

**EFFICIENT GREEN SYNTHETIC ROUTES TO BIO-BASED POLYURETHANES
FROM SOYMEAL**

By

Siva Rama Krishna Chalasani

A DISSERTATION

Submitted to
Michigan State University
in partial fulfillment of the requirements
for degree of

Packaging - Doctor of Philosophy

2014

ABSTRACT

EFFICIENT GREEN SYNTHETIC ROUTES TO BIO-BASED POLYURETHANES FROM SOYMEAL

By

Siva Rama Krishna Chalasani

Polyurethane, a versatile polymer, can be produced in various forms like flexible foams, rigid foams, elastomers, coatings and adhesives with a wide range of properties. Traditionally, polyurethanes are prepared by reacting polyols and diisocyanates. The overall objective of this research was to investigate the feasibility of using readily available and relatively cheap soy meal as a starting material to produce biobased urethane polyols for polyurethane. The amine groups, already present in the soy meal protein, can be converted to urethane polyols.

In this study, these hydroxyl-terminated urethanes were further reacted with dimethyl terephthalate in a two-step reaction to obtain polyurethanes without employing the toxic isocyanate reagent. Glycine, an amino acid found in soy meal was used as a model compound for this study for understanding the chemistry and developing the process. The structures, properties of the intermediates and products were characterized by ^1H NMR, FTIR, acid, amine and hydroxyl values, as well as the key thermal, rheological, morphological properties of the polymer were analyzed..

In the next phase of this study, these developed polyols were further reacted with isocyanates and evaluated in rigid polyurethane foams. A commercial sucrose based polyol was used as a reference petroleum-based polyol. Foams were prepared at Isocyanate Index of 105-110. PU rigid foams with 25% and 50% soy meal polyol formulations exhibited comparable properties to foams prepared with 100% commercial conventional polyols for rigid foams,

including density, compressive strength, compressive strain at yield, friability, water absorption, burning rate and dimensional stability with aging.

A relatively simple method was developed for routine determination of hydroxyl values for a wide range of hydroxyl containing compounds including soybean oil polyols, polyether polyols, ethylene glycol and their blends. This method was based on reacting the hydroxyl compound with hexamethyldisilazane (HMDS) and determining the FTIR peak area of the silylated product at 1251 cm^{-1} . This method is simple and accurate and is not limited to a specific family of polyol compounds. It does not require any special equipment or hazardous chemicals and can be carried out by non-technical staff as a rapid and convenient method for quantitative determination of hydroxyl values. An excellent linear correlation was obtained between this spectroscopic method and conventional titration methods for different types of polyols over a wide range of hydroxyl values. Furthermore, unlike the titration methods the current method is not affected by the presence of acid, base or small amounts of water in the test sample.

Further, the soy meal polyol and castor oil have been further utilized for synthesizing aqueous polyurethane dispersions for coating applications on paper and cellophane substrates. The coatings were evaluated for various properties using contact angle analysis, viscosity measurements, scanning electron microscopy, barrier properties against water vapor and oxygen permeation.

In the last phase, biodegradability studies that were carried out during the course of the study on polyvinyl alcohol, soy meal polyol and castor oil based polyurethane films according to different standards are reported and discussed.

To Lord Sri Krishna

ACKNOWLEDGEMENTS

A dissertation of this scope certainly cannot be accomplished without a wealth of support. I take this opportunity to express my deep gratitude to my major professor Dr. Ramani Narayan whose support and guidance were invaluable. He was always a constant source of motivation, inspiration and had been my role model. I thank my major professor at the school of Packaging Dr. Susan Selke for her guidance and constant support. Her patience and helpfulness was always a great source of strength. My special thanks to Dr. Daniel Graiver, who guided me at various stages of my research. He was available all the time for offering valuable suggestions and was always a great source of motivation. My special thanks to Dr. Laurent Matuana and Dr. Diana Twede for their constructive criticisms and suggestions which helped shape and improve this dissertation.

My special thanks to Dr. Elodie Hablot, post-doctoral candidate who worked in our group for her guidance and help at various stages of my research. I thank my friend Dr. Zhiguan Yang, whose company was always a great source of relief and help. I would also like to thank Dr. Xiangke Shi for his enthusiasm and help in all the activities of our group. My special thanks to other members of our Biobased Materials Research Group Atishi Bali, Sudhanwa Dewasthale, Chetan Thambe, Jeff Schneider, Yanjie Zhao and Samaneh Rahimi. Their diverse talents, enthusiasm and skills supplemented my research and the cohesion in the group was always a great source of strength. Also my special thanks to Ken Farminer, who was also a great source of support and strength.

I am thankful to Mike Rich at the MSU Composite Materials and Structures Center for his help in getting me trained on various analytical instruments. My special

thanks to Dr. Ajay Katuria and Aaron Walworth for their training on the special equipment available at the School of Packaging.

I wish to express my gratitude towards my parents and grand parents whose blessings made this possible. My special thanks to my wife Sushma whose understanding, support, cooperation and encouragement greatly helped me in accomplishing this task. Also special thanks to my little son Mokshagna whose presence at home always relieved me of the tensions associated with this work.

And finally I bow in reverence to Almighty Lord Sri Krishna for giving me the strength to accomplish these tasks and granting me success in my endeavors.

TABLE OF CONTENTS

LIST OF TABLES	xi
LIST OF FIGURES	xiii
Chapter 1 Introduction	1
1.1 Polyurethanes	1
1.2 Application of polyurethanes in packaging	2
1.3 Raw materials.....	3
1.3.1 Isocyanates	3
1.3.2 Polyols	4
1.4 Goals and objectives	5
1.5 PhD dissertation outline	6
REFERENCES	8
Chapter 2 Synthesis of polyurethanes from soymeal by a non-isocyanate route	10
2.1 Introduction.....	10
2.2 Literature review	12
2.2.1 Utilization of soybean.....	12
2.2.2 Hydrolysis of soy proteins.....	14
2.2.3 Protection of carboxylic acid groups.....	16
2.2.4 Synthesis of hydroxy-terminated urethane polyols	17
2.3 Materials and methods	19
2.3.1 Measurements.....	20
2.4 Experimental procedure	21
2.4.1 Synthesis of aminated glycine (Gly-ED).....	21
2.4.2 Synthesis of hydroxy-terminated urethane monomer (Gly-OH).....	22
2.4.3 Synthesis of poly(amide-urethane-ester)s from glycine (Gly-OH-DMT[P]).....	22
2.4.4 Acid hydrolysis of soy meal	25
2.4.5 Amination of soy hydrolyzate	25
2.4.6 Synthesis of hydroxy-terminated urethanes from soymeal	25
2.4.7 Poly(amide-urethane-ester)s from soymeal(SMS-OH- DMT[P]).....	25
2.5 Results and Discussion	26
2.5.1 Synthesis of hydroxyl-terminated amide urethane monomers	26
2.5.2 Synthesis of poly(amide-urethane-ester)s	33
2.6 Conclusions.....	40
REFERENCES	42
Chapter 3 Rigid polyurethane foams based on soy meal polyols	48
3.1 Introduction.....	49
3.2 Literature review	50

3.2.1 Synthetic routes to vegetable oil-based polyols	54
3.2.2 Rigid polyurethane foams from vegetable oil-based polyols	59
3.3 Experimental methods	61
3.3.1 Preparation of rigid polyurethane foams	65
3.4 Results and discussion	67
3.4.1 Rigid polyurethane foams.....	69
3.4.2 Soymeal rigid PU foams vs. commercial packaging PU foams	72
3.5 Conclusions.....	72
REFERENCES	74
Chapter 4 A spectroscopic method for hydroxyl value determination of polyols	80
4.1 Introduction.....	80
4.2 Materials and methods	83
4.2.1 Materials	83
4.2.2 Instrumentation.....	84
4.2.3 Silylation of polyols with HMDS.....	84
4.2.4 OHV determination by titration.....	85
4.2.5 OHV determination by FTIR.....	85
4.3 Results and discussion	86
4.3.1 Method development	88
4.3.2 Precision and accuracy	89
4.3.3 Structural considerations	92
4.3.4 Correlation with the titration method	94
4.3.5 Interferences	95
4.4 Conclusions.....	97
REFERENCES	98
Chapter 5 Evaluation of PU coatings derived from soymeal polyol and castor Oil.....	101
5.1 Introduction.....	101
5.2 Literature review	103
5.2.1 Isocyanates, polyols and catalysts	107
5.2.2 Waterborne polyurethane dispersions	108
5.2.3 Applications of PU dispersions	114
5.2.4 Castor oil based polyurethanes	115
5.3 Material and methods.....	119
5.3.1 Measurements.....	119
5.3.1.1 Attenuated total reflection-fourier transform infrared (ATR-FTIR)	119
5.3.1.2 End group analysis	119
5.3.1.3 Differential scanning calorimetry (DSC).....	120
5.3.1.4 Thermogravimetric analysis (TGA).....	120
5.3.1.5 Barrier properties against water vapor and oxygen permeation.....	120
5.3.1.6 Water absorption resistance test of coatings (Cobb test)	121
5.3.1.7 Scanning electron microscopy	121
5.4 Experimental procedures	122
5.4.1 Soymeal-based polyurethane dispersions.....	122

5.4.1.1 Aqueous alcoholic treatment of soymeal	122
5.4.1.2 Synthesis of soymeal polyurethane dispersions	122
5.4.2 Synthesis of castor oil based polyurethane dispersions (CO-PUDs).....	123
5.5 Results and discussion	123
5.5.1 Soymeal polyol PUDs	123
5.5.2 Castor oil PUDs	134
5.5.3 Comparison between soymeal polyol and castor oil based PUDs	142
5.5 Conclusions	143
REFERENCES	144
 Chapter 6 Biodegradability studies	 153
6.1 Introduction	153
6.2 Literature review	154
6.2.1 Various factors affecting the biodegradability of polymers	154
6.2.2 Influence of environmental conditions on biodegradability.....	158
6.2.3 Affects of polymers properties on their biodegradability.....	159
6.2.4 Standard test methods.....	160
6.3 Biodegradability testing of polyvinyl alcohol in aqueous medium	162
6.3.1 Introduction	162
6.3.2 Experimental methods	163
6.3.2.1 Materials.....	163
6.3.2.2 Microbial source.....	164
6.3.2.3 Biodegradation tests in aqueous medium.....	165
6.3.3 Biodegradation kinetics	169
6.3.4 Results and discussion.....	171
6.3.4.1 Biodegradation of PVA in non-acclimatized medium	171
6.3.4.2 Biodegradation of PVA in the presence of acclimatized inoculum	174
6.3.5 Conclusions	177
6.4 Biodegradability testing of castor oil PU films and soymeal polyol using Microbial oxidation degradation analyzer (MODA)	 177
6.4.1 Introduction	177
6.4.2 Experimental methods	178
6.4.2.1 Materials.....	178
6.4.2.2 Gravimetric measurement respirometric system.....	179
6.4.2.3 Preparation of compost	180
6.4.3 Results and discussion.....	182
6.4.3.1 Biodegradation of castor oil based PU films	182
6.4.3.2 Biodegradation of soymeal polyol	184
6.4.3.3 Biodegradation kinetic studies	187
6.4.4 Conclusions	190
REFERENCES	191
 Chapter 7 Summary and recommendations for future work.....	 196
7.1 Summary	196
7.1.1 Synthesis of polyurethanes from soymeal by a non - isocyanate route.....	196
7.1.2 Rigid polyurethane foams based on soymeal polyols	196

7.1.3 Spectroscopic method for hydroxyl value determination.....	197
7.1.4 Evaluation of PU coatings based on soymeal polyol and castor oil.....	197
7.1.5 Biodegradability studies	198
7.2 Recommendations for future work	199
7.2.1 Synthesis of soymeal polyols suitable for flexible polyurethane foams	199
7.2.2 Evaluation of soymeal polyols for adhesive formulations	199
7.2.3 Shelf life studies for packaging applications.....	199

LIST OF TABLES

Table 1.1: US. polyurethane production by end-use market, 2010	3
Table 1.2: Estimated global PU raw material demand (MMlbs) 2012	4
Table 2.1: Composition of amino acids	15
Table 2.2: End group analysis of PU and its intermediates synthesized from glycine	28
Table 2.3: End group analysis of PU and its intermediates synthesized from soy meal.....	32
Table 2.4: Mw of Gly-OH-DMT[P] as a function of OH values.....	34
Table 3.1: The most common fatty acids found in vegetable oils	53
Table 3.2: Typical formulation of rigid foams derived from propoxylated soymeal polyol	66
Table 3.3: Foam characterization methods	66
Table 3.4: End group analysis and viscosity of polyols	69
Table 3.5: Properties of rigid PU foams prepared from propoxylated soy meal urethane polyols	71
Table 3.6: Properties comparison between soymeal polyol foams and commercial PU packaging foams.....	72
Table 4.1: Statistical analysis of the areas under the silylated FTIR bands.....	89
Table 4.2: Reproducibility of FTIR peak areas of silylated polyols.....	91
Table 4.3: Effect of acid, base and water on the OHV	97
Table 5.1: Different types of coatings by ASTM classification	106
Table 5.2: Castor oil composition.....	116
Table 5.3: Carbohydrate content analysis in soymeal	124

Table 5.4: End group analysis of soymeal polyol.....	128
Table 5.5: Glass transition and degradation temperatures of soymeal polyol PUD film	131
Table 5.6: Cobb values, WVTR and contact angles of soymeal polyol PUD coatings	132
Table 5.7: Properties of castor oil PUDs & coatings	136
Table 5.8: Glass transition and degradation temperatures of castor oil PUD films	138
Table 5.9: Cobb values, contact angles, WVTR and OTR results of castor oil PUD coatings	140
Table 6.3.1: Kinetic parameters of PVA degradation in acclimatized and non-acclimatized inoculum	172
Table 6.4.1: Percent biodegradation of castor oil PU film as a function of time.....	184
Table 6.4.2: Biodegradation kinetic parameters of castor oil PU and soymeal polyol	187

LIST OF FIGURES

Figure 1.1: Polyurethane synthesis, with urethane groups -NH-(C=O)-O- linking the molecular chains	2
Figure 2.1: Composition of soybeans	13
Figure 2.2: Schematic representation of soy proteins containing functional side groups	15
Figure 2.3: Synthesis of methyl carbamate.....	17
Figure 2.4: Conversion of peptide-carbamates to hydroxy pre-polymers & polyurethanes.....	18
Figure 2.5: Synthesis of hydroxyl terminated (amide-urethane) oligomers from glycine.....	22
Figure 2.6: Synthesis of poly(amide-urethane-ester)s using dimethyl terephthalate	24
Figure 2.7: ATR-FTIR of (A) Gly, (B) Gly-ED, (C) Gly-OH and (D) the final polymer	27
Figure 2.8: ¹ H NMR of Gly-OH	30
Figure 2.9: FTIR data of (A) SMS, (B) SMS-ED, (C) SMS-OH, (D) SMS-OH-DMT, (E) SMS-OH-DMT[P]	31
Figure 2.10: Mw of Gly-OH-DMT[P] as a function of OH values	34
Figure 2.11: TGA of PU from (A) glycine and (B) soy meal.....	35
Figure 2.12: DSC of PU from (A) glycine and (B) soy meal	36
Figure 2.13: Storage (G') and loss modulus (G'') of PU from glycine as a function of temperature.....	37
Figure 2.14: Storage (G') and loss modulus (G'') of PU from soy meal as a function of temperature.....	37
Figure 2.15: Viscosity of PU from glycine as a function of reaction time	38

Figure 2.16: Viscosity of PU from soy meal as a function of reaction time.....	39
Figure 2.17: Log viscosity Vs log shear rate chart of PUs from glycine (A) and soy meal (B) at a temperature of 180 °C.....	39
Figure 2.18: TEM images of PU synthesized from glycine (left) and soy meal (right) showing the phase separation between soft and hard segments	40
Figure 3.1: Triglyceride structure, where R ¹ , R ² , R ³ are fatty acids	52
Figure 3.2: Polyol synthesis from epoxidized vegetable oils	55
Figure 3.3: Ozonolysis route to synthesis of polyols from vegetable oil.....	57
Figure 3.4: Synthesis of polyols from vegetable oils by hydroformylation	58
Figure 3.5: Preparation of hydroxyl-terminated urethane monomer	62
Figure 3.6: Propoxylation of soymeal polyol	64
Figure 3.7: Samples of rigid polyurethane foams prepared with combination of water and Enovate 3000 blowing agent; A - reference formulations (0% soy mealpolyol); B - fomulations with 25% soy meal polyol; C - formulations with 50% soy meal polyol	70
Figure 4.1: Silylation of polyols with HMDS.....	84
Figure 4.2: FTIR spectra of a sample polyol (A), the same sample after silylation (B) and after subtraction (insert).....	86
Figure 4.3: Accuracy of the method as determined by comparing the experimental to calculated OHVs.....	90
Figure 4.4: Correlation of the FTIR method with the calculated OHV	91
Figure 4.5: Correlation of the FTIR method with the titration method	93
Figure 4.6: Normal probability plot	94
Figure 4.7: Residual plot of OHV	95
Figure 5.1: Reactions of polyisocyanates in PU coating systems.....	104
Figure 5.2: Synthesis of anionic waterborne PU dispersions	109

Figure 5.3: 1 st generation, polyether modified hydrophilic polyisocyanate	112
Figure 5.4: 2 nd generation, polyether modified hydrophilic polyisocyanate (allophanate)	112
Figure 5.5: 3 rd generation, aminosulfonate modified hydrophilic polyisocyanate	113
Figure 5.6: Breakdown of the US coating market in 2010	114
Figure 5.7: Structure of castor oil	115
Figure 5.8: Flow chart for the synthesis of PUDs from soymeal.....	126
Figure 5.9: FTIR of soymeal polyol and its intermediates	127
Figure 5.10: FTIR spectra of coatings made using soymeal polyol PUDs	129
Figure 5.11: TGA and its derivate curve for soymeal polyol PUD films	130
Figure 5.12: DSC scan for the soymeal polyol based PUD films.....	131
Figure 5.13: Surface (left) and cross-sectional (right) SEM images of Form-WB uncoated substrate	132
Figure 5.14: Surface (left) and cross-sectional (right) SEM images of soymeal polyol PUD coatings	132
Figure 5.15: Flow chart for the synthesis of PUDs from castor oil	135
Figure 5.16: Viscosity of the castor oil PUDs as a function of time at different RPMs.....	135
Figure 5.17: FTIR spectrum of castor oil PUD coated film	136
Figure 5.18: TGA and its derivative curve for castor oil PUD film	137
Figure 5.19: DSC scan for the castor oil PUD film	138
Figure 5.20: SEM photographs of uncoated (left) and coated (right) cellophane substrate (top): SEM photographs showing the cross-sections of the uncoated (left) and coated (right) cellophane substrates (bottom)	139
Figure 6.1: Various factors that affect biodegradation	156
Figure 6.2: General mechanism for the biodegradation of plastics by microorganisms	158

Figure 6.3.1: Chemical structure of poly(vinyl alcohol).....	164
Figure 6.3.2: Schematic of the experimental setup.....	166
Figure 6.3.3: A typical biodegradation curve showing CO ₂ evolved as a function of time.....	169
Figure 6.3.4: Biodegradation curves of PVA and cellulose in the presence of municipal sewage sludge.....	171
Figure 6.3.5: Graph of $\ln(1-y/a)$ versus time for cellulose in municipal sewage water.....	173
Figure 6.3.6: Biodegradation of PVA, cellulose and starch in the presence of acclimatized inoculum.....	174
Figure 6.3.7: Biodegradation kinetics of PVA-88 in the presence of acclimatized inoculum.....	176
Figure 6.3.8: Biodegradation kinetics of PVA-99 in the presence of acclimatized inoculum.....	176
Figure 6.4.1: Schematic representation of the MODA system.....	179
Figure 6.4.2: Evolved carbon dioxide as a function of time for cellulose, blank and castor oil PU film.....	183
Figure 6.4.3: Percent biodegradation as a function of time for cellulose and castor oil PU film.....	184
Figure 6.4.4: Cumulative CO ₂ evolved over time in soymeal polyols, cellulose and blank.....	186
Figure 6.4.5: Percent biodegradation as a function of time for cellulose and soymeal polyol.....	186
Figure 6.4.6: Graph of $\ln(1-y/a)$ versus time for cellulose.....	188
Figure 6.4.7: Graph of $\ln(1-y/a)$ versus time for castor oil PU films.....	189
Figure 6.4.8: Graph of $\ln(1-y/a)$ versus time for soymeal polyol.....	189
Figure 6.4.9: Comparison between experimental and estimated data generated by the kinetic model.....	190

Chapter 1 Introduction

1.1 Polyurethanes

Polyurethanes are a class of polymers consisting of organic units joined together by urethane linkages. Polyurethanes are formed by reaction between a diisocyanate or a polymeric isocyanate with a polyol in the presence of suitable catalysts and additives (Figure 1.1). This reaction between the isocyanate group and the hydroxyl compound was originally described in the 19th century, but the credit for pioneering the work on polyurethane polymers goes to Otto Bayer and his coworkers in 1937 at the laboratories of I.G.Farben in Leverkusen, Germany [1]. The condensation reaction of difunctional hexamethylene diisocyanate and 1,4-butanediol produced the polyurethane product, which found special uses compared to already existing plastics[2]. The first commercial applications of polyurethane polymers, elastomers, coatings and adhesives were developed between 1945 and 1947, followed by flexible polyurethane foams in 1953 and rigid polyurethane foams in 1957.

The nature of the chemistry allows polyurethanes to be adapted to solve challenging problems, to be molded into unusual shapes and to enhance industrial and consumer products, making polyurethanes one of the most versatile plastic materials. A variety of diisocyanates and a wide range of polyols can be used to produce a broad spectrum of polyurethanes, including flexible foams, rigid foams, coatings, adhesives, sealants and elastomers (CASE) etc., to meet the needs of a broad variety of applications[3,4]. The global consumption of polyurethanes has been on the rise with an average annual rate of 7% for the last 15 years. Therefore it is not surprising

that polyurethanes are all around us, from furniture to automobile parts, footwear, electronics, textiles, insulations in refrigerators and homes, making them essential to a multitude of end-use applications.

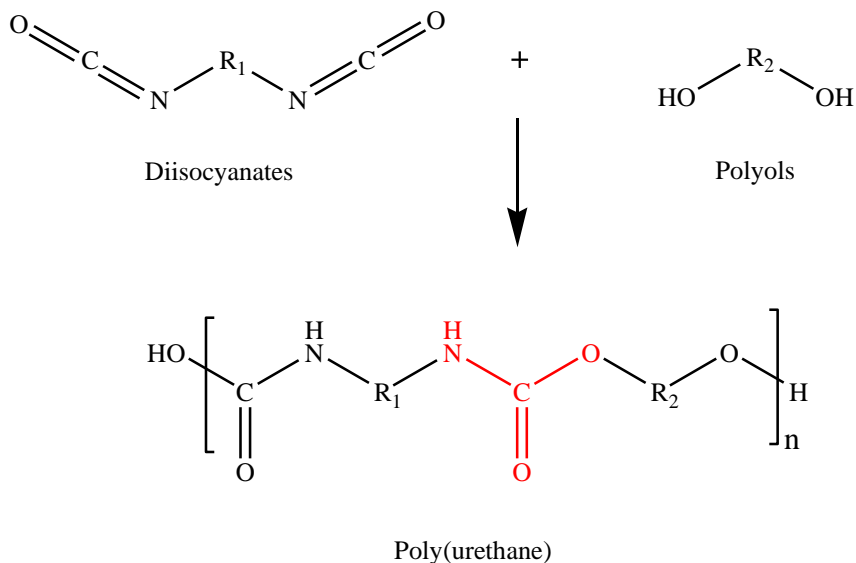


Figure 1.1: Polyurethane synthesis, with urethane groups -NH-(C=O)-O- linking the molecular chains

1.2 Applications of polyurethanes in packaging

Polyurethane packaging foams provide cost-effective, custom form-fitting cushioning to effectively and securely protect items that need to stay safely in-place during transit. Because of their excellent shock absorbency, water resistance and resiliency, 29 million pounds of flexible polyurethane foams are used to protect and cushion especially sensitive products, i.e., computers and other electronics. Rigid polyurethane foams that are poured-in-place to create a tight, impact-resistant cushion also are used to protect sensitive or fragile items. Polyurethane adhesives provide excellent barrier properties and bond strength and are used in packaging for cereals, snack foods and lunch meats (Table 1.1).

Approximately 172 million pounds of polyurethane, which is 4.1% of the total U.S. polyurethane consumption, caters to the needs of the packaging industry. Polyurethanes used in packaging generated a revenue of \$2.9 billion in shipments in 2010 and supported 9,200 jobs in 200 locations throughout the U.S. [5].

Table 1.1: US. polyurethane production by end-use market, 2010

End-use markets for polyurethanes	Million Pounds	% of Total
Building and Construction	1,432	34.60
Transportation and Marine	770	18.60
Furniture and Bedding	730	17.60
Machinery and Foundry	294	7.10
Appliances	230	5.50
Packaging	172	4.10
Textiles, Fibers and Apparel	39	0.90
Electronics	30	0.70
Footwear	19	0.50
Others	428	10.30
Total Polyurethanes Production	4,143	100.00%

1.3 Raw materials

Isocyanates and polyols are the two major raw materials for making polyurethanes.

1.3.1 Isocyanates

Isocyanates form the A-side component in polyurethane chemistry with the functional group $-N=C=O$. Isocyanates are commonly produced by the phosgenation of amines. This reaction is usually completed in a chlorinated aromatic solvent in order to remove excess phosgene in later purification stages.

Methylene diphenyl diisocyanate (MDI) and toluene diisocyanate (TDI) are the two major isocyanates utilized in the global isocyanate market. In 2012, approximately

70.1% of isocyanates utilized in the global market were MDI, 25.9% were TDI, and approximately 3.9% were other types of isocyanate [6]. Other types of isocyanates like 1,6-hexane diisocyanate (HDI), isophorone diisocyanate (IPDI), 1,5-naphthalene diisocyanate (NDI) and 1,4-phenylene diisocyanate (PDI) are also used in different applications (Table 1.2).

Table 1.2: Estimated global PU raw material demand (MMlbs) 2012

PU Raw materials	NAFTA	S.America	EMEA	Asia Pacific	China	Total (MMlbs)
MDI	2105	275	3640	1985	3085	11090
TDI	595	330	1380	465	1325	4095
Aliphatic Iso.	145	20	140	55	265	625
Polyester polyols	770	120	880	450	1100	3320
Polyether polyols	2205	830	4960	1785	4850	14630
Additives	1125	210	950	935	2645	5865
Total	6945	1785	11950	5675	13270	39625

1.3.2 Polyols

The polyols are a source of multifunctional hydroxyl groups and form the B-side component in the synthesis of polyurethane products. Polyether polyols and polyester polyols are the two major petroleum-based polyols utilized in the global polyols market [6]. In general, polyether polyols are synthesized by the reaction of ethylene glycol, propylene glycol and other initiators like glycerin with alkylene oxides to form primary hydroxyl groups [7]. Polyester polyols are synthesized by the reaction between glycols

such as 1,6-hexanediol or polyols such as glycerin with diester or diacid to form primary polyester polyols [8].

Polyols have different physicochemical properties that play an important role in the properties of the final polyurethane products. The important properties for characterizing the polyols are described below.

Acid number (mg KOH/g) is defined as the amount in milligrams of potassium hydroxide required to neutralize the acid present in one gram of a polyol sample. Functionality and equivalent weight are the other important properties. The functionality of polyols can be defined as the average number of functional groups reacting with isocyanate per molecule of polyols. Hydroxyl equivalent weight is the amount in grams of a sample having one equivalent weight (17.008g) of hydroxyl in the sample. The equivalent weight can be calculated from the hydroxyl number according to the following equation

$$\text{Equivalent weight} = 56100/\text{Hydroxyl number}$$

Hydroxyl number (mg KOH/g) is a measure of the amount of reactive hydroxyl groups available for reaction and is usually reported as milligrams of potassium hydroxide equivalent to the hydroxyl groups found in one gram of polyols.

1.4 Goals and objectives

Traditionally, polyurethanes are prepared by reacting polyols and diisocyanates. However, there are concerns about the toxicity of the isocyanates as well as phosgene, which is used to prepare these isocyanates. Further, the dwindling reserves of petroleum resources, geopolitical issues and price instability of these basic materials used in the

production of polyurethanes are also major concerns. These concerns have led to a high demand for the use of bio-based resources as alternative starting materials in the production of polyurethanes.

The overall objective of this research was to investigate the feasibility of using readily available and relatively cheap soy meal as a starting material to produce soy-based urethane polyols for polyurethane. The initial focus was to determine “proof of concept” of the product and economic feasibility of the process. Upon successful completion of this work, other specific objectives of this dissertation are to evaluate these polyols in synthesizing polyurethanes avoiding the toxic isocyanates, as well as utilization in rigid foam formulations to produce foams with increased bio-based content and thus reduced carbon footprint.

1.5 PhD dissertation outline

The PhD dissertation thesis outline is divided into a Literature Review section (Chapter 2) to review the composition, current applications of soy bean meal and to understand and acquire knowledge regarding the various steps of producing bio-based polyols from soymeal. The research work that follows contain the synthesis and characterization of polyurethanes from soymeal polyols by a non-isocyanate route. The hydroxy-terminated urethane polyols made from soymeal were further reacted with dimethyl terephthalate in a two-step reaction to obtain polyurethanes without employing the toxic isocyanate reagent. Glycine, an amino acid found in soy meal, was used as a model compound in this study for understanding the chemistry and optimize the preparation process. The structures, morphology, thermal and rheological properties of

the intermediates and the products were characterized by ^1H NMR, FTIR, acid, amine and hydroxyl values.

In chapter 3 the developed polyols were further reacted with isocyanates and evaluated in rigid polyurethane foam formulations. A commercial sucrose based polyol was used as a reference petroleum-based polyol. Key properties of the PU rigid foams made with 25% and 50% soymeal polyols such as the density, compressive strength, compressive strain at yield, friability, water absorption, burning rate and dimensional stability with aging were analyzed.

In chapter 4, a novel and general spectroscopic method for the determination of hydroxyl values for a wide range of polyols including soybean oil polyols, polyether polyols, ethylene glycol etc. is presented. This method is based on reacting the polyols with hexamethyldisilazane and determining the hydroxyl value from the FTIR peak area of the silylated product. The accuracy and precision, as well as interferences from acids, bases and water of the method on the hydroxyl value determination were measured and compared with the standard titration methods.

In chapter 5, soymeal polyol and castor oil were utilized for synthesizing aqueous polyurethane dispersions for coating applications on paper and cellophane substrates. The coatings were further evaluated for various properties using contact angle analysis, viscosity measurements, scanning electron microscopy, barrier properties against water vapor and oxygen permeation.

In the last chapter, biodegradability studies that were carried out during the course of the study on polyvinyl alcohol, soymeal polyol, and castor oil based polyurethane films according to different standards are reported and discussed.

REFERENCES

REFERENCES

1. Bayer O (1947) Das Di-Isocyanat-Polyadditionsverfahren (Polyurethane). *Angew Chem* 59:257-272
2. Seymour RB, Kauffman GB (1992) Polyurethanes: A Class of Modern Versatile Materials. *J Chem Educ* 69:909-910
3. Saunders JH, Frisch KC (1964) Polyurethanes, Chemistry and Technology Part II, Technology, Interscience Publishers.
4. Oertel G, Abele L (1985) Polyurethane Handbook: Chemistry-Raw Materials-Processing-Application-Properties. Hanser Publishers.
5. American Chemistry Council (2012) CPI 2010 End-Use Market Survey on the Polyurethane Industry
6. American Chemistry Council (2013) 2012 End-Use Market Survey on the Polyurethanes Industry in the United States, Canada and Mexico
7. Garcia JL, Jang EJ, Alper H (2002) New heterogeneous catalysis for the synthesis of poly(ether polyol)s. *J Appl Polym Sci* 86(7):1553-1557
8. Kadkin O, Osajda K, Kaszynski P, Barber TA (2003) Polyester Polyols: Synthesis and Characterization of Diethylene Glycol Terephthalate Oligomers. *J Polym Sci Part A: Polym Chem* 41(8):1114-1123

Chapter 2 Synthesis of polyurethanes from soy meal by a non-isocyanate route

Poly(amide-urethane-ester)s were synthesized from renewable soy meal without employing the typical toxic isocyanate reagent. In this process, soy meal was hydrolyzed to a mixture of amino acids, which were then condensed with ethylene diamine to produce amine terminated amide monomers. In a second step, these monomers were reacted with ethylene carbonate to yield hydroxyl-terminated amide urethanes. These hydroxyl-terminated urethanes were further reacted with dimethyl terephthalate in an urethane exchange reaction to obtain poly(amide-urethane-ester)s. Glycine, an amino acid found in soy meal, was used as a model compound for this study for understanding the chemistry and developing the process. The structures, properties of the intermediates and products were characterized by ^1H NMR, FTIR, acid, amine and hydroxyl values, and the key thermal, rheological, morphological properties of the polymers were analyzed. The polymers obtained were amorphous and thermally stable up to 270 °C.

2.1 Introduction

Polyurethanes are one of the most versatile polymeric materials available today. They have a wide range of applications in industries such as flexible foams in upholstered furniture, rigid insulation foams in walls and roofs, thermoplastic materials used in medical devices and footwear, coatings, adhesives, sealants and elastomers used on floors and automotive interiors[1]. Polyurethanes are usually synthesized by the reaction between diols and diisocyanates. Isocyanates are commercially prepared by the reaction of amines with phosgene. Although this reaction is convenient and widely used in the

industry, issues related to handling of phosgene gas, its hazardous and toxicity characteristics as well as its corrosiveness are problematic [2,3]. Consequently, various non-isocyanate routes for synthesizing polyurethanes gained momentum in the last few decades. In particular, the reactive applications of cyclic alkylene carbonates have been the subject of considerable research. Alkylene carbonates react with aliphatic diamines to give difunctional hydroxyalkyl urethanes, which could replace toxic diisocyanates [4-17]. Furthermore, there is also a growing interest in the manufacture and use of biobased plastics and products. Switching the petro-fossil carbon feedstock to a bio-renewable carbon feedstock offers the "value proposition" of a reduced material carbon and environmental footprint [18,19]. The increasing awareness about environmentally friendly materials produced from annually renewable biodegradable resources have led to intensified research for the development of plastics from soy based materials. Soybean oil based polyols are available in the polyurethane market and much work has been published in the literature regarding synthesis of polyurethanes utilizing these polyols [20,21]. Huafeng et al. [22] proposed blending soy protein isolate with waterborne polyurethane through casting and evaporation methods to produce films with improved water resistance and flexibility. The bulk of the soy meal is utilized as animal feed, soy protein is also used in human nutrition. In spite of this, the proportion of soy protein availability is high and there is a need to look into the alternative industrial uses of soy protein [23]. However to the best of our knowledge, no other studies are available in the literature utilizing soybean meal as a renewable biomass resource for synthesizing polyurethanes.

This chapter reports a novel route to the synthesis of biobased poly(amide-urethane-ester)s from soy meal by a non-isocyanate route. Hydrolysis of soy proteins to individual amino acids or low molecular weight peptides[24-28], amidation of the hydrolyzed product mixture with ethylene diamine, urethane monomer synthesis by reacting the aminated hydrolyzate with cyclic ethylene carbonate and reaction of the resulting hydroxyl-terminated urethanes with dimethyl terephthalate in a final two step reaction were the steps involved in the synthesis of poly(amide-urethane-ester)s from soy meal. In order to gain insight into the chemistry of the process and better understand the reaction mechanism, glycine, a common amino acid found in soy proteins, was used as a model compound. The overall objective was to investigate the feasibility of using soy meal to produce biobased poly(amide-urethane-ester)s by a non-isocyanate route. The chemical structures and key properties of all intermediates as well as the final poly(amide-urethane-ester)s are reported.

2.2 Literature review

2.2.1 Utilization of soybean

Soybeans, which are abundantly available, low in cost and often referred to as the miracle crop, can provide a sustainable and alternative source to petrochemicals. Soy is grown throughout the world and soybean production has increased more than 500% in the last forty years [29]. The typical composition of soybeans is given in Figure 2.1. A mature soybean consists of about 38% protein, 30% carbohydrates, 18% oil and 14% moisture, ash and hull [30]. Soybean composed of both protein and oil can open the door for a variety of uses. Soybean processors can divide soy's components into soy protein

(soybean meal) and soy oil. Soy oil can be extracted from the bean either by mechanical pressing or using solvent extraction methods. Soy oil constituting around 18% of soybeans has already made its way into the polyol market. Soy oil based polyols are also commercially available in the polyurethane market and more and more researchers and companies are getting into this area. The Dow Chemical Company, Biobased Technologies®, Arkema Inc., Cognis Oleochemicals and Urethane Soy Systems are some of the leading companies along with other smaller independent companies in the U.S. with research programs on soy based polyols. Academic research based on soybean oil and polyurethane development includes the laboratories of Dr. J. Massingill (Texas State University), R.P.Wool (University of Delaware), Z. Petrovic (Pittsburg State University), R. Larock (Iowa State University), G.Suppes/F. Hsieh (University of Missouri-Columbia) and G.Wilkes (Virginia Tech. University).

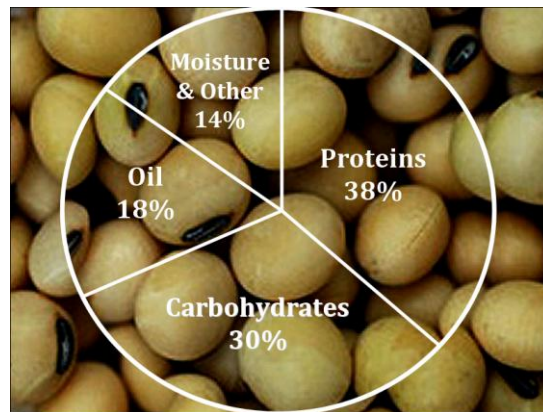


Figure 2.1: Composition of Soybeans

Soybean meal is the product remaining after extracting most of the oil from whole soybeans. Soybean meal which comprises up to 80% of the soybeans, is high in protein content and primarily serves as animal diet for pig, chicken, cattle, horse, sheep and fish

feed. Currently, only a small percentage of the soybean meal is being utilized for industrial purposes, mainly for synthesis of adhesives, insecticides, paints, paper coatings, fire-resistant coatings, cosmetics, printing inks and emulsions [31].

2.2.2 Hydrolysis of soy proteins

The hydrolysis of proteins, including soy proteins, to amino acids by acid hydrolysis is a well known process. Generally, the hydrolysis proceeds smoothly provided a sufficient amount of water is present. The hydrolysis rate depends on the temperature, pH, the size of anion (or cation) and the concentrations of additives that are be used. Standard hydrolysis procedures involve 24 hours of acid hydrolysis using 6 M HCl at 110°C [32-34], although other acids, such as ethanesulfonic acid and p-toluenesulfonic acid, have also been used. The effect of hydrolysis time (16-72 h) has been studied on soy proteins and its effect on the release of amino acids as well as the composition of the hydrolyzed product mixture as these hydrolysis products are widely used in animal nutrition [35]. The effect of acid concentration on the hydrolysis of soy protein and the composition of the released amino acid has also been investigated [36] and it was found that there was no indication of any degradation during hydrolysis provided 9 molar HCl or less was used. If however, higher concentrations of HCl were used (e.g. 12M), some of the amino acids (primarily threonine) were degraded and the extent of the degradation was directly proportional to the hydrolysis time. Typically, the acid hydrolysis product mixture in this process ends up as the chloride salt of the amine. The composition of the individual amino acids from the acid hydrolysis is listed in Table 2.1 [37].

Schematically (Figure 2.2), the hydrolysis breaks up the amide bonds between the primary amide linkages of the protein as well as the secondary, tertiary and quarterly linkages (e.g. intramolecular hydrogen bonds, disulfide bonds, and ionic interactions) between the protein molecules. The end result is a mixture of small molecular weight peptides and individual amino acids

Table 2.1: Composition of amino acids

	Nutrient	Soybean Meal (dehulled)	Soy Protein Concentrate
Amino Acids %			
1	Arginine	3.56	4.68
2	Histidine	1.29	1.74
3	Isoleucine	2.16	2.94
4	Leucine	3.67	4.97
5	Lysine	2.97	4.08
6	Methionine	0.65	0.90
7	Cystine	0.76	1.07
8	Phenylalanine	2.43	3.24
9	Tyrosine	1.70	2.29
10	Tryptophan	0.61	0.83
11	Threonine	1.83	2.55
12	Valine	2.31	3.15
13	Aspartic acid	5.29	7.16
14	Serine	2.26	3.11
15	Glutamic acid	8.59	11.53
16	Proline	2.37	3.24
17	Glycine	1.97	2.68
18	Alanine	2.07	2.81

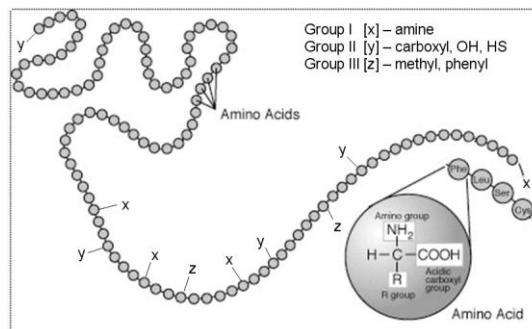


Figure 2.2. Schematic representation of soy proteins containing functional side groups

It should also be mentioned here that soy protein, either as defatted flours, grits, meal, concentrate, or isolates can be used in this hydrolysis process, although each of these grades contains different amounts of proteins, fibers, lecithin, fat, carbohydrates, ash, and moisture. Accordingly, the cost of the process, which depends on the grade of the starting proteins, will increase in proportion to the purity of the starting materials.

2.2.3 Protection of carboxylic acid groups

Close examination of the amino acid composition reveals that several amino acids (aspartic acid, threonine, cysteine, glutamic acid, serine and tyrosine) contain more than one carboxylic acid. Indeed, other amino acids contain several amines and only a single carboxylic group (arginine, lysine, tryptophan and histidine). After the hydrolysis, the carboxylic acids of each amino acid must be protected or converted to other functional groups so that they will not interfere in the subsequent reactions. There are several examples in the literature of methods to achieve this task; one such example [38] is to react the amino acid mixture with trimethylchlorosilane. Another example is to esterify the carboxylic acid of the amino acids with an alcohol to yield the corresponding alkyl esters [39] respectively. It is apparent that some of these protection schemes are not useful commercially and/or are too expensive. For example, using trimethylchlorosilane is a fast and convenient reaction but it yields a Si-O-C bonds which are hydrolytically unstable. The by-product, HCl, also reacts with the amino group to yield the chloride salt, which would negatively impact subsequent reactions of the amine.

The amination of the carboxylic acid could also be achieved using carbodiimides in water [40, 41]. Under these mild conditions the reaction could proceed in the water phase, eliminating the need to distill out the water from the hydrolysis step. This amination of carboxylic groups is widely used in biochemistry “to convert the carboxylic groups into more potent nucleophile and at the same time provides an extended arm from the protein to avoid steric hinderance”. It has also been used to change the surface chemistry of solid particles for protein immobilization. Thus, 1-ethyl-3-(3-dimethyl aminopropyl)-carbodiimide (EDC) was reacted with the hydrolyzed soy protein water solution after the pH was adjusted to 4.5-5.0 as required for this reaction. Although this method of protecting and converting the carboxylic groups appeared successful, the relatively high expense associated with the EDC reagent did not justify its use.

2.2.4 Synthesis of hydroxy-terminated urethane polyols

Carbamates are known protecting groups in organic chemistry, and in particular in peptide synthesis [42-44] where they are generally obtained by the reaction of various amines with an alkyl chloroformate in the presence of a base [45,46] or a Lewis acid [47,48]. Carbamates, also called urethanes are the monomers of polyurethanes. The conversion of the amine functional hydrolyzed product mixture to carbamates [49] was achieved by reacting it with methyl chloroformate using zinc as a catalyst (Figure 2.3).

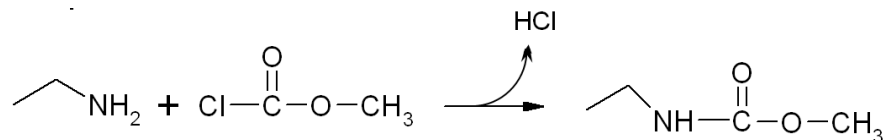


Figure 2.3: Synthesis of methyl carbamate

Methyl chloroformate is a highly reactive reagent. Its reaction with amine is fast, usually completed in a few minutes at room temperature with a wide choice of catalysts. However, it has been found that extreme care must be taken to chelate and capture the HCl that is released in the course of the reaction. Otherwise, HCl will react with the amine functional proteins to yield chloride salts which will cause it to precipitate from the solution and prevents any further reaction. It was found that this premature precipitation and salt formation can be avoided by using a chelating agent (pyridine or zinc powder appeared to work fine) and, most importantly, by adding the amine functional reagent dropwise to a solution of methyl chloroformate containing the chelating agent. This way, the amine is reacted with the chloroformate and any HCl by-product is captured by the chelating agent. If, however, the chloroformate is added to the amine reagent, the HCl by-product will react with the amine instead of being removed by the chelating agent.

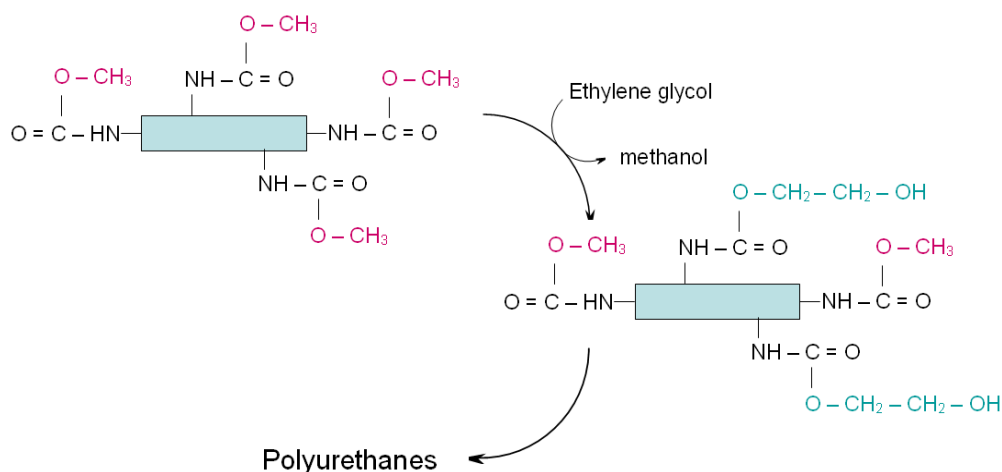


Figure 2.4: Conversion of peptide-carbamates to hydroxy pre-polymers & polyurethanes

L. Ubags [50] reported that polyurethanes can be synthesized by polycondensation of bis(phenyl carbamate)s with ethylene glycol. This procedure can be applied to the carbamate produced from the previous reactions mentioned above and polyol terminated urethane prepolymers can be achieved by exchanging the methoxide group on the carbamate with ethylene glycol as depicted in Figure 2.4.

During the course of this study, it was realized that hydroxy-terminated urethane monomers can be synthesized in a much more direct way than in the methods mentioned above: by reacting diamines with ethylene carbonates. Rokicki and Piotrowska [51] investigated the reaction of diamines with ethylene carbonate to synthesize hydroxy-terminated urethane monomers finding that it can be done at much milder conditions (room temperature, no catalyst required) and the reaction can be monitored by the disappearance of the C=O stretch of ethylene carbonate at 1800 cm^{-1} using FTIR. The usage of cyclic carbonates as alternative materials for synthesizing polyurethanes by isocyanate-free routes is widely reported in the literature [52-55].

2.3 Materials and methods

Glycine (Gly), ethylene diamine (ED), ethylene carbonate (EC), titanium (IV) butoxide $\text{Ti}(\text{O}i\text{Bu})_4$ and dimethyl terephthalate (DMT) as well as all the reagents required for the titrations (e.g. butanol, pyridine, acetic anhydride, hydrochloric acid, potassium hydroxide, sodium hydroxide, phenolphthalein and bromophenol blue) were purchased from Sigma Aldrich. Defatted soy meal (SMS) was obtained from Zeeland farms, Michigan. All chemicals were used as received unless otherwise noted.

2.3.1 Measurements

Proton-nuclear magnetic resonance (^1H NMR) spectra were recorded on a 500 MHz NMR spectrometer (Varian Inc., USA, Unity Plus 500MHz) using the solvent peak as an internal standard.

The attenuated total reflection-Fourier transform infrared (ATR-FTIR) spectra were acquired on a FT-IR (Shimadzu Co., Tokyo, Japan, IRAffinity-1) equipped with a single reflection ATR system (PIKE Technologies, Madison, USA, MIRacle ATR).

Differential scanning calorimetry (DSC) measurements were performed using DSC Q2000 TA Instruments under nitrogen flow. To determine the thermal property profile, a sample (5-10 mg placed in an aluminium pan) was heated up to 200 °C at 10 °C/min, held at this temperature for 3 min to remove the thermal history, then cooled to -70 °C at 10 °C/min and finally heated again to 200 °C at 10 °C/min. The glass transition temperature T_g was determined from the inflection point from the second heating scan.

Thermogravimetric analysis (TGA) measurements were conducted under nitrogen flow using a Hi-Res TGA 2950 apparatus from TA Instruments. In a typical experiment, a sample (10-20 mg placed in an aluminium pan) was heated up to 550 °C at 10 °C/min in a nitrogen atmosphere. The characteristic degradation temperature was taken as the maximum temperature of the derivative thermogram (DTG) curve (T_{dmax}) for each degradation step.

Dynamic mechanical analysis (DMA) was performed using a TA Q800 instrument, samples evaluated using a three point bend geometry at a constant frequency of 1 Hz, scanning rate of 4 °C/min from 23°C to 150°C providing measurements of storage modulus (G') and loss modulus (G'') as a function of temperature.

Viscosity measurements were made with an ARES – G2 Rheometer using parallel-plate geometry with diameter 25.4 mm in a frequency/temperature sweep test type.

Transmission electron microscopy was performed using a JEOL 2200FS 200 k V field emission transmission electron microscope (TEM).

Acid values (mgKOH/g) were determined in accordance with ASTM D1980-87 [56]. Samples were dissolved in water and were then titrated with 0.2N KOH in water in the presence of phenolphthalein as the indicator. Amine values (mgKOH/g) were determined in accordance with ASTM D2073-92 [57]. Samples were dissolved in water and were then titrated with freshly standardized 0.2N HCl in water by using bromophenol blue solution as indicator. Hydroxyl values were determined in accordance with ASTM D1957-86 [58]. Samples were dissolved in pyridine containing acetic anhydride solution and boiled using a steam bath for 2 hours. The solution was then cooled down with distilled water. The remaining acetic anhydride was thus transformed into acetic acid. Butanol was added to the solution and the remaining acetic acid was titrated back with freshly standardized 0.2N KOH in methanol using phenolphthalein as the indicator.

2.4 Experimental procedures

2.4.1 Synthesis of aminated glycine (Gly-ED)

Glycine (200.86 g, 2.67 mol) and an excess of ED (798.27 g, 13.28 mol) were charged into a polycondensation reactor (PAAR, Serie 4530, 2000 mL) equipped with a mechanical stirrer, a thermocouple, a nitrogen inlet and a Dean-Stark trap. The mixture was first flushed with nitrogen for 20 min. The temperature of the reaction mixture was initially raised to 150°C under a pressure of 150 psi for 1 hour and then the reaction was

run at a temperature of 110°C under atmospheric pressure for 5 more hours under nitrogen. Samples were taken out periodically and were analyzed by titration (acid and amine values). The final reaction mixture was then precipitated in tetrahydrofuran (THF) and then washed thrice with THF to obtain a pure aminated glycine product (Gly-ED) which was further analyzed by FTIR, acid and amine value titrations..

2.4.2 Synthesis of hydroxy-terminated urethane monomers (Gly-OH)

Gly-OH was synthesized in the same vessel used for the synthesis of Gly-ED. In a typical procedure, Gly-ED monomer (75.5 g, amine value = 825.95 mgKOH/g) was heated at 80°C, EC (98.9 g, 1.12 mol) that was previously melted in an oven at 60 °C for 2 h, was then charged into the vessel. The ratio of total amine equivalents to the total carbonate equivalents was kept close to 1. The reaction was carried out in the bulk at 80°C for 2 hours under a nitrogen atmosphere. The final material Gly-OH was analyzed by titration (amine, acid and hydroxyl values), ¹H NMR and FTIR.

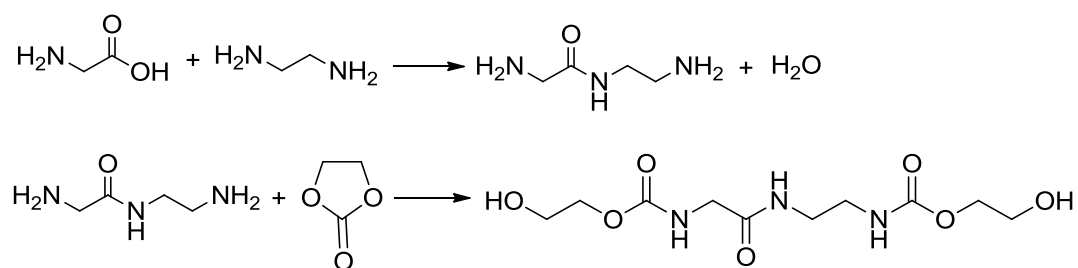


Figure 2.5: Synthesis of hydroxyl terminated (amide - urethane) oligomers from glycine

2.4.3 Synthesis of poly(amide-urethane-ester)s from glycine (Gly-OH-DMT[P])

The preparation of Gly-OH-DMT[P] consists of two steps : (a) the first step afforded the transesterification of Gly-OH with Dimethyl terephthalate (DMT). Gly-OH

(99.8 g, 0.67 molar eqv.), DMT (59.2 g 0.3 mol) added as a melt and titanium (IV) butoxide (2.9 g, 1.8 wt%) as catalyst were added to the reactor which was pre-heated to a temperature of 150°C. The ratio of OH/esters was kept at 1:0.9. The reaction was then continued for 5 hours at a temperature of 150 - 155 °C under nitrogen flow. After the first step, a vacuum of 50 – 10 mbar was applied gradually. The by-product of the transesterification reaction, methanol, was collected in the arm of the Dean-Stark condenser. Samples (SMS-OH-DMT) were taken for FTIR and hydroxyl value titrations.

(b) The second step was applied to continue the urethane-exchange reaction by removing ethylene glycol as a by-product to achieve a higher molecular weight. The temperature of the reactor was maintained at 200 - 210°C under a vacuum pressure of 250 pascals. The reaction was continued for a total time of 5 hours and the evolved ethylene glycol was collected in the Dean-Stark condenser. Samples (GLY-OH-DMT[P]) were collected at regular time intervals for analysis. Pure hydroxyl-terminated poly(amide-urethane-ester)s were obtained by dissolving the reaction mixture in DMSO, then precipitating it in de-ionized water, followed by washing twice and drying overnight.

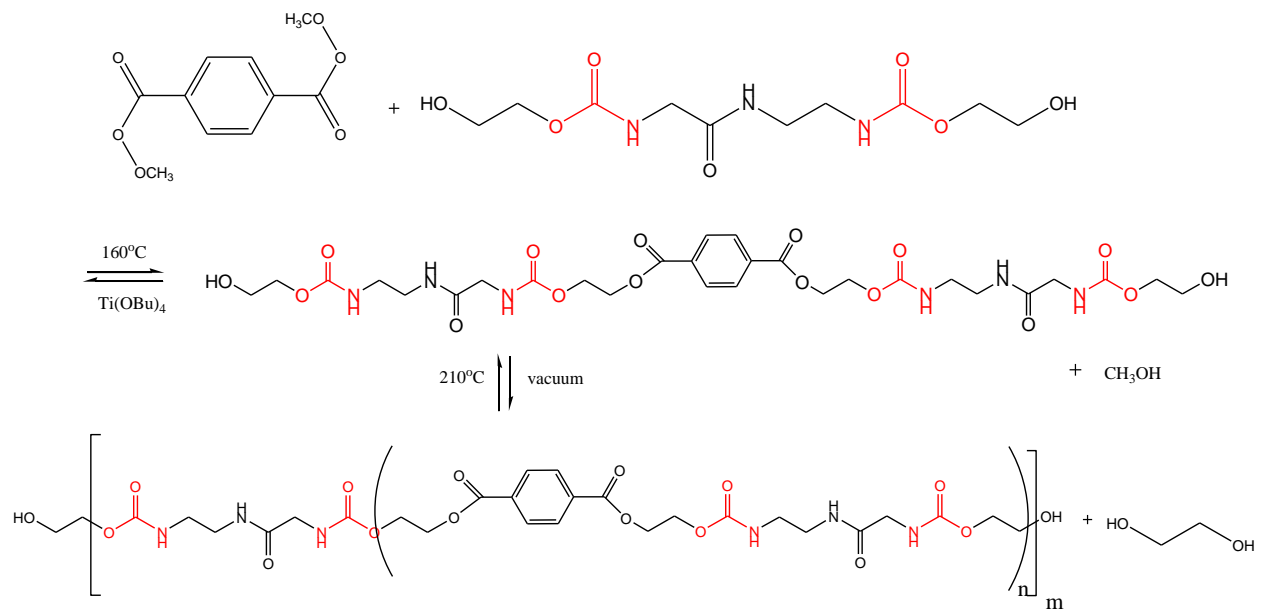


Figure 2.6: Synthesis of poly(amide-urethane-ester)s using dimethyl terephthalate

2.4.4 Acid hydrolysis of soy meal

Soy meal (1250 g) was added to a 12 L three necked round bottom flask fitted with a mechanical stirrer, condenser and then hydrolyzed using 5 L of 3 N HCl under continuous stirring at a temperature of 100°C for 45 hours. After the hydrolysis, the mixture was neutralized by adding NaOH solution (36%). The final pH of the mixture was 4.3. The insoluble part was then filtered and removed, which represented 25% of the initial weight on a dry basis. The neutralized soy hydrolyzate (SMS) was then distilled under vacuum at a temperature of 80°C to remove water (3.68 L) from the system.

2.4.5 Amination of soy hydrolyzate

The concentrated soy hydrolyzate (4.33 Kg) was then reacted with excess ED (1.62 Kg) and this condensation reaction was carried out under continuous stirring at a temperature of 110°C for 6 hours. After the completion of the reaction, the aminated hydrolyzate (SMS-ED) mixture was distilled under vacuum to remove excess ED and water. Samples were collected and analyzed by amine value, acid value titrations and FTIR.

2.4.6 Synthesis of hydroxyl-terminated urethanes from soymeal

The aminated hydrolyzate (SMS-ED) (2.53 Kg, 21.8 amine equivalents) was reacted with ethylene carbonate (1.92 Kg, 21.8 moles) under continuous stirring at a temperature of 80°C for 3 hours. After the completion of the reaction, the product (SMS-OH) was then analyzed by acid value, amine value, hydroxyl value titrations and FTIR.

2.4.7 Poly(amide-urethane-ester)s from soymeal (SMS-OH-DMT[P])

The preparation of SMS-OH-DMT[P] consists of two steps: (a) the first step afforded the transesterification of SMS-OH with Dimethyl terephthalate (DMT). SMS-OH

(450.36 g, 2.6 molar eqv.), DMT (185.4 g 1.9 mol) added as a melt and titanium (IV) butoxide (10.94 g, 1.7 wt%) as catalyst were added to the reactor which was pre-heated to a temperature of 150°C. The ratio of OH/esters was 1:0.7. The reaction was then continued for a total reaction time of 4 hours under nitrogen flow. After the first step, a vacuum of 50 – 10 mbar was applied gradually. The by-product of the transesterification reaction, methanol, was collected in the arm of the Dean-Stark condenser. Samples were taken for FTIR and hydroxyl value titrations.

(b) the second step was applied to continue the urethane-exchange reaction by removing ethylene glycol as a by-product to achieve a higher molecular weight. The temperature of the reactor was maintained at 200°C under a vacuum pressure of 230 pascals. The reaction was continued for a total time of 6 hours and the evolved ethylene glycol was collected in the Dean-Stark condenser. Samples were collected at regular time intervals for analysis. Purification procedures were similar to the poly(amide-urethane-ester)s obtained from glycine.

2.5 Results and discussion

2.5.1 Synthesis of hydroxyl-terminated amide urethane monomers

The synthesis of hydroxyl-terminated amide urethane monomers from amino acids was guided by two basic steps: protecting the carboxylic groups by reacting them with ethylene diamine to form an amide linkage and reacting the terminal amines with ethylene carbonate to yield hydroxyl terminated amide urethane monomers as shown in Figure 2.5. The protection of carboxylic groups in glycine to yield the desired amino-amide (Gly-ED) was confirmed by ATR-FTIR as shown in Figure 2.7.

Significant changes from glycine (A) to Gly-ED (B) spectra were the appearance of the new peak at 1651 cm^{-1} corresponding to the C=O deformation and a shift in the N-H stretch of the primary amine at 1500 cm^{-1} to 1535 cm^{-1} , which is attributed to the transformation of amine in amide. The results were further confirmed by amine and acid values as presented in Table 2.2. It should be noted that although the experimental amine and acid values of the model amino acid compound glycine were lower than the expected values, this is undoubtedly due to the zwitterion structure of glycine. The acid value (0 mgKOH/g) of Gly-ED testified that no free carboxylic groups were present in the product. A significant increase in the amine value (825.95 mgKOH/g) was observed after the reaction with ethylene diamine to convert the carboxylic acid groups to amides and produce the diamine derivative (Gly-ED). The ratio between the experimental and the calculated amine value indicated that the conversion of glycine to Gly-ED was 86.25%. Gly-ED was then reacted with ethylene carbonate to yield Gly-OH.

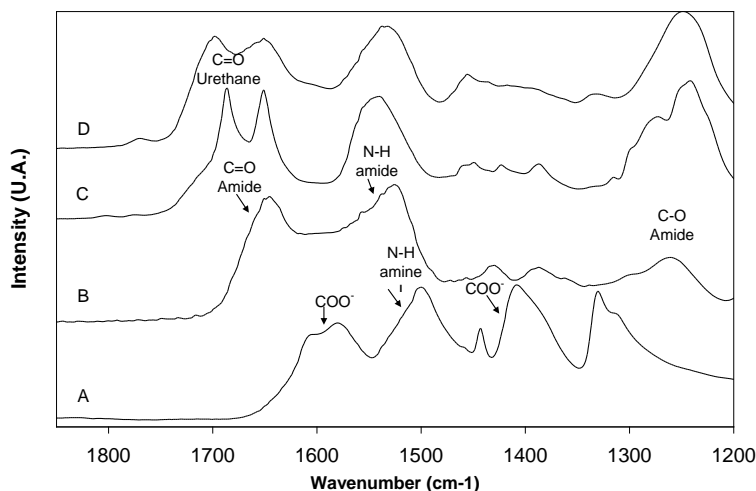


Figure 2.7: ATR-FTIR of (A) Gly, (B) Gly-ED, (C) Gly-OH and (D) the final polymer

Table 2.2: End group analysis of PU and its intermediates synthesized from glycine

	Amine value (mgKOH/g)		Acid value (mgKOH/g)		Hydroxyl value (mgKOH/g)	
	Calc.	Exp.	Calc.	Exp.	Calc.	Exp.
Glycine	747.30	60.85 ± 1.6	747.30	18.33 ± 0.4	-	-
Gly-ED	957.58	825.95 ± 2.8	0	0	-	-
Gly-OH	0	37.72 ± 2.2	0	0	383.71	377.55 ± 2.4
Gly-OH-DMT	0	-	0	-	-	164.66± 0.3
Gly-OH-DMT[P]	0	-	0	-	-	12.24± 2.6

The ATR-FTIR of this hydroxyl-terminated monomer is presented in Figure 2.7. The formation of urethane in this reaction was confirmed by the appearance of a peak corresponding to C=O stretching of urethane groups at 1697 cm^{-1} . ^1H NMR spectrum of Gly-OH is shown in Figure 2.8 which further confirms these results. The appearance of peaks at 4.21 ppm and 4.16 ppm are characteristic of the ethylene protons obtained from the ring opening reaction of ethylene carbonate with the amine groups. The peaks at 3.37 and 3.28 correspond to the protons near the nitrogen atoms. The yield of the reaction of ethylene carbonate with the GLY-ED was found to be 96% by dividing the area under the peak of the unreacted ethylene carbonate at 4.64 ppm and the summation of all peaks due to the reacted ethylene carbonate at 4.21 ppm, 4.16 ppm and 3.68 ppm respectively. The amine and hydroxyl values of Gly-OH are presented in Table 2.2. A comparison of the amine values of Gly-ED and Gly-OH, shows a decrease in the amine values from 825.95 mgKOH/g to 37.72 mgKOH/g indicating essentially complete reaction of GLY-ED with ethylene carbonate. The conversion of amine groups to urethane hydroxyl-terminated groups equals 95.4% which matches with the results (96%) obtained from the ^1H NMR. The experimental hydroxyl value obtained was 377.55 mgKOH/g, which was also very close to the expected value (387.71 mgKOH/g).

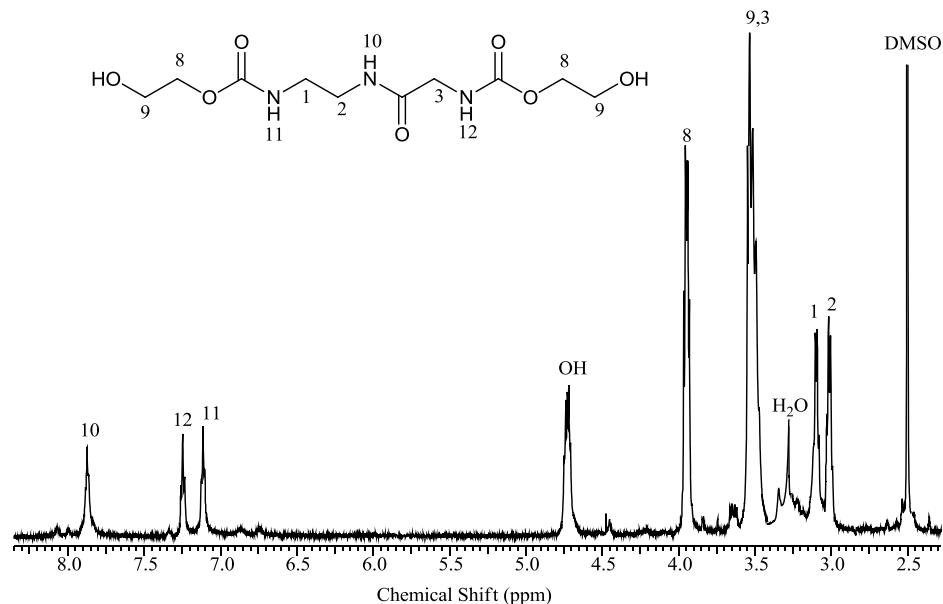


Figure 2.8: ¹H NMR of Gly-OH

The hydrolysis of soy meal to cleave the amide linkages in the proteins to individual amino acids was done using 3N HCl at a temperature of 100°C for 45 hours. The rate of hydrolysis is directly proportional to the temperature and the concentration of the acid in the system. The temperature of the reaction can be increased above 100°C by running the hydrolysis under pressure. However, it is well known that excessive temperature (as well as excessive concentrations of acid) leads to the degradation of amino acids. Therefore relatively mild conditions and long reaction times were used to ensure complete hydrolysis and minimum degradation of the resulting amino acids. The composition of the amino acids from the hydrolysis of the soy proteins is well known [59]. The soy protein hydrolyzate (SMS) as analyzed by FTIR in Figure 2.9 shows a peak at 1625 cm⁻¹ which is typical of the C=O stretch of carboxylic acids in the amino acid mixture. The amine and acid values of SMS as shown in Table 2.3 do not match with the calculated values, this is most likely due to the zwitterionic nature of the amino acids. The protection of carboxylic groups in the hydrolyzate by ethylene diamine to yield the

amino-amides (SMS-ED) was confirmed by FTIR in Figure 2.9. A significant change observed from SMS to SMS-ED spectrum was the shift in the C=O stretch from 1625 cm^{-1} to 1656 cm^{-1} . The new peak at 1583 cm^{-1} was typical of the N-H bend of amides.

The aminated hydrolyzate (SMS-ED) was further analyzed by acid and amine value titrations as shown in Table 2.3. A significant increase in the amine value (484.2 mgKOH/g) was observed, followed by a decrease in the acid value (14.1 mgKOH/g), indicating the amidation of the carboxylic groups by the addition of ethylene diamine. SMS-ED was then reacted with ethylene carbonate to yield SMS-OH. The ATR-FTIR of this hydroxyl-terminated urethane compound is shown in Figure 2.9. The formation of urethane in this reaction was confirmed by the appearance of a peak corresponding to the C=O stretch of the urethane groups at 1697 cm^{-1} . The decrease in the amine value (59.8 mgKOH/g) followed by hydroxyl value (324.18 mgKOH/g) signifies the conversion of amines to hydroxyl-terminated urethane monomers.

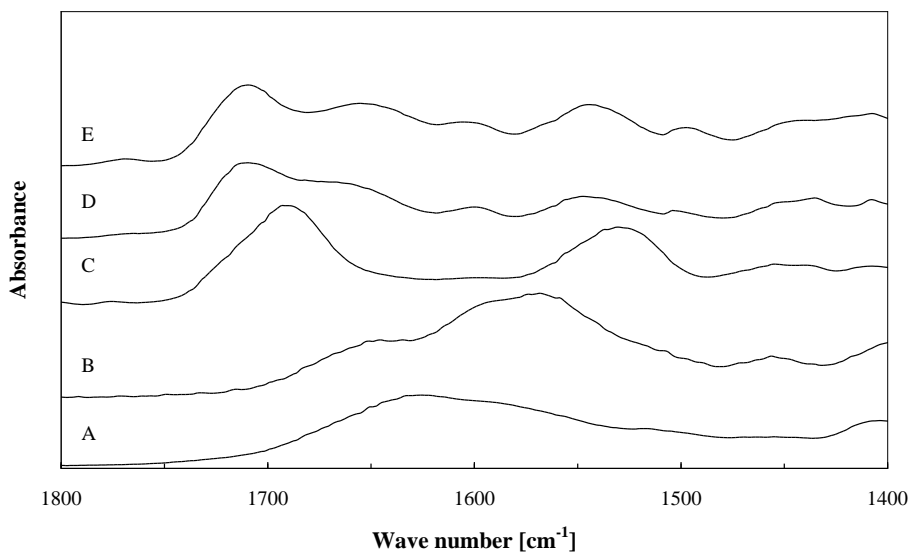


Figure 2.9: FTIR data of (A) SMS, (B) SMS-ED, (C) SMS-OH, (D) SMS-OH-DMT, (E) SMS-OH-DMT[P]

Table 2.3: End group analysis of PU and its intermediates synthesized from soy meal

	Amine value (mgKOH/g)		Acid value (mgKOH/g)		Hydroxyl value (mgKOH/g)	
	Calc.	Exp.	Cal.	Exp.	Calc.	Exp.
SMS	483.7	33.7± 0.8	549.4	64.9± 1.2	-	-
SMS-ED	726.7	484.2± 2.3	0	14.1± 3.1	-	-
SMS-OH	0	59.8± 3.1	0	15.8± 0.2	456.23	324.18± 2.1
SMS-OH-DMT	0	-	0	-	-	263.56± 3.6
SMS-OH-DMT[P]	0	-	0	-	-	39.4± 2.4

2.5.2 Synthesis of poly(amide-urethane-ester)s

The synthesis of Poly(amide-urethane-ester)s was accomplished by reacting the hydroxyl-terminated amide urethane monomers with dimethyl terephthalate using titanium (IV) butoxide as a catalyst in a two step reaction. In the first step, an excess of hydroxyl-terminated amide urethane monomers was reacted with dimethyl terephthalate to produce intermediate oligomers yielding methanol as the by-product. These intermediate oligomers were further transesterified in the second step under high temperature and vacuum conditions to obtain high molecular weight poly(amide-urethane-ester)s by removing ethylene glycol as a by-product (Figure 2.6). In the reaction using the model compound glycine, Gly-OH was reacted with DMT using titanium (IV) butoxide as catalyst to obtain intermediate oligomers (Gly-OH-DMT) in the first step. ATR-FTIR of Gly-OH-DMT is shown in Figure 2.7. A shift in the C=O stretch at 1697 cm^{-1} typical of urethanes to 1709 cm^{-1} typical of C=O stretch of esters was observed followed by a decrease in the intensity of the O-H stretch peak at 3300 cm^{-1} . Similarly, a decrease in the hydroxyl values (Table 2.2) of Gly-OH from 377.55 mgKOH/g to 164.66 mgKOH/g of Gly-OH-DMT was determined that indicates the conversion of OH groups to esters by a transesterification reaction between DMT and Gly-OH. The FTIR of the Gly-OH-DMT[P] was similar to the one of Gly-OH-DMT; however, a decrease in the intensity of the peaks at 1709 cm^{-1} and 3300 cm^{-1} was observed. The lower concentration of hydroxyl groups as a result of removal of ethylene glycol was further confirmed by the hydroxyl value (12.24 mgKOH/g) as listed in Table 2.2. The theoretical molecular weight based on the hydroxyl value was calculated to be around 9250 g/mol

with a degree of polymerization (DPn) equal to 13 (Table 2.4 and Figure 2.10). By applying the equation of Carother's, the conversion obtained was 92%.

Table 2.4: Mw of Gly-OH-DMT[P] as a function of OH values

DPn	Mw	OH values (mgKOH/g)
1	716.68	156.55
2	1371.29	81.82
3	2087.97	53.74
4	2804.65	40.00
5	3521.33	31.86
6	4238.01	26.47
7	4954.69	22.65
8	5671.37	19.78
9	6388.05	17.56
10	7104.73	15.79
11	7821.41	14.35
12	8538.09	13.14
13	9254.77	12.12
14	9971.45	11.25
15	10688.13	10.50

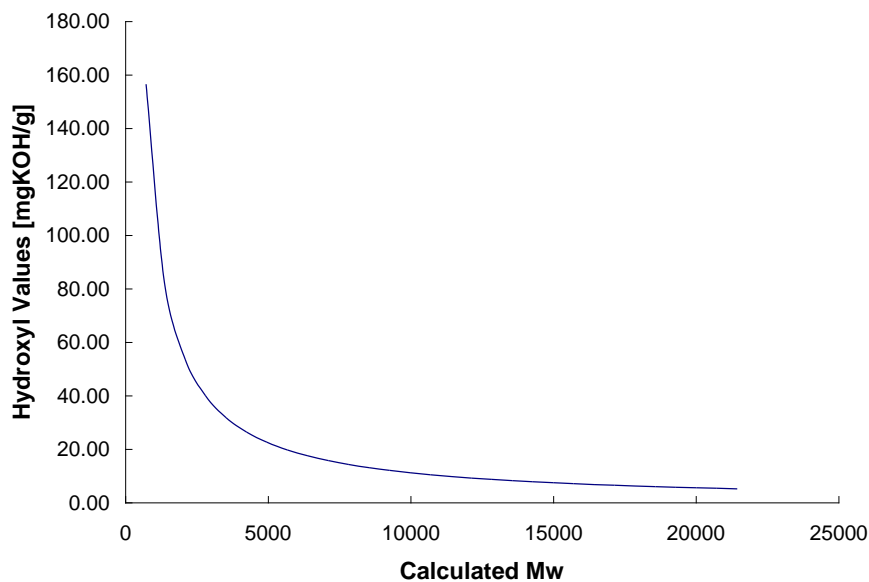


Figure 2.10: Mw of Gly-OH-DMT[P] as a function of OH values

The FTIR of SMS-OH-DMT is shown in Figure 2.9. Peak shifts similar to the one obtained in the case of Gly-OH-DMTP were observed, a shift in the C=O stretch at 1695 cm^{-1} to 1714 cm^{-1} . The hydroxyl value decreased from 324.18 mgKOH/g to 263.56

mgKOH/g (Table 2.3) indicating a decrease in the OH groups of SMS-OH upon the transesterification reaction with DMT. The FTIR spectrum of SMS-OH-DMT[P] was similar to the intermediate SMS-OH-DMT and no peak shifts were observed except for the decrease in the intensity of the peaks, similar to the results obtained from the model compound glycine. A decrease in the hydroxyl value as shown in Table 2.3 from 263.56 mgKOH/g to 39.4 mgKOH/g as a result of removal of ethylene glycol due to the urethane-exchange reaction, also indicating an increase in the molecular weight.

The thermal stability of the prepared poly(amide-urethane-ester)s was determined by TGA. From Figure 2.11, it is clear that both the poly(amide-urethane-ester)s were thermally stable up to 240 °C. $T_{d\ 5\%}$ and $T_{d\max}$ for SMS-OH-DMT[P] were 265.2 °C and 378.48 °C, respectively. Similarly $T_{d\ 5\%}$ and $T_{d\max}$ for Gly-OH-DMT[P] were 276.2 °C and 379.66 °C, respectively. The thermal stability of Gly-OH-DMT[P] was slightly higher than SMS-OH-DMT[P].

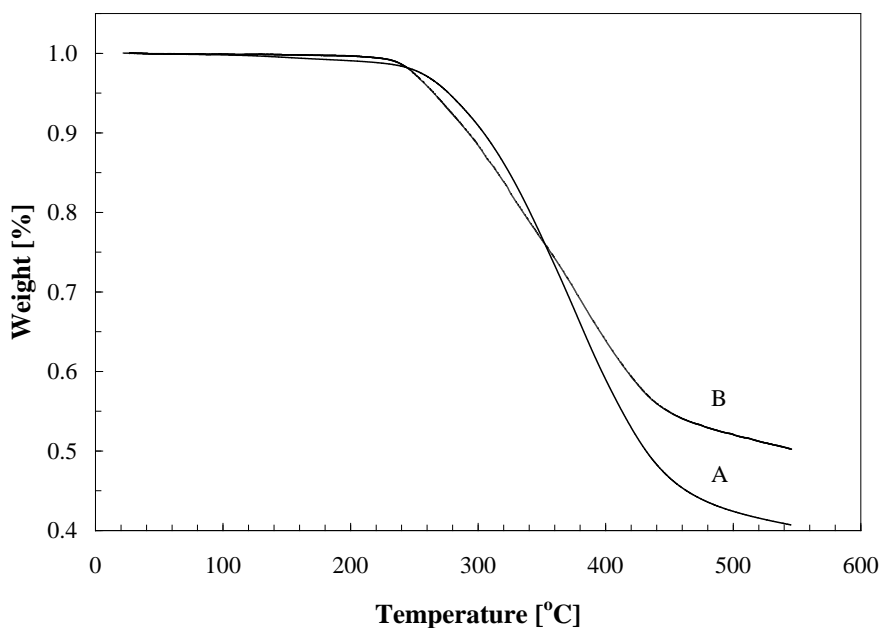


Figure 2.11: TGA of PU from (A) glycine and (B) soy meal

The glass transition temperatures T_g were measured by DSC (curves A and B in Figure 2.12). The T_g of Gly-OH-DMT[P] and SMS-OH-DMT[P] were 123.59 °C and 103.06 °C, respectively. No crystallization peak (or melting peak) was observed and only a glass transition was observed in both the polymers, thus indicating that they were totally amorphous.

The temperature dependency of the modulus of the polyurethane materials was studied by DMA. The storage modulus (G') and loss modulus (G'') curves for Gly-OH-DMT[P] and SMS-OH-DMT[P] are shown in Figure 2.13 and Figure 2.14, respectively. The temperature at which the maximum G'' is reached in the loss modulus curve indicates the glass transition (T_g) at which the polymer turns from a glassy material into a viscous material. The T_g of the Gly-OH-DMT[P] observed here was 124.64 °C, which agreed with the value detected by the DSC (123.59 °C). Similarly, the T_g of the SMS-OH-DMT[P] observed at the maximum loss modulus temperature of 101.67 °C, was very close to the value obtained from the DSC (103.06 °C).

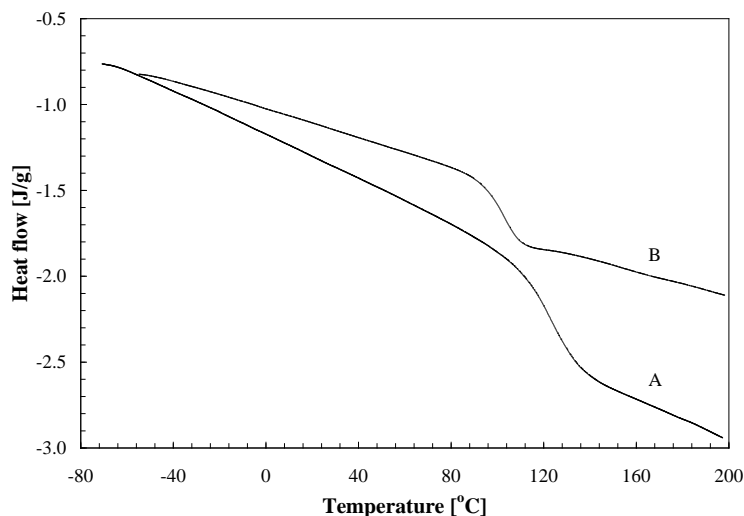


Figure 2.12: DSC of PU from (A) glycine and (B) soy meal

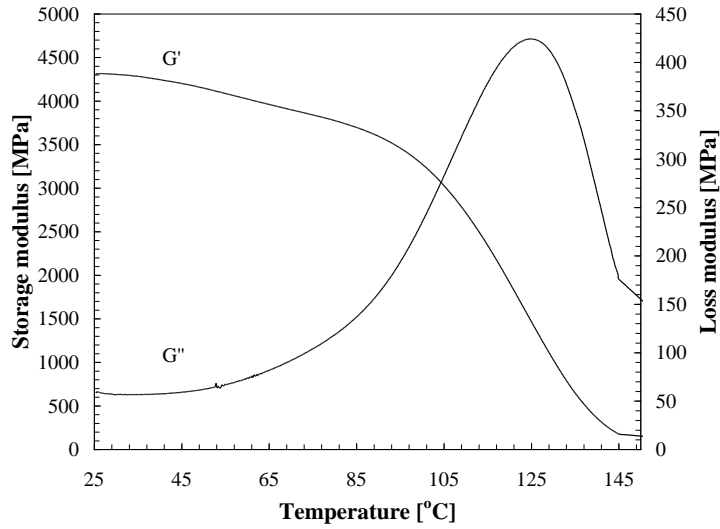


Figure 2.13: Storage (G') and loss modulus (G'') of PU from glycine as a function of temperature

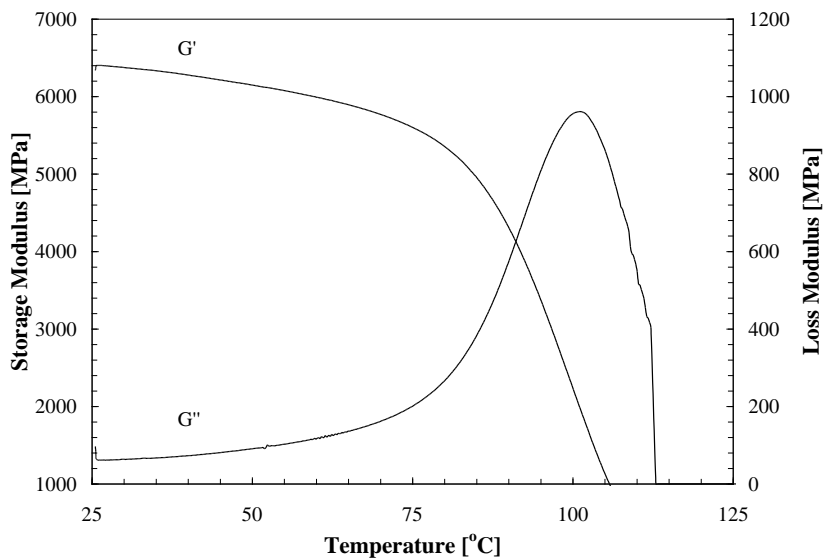


Figure 2.14: Storage (G') and loss modulus (G'') of PU from soy meal as a function of temperature

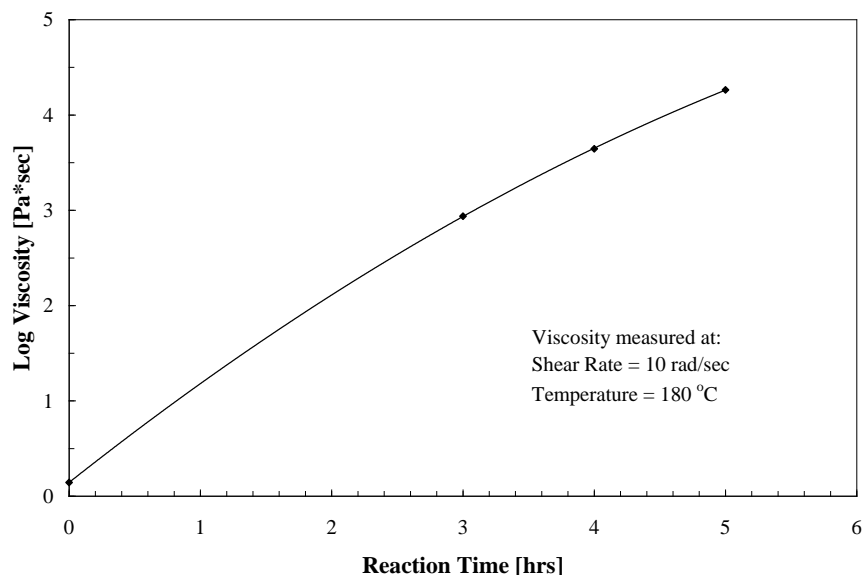


Figure 2.15: Viscosity of PU from glycine as a function of reaction time

Viscosity measurements as a function of shear rate at different temperatures were run on Gly-OH-DMT[P] and SMS-OH-DMT[P] samples that were collected at different time intervals during the course of the polymerization reaction. Figure 2.15 and Figure 2.16 show the viscosity of the PU from glycine and soy meal, respectively, plotted against different reaction times, at a shear rate of 10 rad/sec and at a temperature of 180 °C. An increase in viscosity was observed in both the cases with an increase in molecular weight as ethylene glycol was distilled out in the polycondensation reaction. The viscosity of the polymers from glycine and soy meal were examined using the Power Law (or Ostwald) Model:

$$\eta = K\gamma^{n-1}$$

where η is the viscosity, K is the consistency coefficient, n is the Power Law Index and γ is the shear rate. the viscosity at 180 °C under different shear rates is shown in Figure 2.17. It was observed that while both the polymers exhibited pseudoplasticity, the PU

from glycine had a higher viscosity than the soy meal-based polymer over the measured range of shear rates and temperature; it was also significantly more shear-thinning (lower Power Law Index).

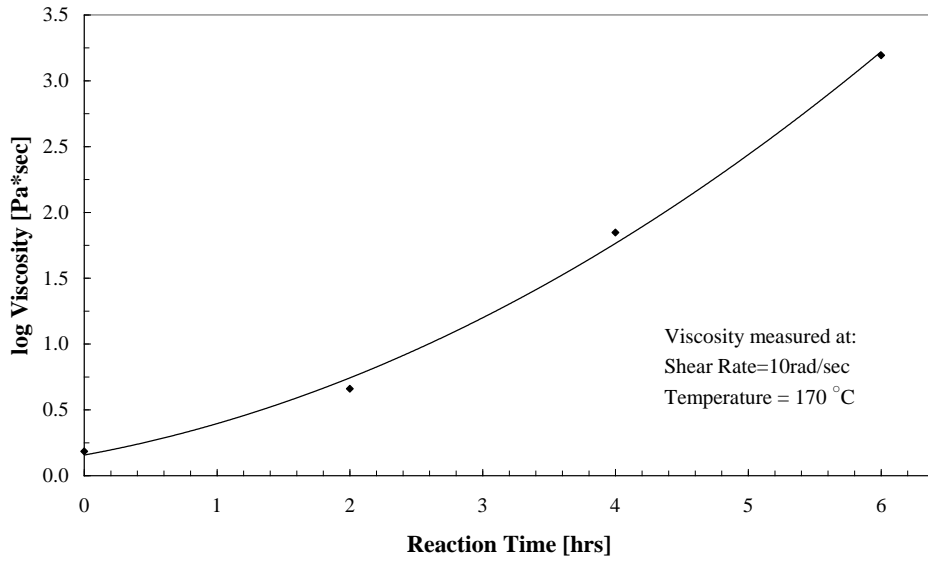


Figure 2.16: Viscosity of PU from soy meal as a function of reaction time

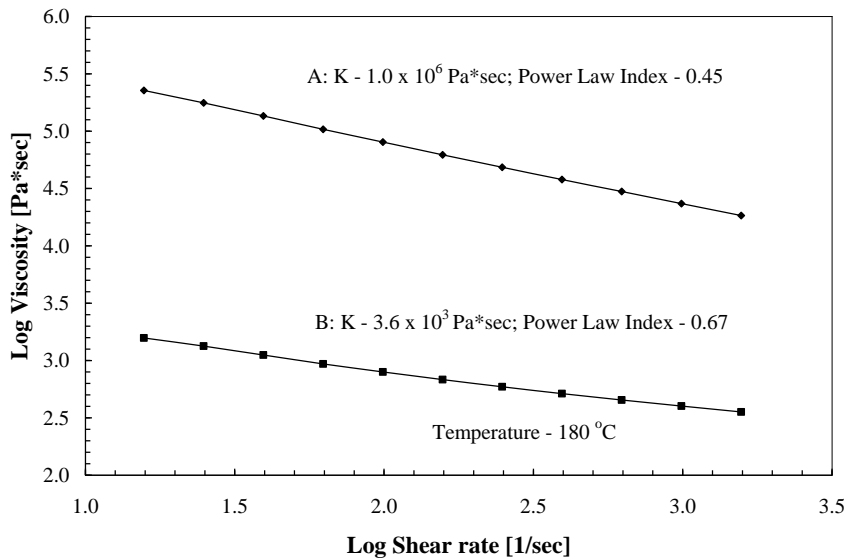


Figure 2.17: Log viscosity Vs log shear rate chart of PUs from glycine (A) and soy meal (B) at a temperature of 180 °C

The morphology of the polymers as observed by TEM is shown in Figure 2.18. As reported in the literature, polyurethanes typically show phase distinctions between soft and hard chain segments [60]. It is apparent from the images in Figure 2.18 that here too, a distinct phase separation is observed where the rigid phase is randomly separated and dispersed in the soft phase throughout the matrix. This phase separation morphology is expected since the methyl phthalates in the PU constitute the hard segments and the alkyl groups are associated with the soft segments. The rigid segments appear to have a typical spherical/elliptical nature randomly distributed throughout the soft phase matrix. The interactions of the rigid segments were localized and very few. This was further collaborated by the DSC data showing a broad glass transition temperature and the absence of a melting point, which indicate the absence of crystallinity and structural regularity in the polymer.

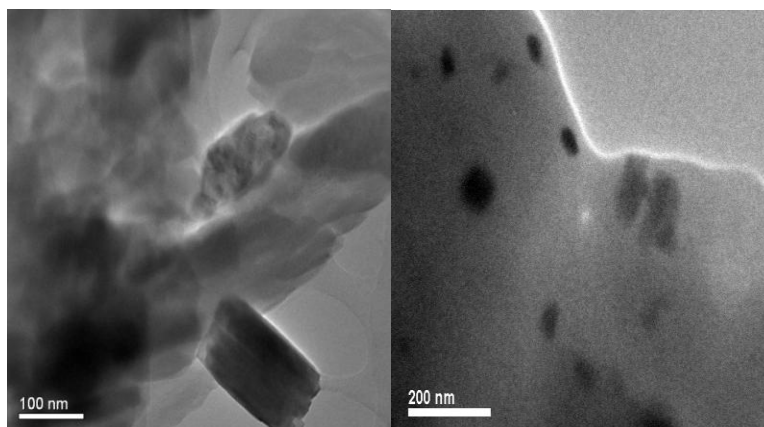


Figure 2.18: TEM images of PU synthesized from glycine (left) and soy meal (right) showing the phase separation between soft and hard segments

2.6 Conclusions

This chapter reports on the first synthesis of biobased poly(amide-urethane-ester)s from the renewable source soy meal through a non-isocyanate route. Glycine, an amino

acid found in soy meal, was used as a model compound for this study. The products and its intermediates analyzed by acid value, amine value, OH value titrations, FTIR, ¹H NMR at various stages confirm the synthesis. Similar procedures were followed for the synthesis of poly(amide-urethane-ester)s from soymeal. However it necessitated an additional acid hydrolysis step for the breakdown of soy proteins to amino acids. In both cases, the final poly(amide-urethane-ester)s were further analyzed for their thermal and rheological properties. The polymers were amorphous and thermally stable up to 270°C. The viscosity measurements made on the polymers at regular time intervals during the course of the polycondensation reaction with dimethyl terephthalate indicated an increase in viscosity with reaction time. However, the estimation of molecular weight based on the end group analysis using OH values indicated the formation of low molecular weight polymers. Of particular interest noted during the course of this study, was the synthesis of hydroxyl-terminated amide urethane monomers from soy meal. These monomers prepared by a “green” environmentally friendly synthetic approach could find potential applications as polyols and replace the petro-based polyols in many PU foam applications.

REFERENCES

REFERENCES

1. Szycher M (1999) Handbook of polyurethanes, CRC Press, Boca Raton, FL.
2. Wild DM, Redlich CA, Paltiel AD (2005) Surveillance for isocyanate asthma: a model based cost effectiveness analysis. *Occup Environ Med* 62:743-749.
3. Pauluhn J (2000) Acute inhalation toxicity of polymeric diphenyl-methane 4,4'-diisocyanate in rats: time course of changes in bronchoalveolar lavage. *Arch Toxicol* 74:257-269
4. Assumption HJ, Mathias LJ (2003) Photopolymerization of urethane dimethacrylates synthesized via a non-isocyanate route. *Polymer* 44:5131-5136
5. Clark AJ, Echenique J, Haddleton DM, Straw TA, Taylor PC (2001) A Nonisocyanate Route to Monodisperse Branched Polyurethanes. *J Org Chem* 66: 8687-8689
6. Clements JH (2003) Reactive Applications of Cyclic Alkylene Carbonates. *Ind Eng Chem Res* 42:663-674
7. Deepa P, Jayakannan M (2008) Solvent-free and non-isocyanate melt transurethane reaction for aliphatic polyurethanes and mechanistic aspects. *J Polym Sci Part A: Polym Chem* 46:2445-2458
8. Helou M, Carpentier JF, Guillaume SM (2011) Poly(carbonate-urethane) : an isocyanate - free procedure from α,ω -di(cyclic carbonate) telechelic poly(trimethylene carbonate)s. *Green Chem* 13:266-271
9. Javni I, Doo PH, Petrovic ZS (2008) Soy-based polyurethanes by nonisocyanate route. *J Appl Polym Sci* 108:3867-3875
10. Li Z, Zhao Y, Yan S, Wang X, Kang M, Wang J, Xiang H (2008) Catalytic Synthesis of Carbonated Soybean Oil. *Catal Lett* 123:246-251
11. Matsumura S, Soeda Y, Toshima K (2006) Perspectives for synthesis and production of polyurethanes and related polymers by enzymes directed toward green and sustainable chemistry. *Appl Microbiol Biotechnol* 70:12-20.
12. Ochiai B, Inoue S, Endo T (2005) One - pot non - isocyanate synthesis of polyurethanes from bisepoxide, carbon dioxide, and diamine. *J Polym Sci Part A: Polym Chem* 43:6613-6618

13. Oestreich S, Struck S (2002) Additives for UV - curable coatings and inks. *Macromol Symp* 187: 333-342
14. Rokicki G, Piotrowska A (2002) A new route to polyurethanes from ethylene carbonate, diamines and diols. *Polymer* 43:2927-2935
15. Tamami B, Sohn S, Wilkes GL (2004) Incorporation of carbon dioxide into soybean oil and subsequent preparation and studies of nonisocyanate polyurethane networks. *J Appl Polym Sci* 92:883-891
16. Yokoe M, Keigo AOI, Okada M (2003) Biodegradable polymers based on renewable resources. VII. Novel random and alternating copolycarbonates from 1,4:3,6-dianhydrohexitols and aliphatic diols. *J Polym.Sci Part A: Polym.Chem* 41:2312-2321
17. Kenar JA (2004) Current perspectives on oleochemical carbonates. *Inform* 15: 580-582
18. Narayan R (2000) Reactive Extrusion Process Produces Biodegradable Films & Injection Molded Products Based on Soy Protein-Polyester. *MRS (Materials Research Society) Bulletin*, Vol. 28:10
19. Narayan R (2006) Rationale, Drivers, Standards, and Technology for Biobased Materials in Renewable Resources and Renewable Energy, CRC Press, Ed Mauro Graziani & Paolo Fornasiero.
20. Shogren R L, Petrovic Z S, Liu Z, Erhan S Z (2004) Biodegradation Behavior of Some Vegetable Oil-based Polymers. *J Polym Environ* 12:173-178
21. Zlatanic A, Lava C, Zhang W, Petrovic ZS (2004) Effect of Structure on Properties of Polyols and Polyurethanes Based on Different Vegetable Oils. *J Polym Sci: Part B: Polym Physics* 42:809-819
22. Tian H, Wang Y, Zhang L, Quan C, Zhang X (2010) Improved flexibility and water resistance of soy protein thermoplastics containing waterborne polyurethane. *Ind Crop Prod* 32(1)13-20
23. Kumar R, Choudhary V, Mishra S, Varma IK, Mattiason B (2002) Adhesives and plastics based on soy protein products. *Ind Crop Prod* 16:155-172
24. Fountoulakis M, Lahm HW (1998) Hydrolysis and amino acid composition analysis of proteins. *J Chromatogr* 826:109-134
25. Zumwalt RW, Absheer JS, Kaiser FE, Gehrke CW (1987) Acid hydrolysis of proteins for chromatographic analysis of amino acids. *J Assoc Off Anal Chem* 70(1):147-151

26. Rowan AM, Moughan PJ, Wilson MN (1992) Effect of hydrolysis time on the determination of the amino acid composition of diet, ileal digesta , and feces samples and on the determination of dietary amino acid digestability coefficients. *J Agric Food Chem* 40(6):981-985
27. Emmert JL, Baker DH (1995) Protein quality assessment of soy products. *Nutr Res* 15:1647-1656
28. Albin DM, Wubben JE, Gabert VM (2000) The influence of hydrochloric acid concentration and measurement methods on the determination of amino acid levels in soya bean products. *Anim Feed Sci Tech* 87:173-186
29. Soyatech (2014) <http://www.soyatech.com/info.php?id=175>
30. WISHH (2014) <http://www.wishh.org/aboutsoy/composition.html>
31. USB (2014) <http://soynewuses.org>
32. Weiss M, Manneberg M, Juranville JF, Lahm HW, Fountoulakis M (1998) Effect of the hydrolysis method on the determination of the amino acid composition of proteins. *J Chromatogr A* 795:263-275
33. Gehrke CW, Wall Sr LL, Absheer J, Kaiser FE, Zumwalt RW (1985) Sample preparation for chromatography of amino acids: acid hydrolysis of proteins. *J Assoc Off Anal Chem* 68:811-821
34. Albin DM, Wubben JE, Gabert VM (2000) Effect of Hydrolysis Time on the Determination of Amino acids in Samples of Soybean Products with Ion-Exchange Chromatography or Precolumn Derivatization with Phenyl Isothiocyanate. *J Agric Food Chem* 48(5):1684-1691
35. Edwards HM, Douglas MW, Parsons CM, Baker DH (2000) Protein and Energy Evaluation of Soybean Meals Processed from Genetically Modified High-Protein Soybeans. *Poult Sci* 79:525-527
36. Albin DM, Wubben JE, Gabert VM (2000) The influence of hydrochloric acid concentration and measurement method on the determination of amino acid levels in soya bean products. *Anim Feed Sci Tech* 87:173-186
37. Campbell MF, Kraut CW, Yackel WC, Yang HS (1985) "Soy Protein Concentrates" in "New Protein Foods", A.M. Altschul and H.L. Wilke, Editors. Vol. 5, p. 301. Academic Press, Inc. Orlando, Florida.
38. Weiberth FJ (1999) "One-pot" preparation of N-(Carbonylamino)amino acids and half -acid/half-ester yrea dipeptides directly from α -amino acids. *Tetrahedron Letters* 40(15):2895-2898

39. Knolker HJ, Braxmeier T (1997) Isocyanates, Part 4. Convenient Phosgene Free-Method for the Synthesis and Derivatization of Enantiopure α -Isocyanato Carboxylic Acid Esters. *Synlett* 8:925-928
40. Shan S. Wong (1991) *Chemistry of Protein Conjugation and Cross-linking*. CRC Press.
41. Nakajima N, Ikada Y (1995) Mechanism of Amide Formation by Carbodiimide for Bioconjugation in Aqueous Media. *Bioconjugate Chem* 6:123-130
42. Green TW, Wuts PGM (1999) *Protective Groups in Organic Synthesis*, 2nd Ed.; Wiley: New York, 503–550.
43. Carpino LA (1987) The 9-fluorenylmethyloxycarbonyl family of base-sensitive amino-protecting groups. *Acc Chem Res* 20(11):401-407
44. Xiuo XY, Ngu K, Choa C, Patel DV (1997) Selective Solid Phase Synthesis of Ureas and Hydantoins from Common Phenyl Carbamate Intermediates. *J Org Chem* 62:6968-6973
45. Yadav JS, Reddy GS, Reddy MM, Meshram HM (1998) Zinc promoted simple and convenient synthesis of carbamates : An easy access for amino group protection. *Tetrahedron Lett* 39: 3259-3262
46. Salvatore RN, Shin S, Nagle AS, Jung KW (2001) Efficient Carbamate Synthesis via a Three - Component Coupling of an Amine, CO₂, and Alkyl Halides in the Presence of Cs₂CO₃ and Tetrabutylammonium Iodide. *J Org Chem* 66:1035-1037
47. Porta F, Cenini S, Pizzotti M (1985) Reaction of amines and related species with transition metal peroxo complexes. *J Organomet Chem* 296:291-300
48. Pandey RK, Dagade SP, Dongare MK, Kumar P (2003) Synthesis of carbamates using yttria-zirconia-based Lewis acid catalyst. *Synthetic Communications* 33(23):4019–4027
49. Greene TW, Wuts PGM (1999) *Protective Groups in Organic Synthesis*. Third Edition. by T.W. Greene, P.G.M. Wuts. John Wiley & Sons, Inc.
50. Ubaghs L (2005) Isocyanate-free Synthesis of (Functional) Polyureas, Polyurethanes, and Urethane-containing Copolymers”, Rheinisch-Westfälische Technische Hochschule Aachen, Fakultät für Mathematik, Informatik und Naturwissenschaften.
51. Rokicki G, Piotrowska A (2002) A new route to polyurethanes from ethylene carbonate, diamines, and diols. *Polym J* 43:2927-2935

52. Rockicki G, Wojciechowski C (1990) Epoxy Resin Modified by Aliphatic Cyclic Carbonates. *J Appl Polym Sci* 41:627
53. Kihara N, Endo T (1993) Synthesis and Properties of Poly(hydroxyurethane)s. *J Polym Sci Part A: Polym Chem* 31:2765-2773
54. Tomita H, Sanda F, Endo T (2001) Structural Analysis of Polyhydroxyurethane Obtained by Polyaddition of Bifunctional Five-Membered Cyclic Carbonate and Diamine Based on The Model Reaction. *J Polym Sci Part A: Polym Chem* 39: 851-859
55. Clements JH (2003) Reactive Applications of Cyclic Alkylene Carbonates. *Ind Eng Chem Res* 42:663-674
56. ASTM Standard D1980-87 (2003) Standard Test Method for Acid Value of Fatty Acids and Polymerized Fatty Acids. ASTM International, West Conshohocken, PA.
57. ASTM Standard D2073-92 (2003) Standard Test Methods for Total, Primary, Secondary, and Tertiary Amine Values of Fatty Amines, Amidoamines, and Diamines by Referee Potentiometric Method. ASTM International, West Conshohocken, PA.
58. ASTM Standard D1957-86 (2003) Standard Test Method for Hydroxyl Value of Fatty Oils and Acids. ASTM International, West Conshohocken, PA.
59. Grieshop CM, Kadzere CT, Clapper GM, Flickinger EG, Bauer LL, Frazier RL, Fahey GC (2003) Chemical and Nutritional Characteristics of United States Soybeans and Soybean Meals. *J Agric Food Chem* 51:7684-7691
60. Elisabetta P, Silvia V, Paola S, Lucia C (2011) The nanostructured morphology of linear polyurethanes observed by transmission electron microscopy. *Micron* 42(1):3-7

Chapter 3 Rigid polyurethane foams based on soy meal polyols

This chapter deals with the preparation of urethanes-based polyols from soy meal that are suitable for polymerization into rigid foams. In this process, soy meal is hydrolyzed to a mixture of amino-acids, which are then condensed with ethylene diamine to produce amine terminated monomers. In a second step, these monomers are reacted with ethylene carbonate to yield hydroxyl terminated urethane oligomers. The carbohydrates that are also present in the meal are propoxylated and converted to active polyols. The final polyol mixture is characterized by low viscosity and high hydroxyl functionality. These new hydroxyl terminated urethanes were then used to produce rigid foams by a conventional process.

The preparation process and characterization of the soy meal-based polyols will be discussed as well as key properties of the rigid foams (e.g. density, compressive strength, compressive strain at yield, friability, water absorption, burning rate, K factor and dimensional stability with aging). It was observed that these polyols are much more reactive than conventional polyols, eliminating the need to add a polymerization catalyst in the foaming process. Furthermore, these soy meal-based polyols are compatible with many conventional polyols, allowing the formulator to adjust the properties of the foams as needed. Thus, polyurethane foams prepared with 25% and 50% soy meal polyols exhibited comparable properties to foams prepared from a conventional polyol. These new biobased polyols with self-catalytic properties are best suited for rigid spray foam formulations that require fast cure and high crosslink density.

3.1 Introduction

The use of biomass as raw materials for production of fuels and chemicals to displace fossil resources has been the focus of many research activities in recent years. These activities are motivated by the possibility of positive contributions to a sustainable resource supply, enhanced national security, and macroeconomic benefits for local communities and the society at large. Much of this activity was directed toward fuel and energy production (e.g. fermentation of biomass to ethanol and transesterification of triglyceride oils to biodiesel). Only limited effort has been directed toward using the protein biomass that is left behind after extracting the oil to produce value added industrial products. Many such products are derived from polyurethanes and include foams, coatings, adhesives, sealants and elastomers (CASE). However, only a few of these synthetic polyurethanes contain biobased components and these are generally prepared by condensation of petroleum-based isocyanates with vegetable oil-based polyols. In comparison, only little attention has been directed toward utilization of protein biomass for value-added polymeric materials. The amino acids in the protein are rich in amine functional groups that can easily be converted to urethanes.

It is well known that soybean contains much more protein than oil. Although the exact composition of the bean depends on many variables including trait, climate, soil, geographical location, maturity, the extraction process, etc. typically the protein content is almost twice the content of the oil (about 38% compared with only 18% oil). Furthermore, the cost of the protein meal is about half the cost of the oil. Thus, the use of the meal as a raw material is attractive considering the economics and its availability.

In the US, soybeans are readily available and are grown in large quantities. After extracting the oil, most of the soy meal is processed into animal feed, primarily for poultry, swine, cattle, and aquaculture. A very small portion is refined to soy flour, soy concentrates, and soy isolates for human consumption and only 0.5% is used for industrial applications. Currently, the small amounts of meal used for industrial applications include its use as adhesives for plywood and particle board with other minor applications such as additives in textured paints, insecticides, dry-wall tape compounds, linoleum backing, paper coatings, fire-fighting foams, fire-resistant coatings, asphalt emulsions, cosmetics and printing inks.

Our objectives were to develop a process for utilizing this relatively inexpensive biomass and convert the amine functional groups to hydroxyl terminated urethanes suitable for use as polyols for rigid polyurethane foams. Unlike previous work, our process is relatively simple; it utilizes non-toxic reactants and intermediates and does not require expensive or specialized equipment.

3.2 Literature review

Rigid polyurethane foams have good insulation properties, adhesion, high strength-to-weight ratio, durability and have been used for many applications in the construction and automotive industries. Polyurethane spray foams are also used widely in the packaging industry for shipping valuable fragile items. They can be formed into very complex shapes and are easy to process [1]. Rigid foams are generally synthesized by the reaction of diisocyanates with polyols having hydroxyl value greater than 300 mgKOH/g. Most of these polyols are derived from petro-based feedstocks. However due to fluctuations in the oil price as well as an increasing trend towards utilizing

environmentally friendly feedstocks, there are efforts to replace these petro-based polyols with renewable biobased resources such as vegetable oils. Vegetable oils like Castor oil, soybean oil, canola oil, palm oil were converted into polyols and further used for synthesizing polyurethane foams [3-10].

Castor oil naturally contains hydroxyl groups that are evenly distributed throughout the triglyceride molecule at approximately 2.7 per triglyceride. Therefore, castor oil was widely used in the production of polyurethanes even before technologies were developed for using other vegetable oils. However, these polyols are secondary hydroxyls with significantly lower reactivity than primary polyols. Castor oil has been further transesterified with an excess of various polyols (like glycerol, pentaerythritol, sorbitol) or converted to amides using diethanolamides to increase the functionality and hydroxyl values, making them suitable for synthesizing rigid polyurethane foams [11, 12]. For example, M. A. Mosiewicki et al. synthesized a low viscosity, highly hydrophilic bio-based polyol from castor oil by alcoholysis using triethanolamine and lithium hydroxide as catalyst. The hydroxyl values of the castor oil derived polyols increased significantly from 169.3 mg KOH/g to 449 mg KOH/g, 2.6 times the original value for the unmodified oil. The resulting polyol was then used in rigid foam formulations using 4,4'-diphenylmethane diisocyanate at an isocyanate index ratio of 1.15 and 1.25. The replacement of the commercial polyol by the castor oil derived polyol helped improve the fire behaviour of the filled foams [13]. Furthermore, G.T Cardoso et al. prepared rigid PU foams using castor oil and characterized the thermogravimetric properties of the foams. They found that the decomposition of the foams began at approximately 170°C,

indicating that these foams had a relatively high resistance to thermal degradation, making them suitable for insulation applications [14].

Vegetable oils are triglycerides, which are esters formed from glycerol and three fatty acids (Figure 3.1) The structures of the fatty acids are given in Table 4.1. Palmitic (C16:0) and stearic acid (C18:0) are the two saturated fatty acids, while oleic (C18:1), linoleic (C18:2), linolenic (C18:3) and ricinoleic acids (C18:1) are the unsaturated fatty acids. The first number is the number of the carbon atoms in the fatty acid and the second number is the number of double bonds. The unsaturated fatty acids have cis-double bonds in their structures. All the most common vegetable oils (Table 3.1) contain significant amounts of palmitic, stearic, oleic, linoleic and linolenic acids, while ricinoleic acid is a major component present in castor oil. Unlike castor oil, nearly all the other vegetable oils do not have the natural hydroxyl groups required for synthesizing polyurethanes. The carbon-carbon double bonds and the ester functionality present in triglycerides can be utilized for further modification to obtain hydroxyl functional groups.

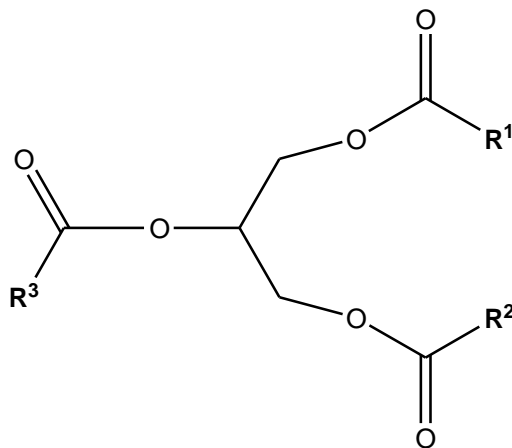
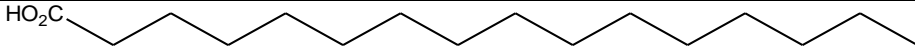
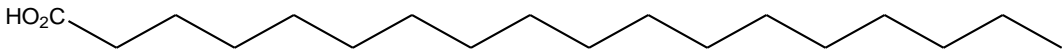
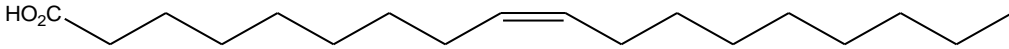
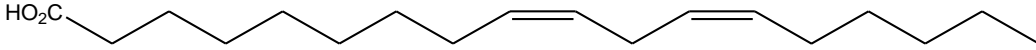
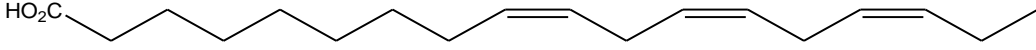
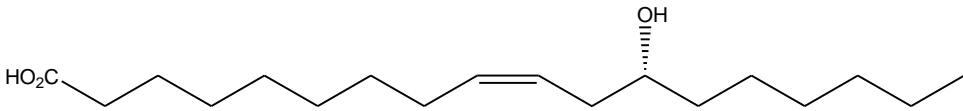


Figure 3.1 Triglyceride structure, where R^1 , R^2 , R^3 are fatty acids

Table 3.1: The most common fatty acids found in vegetable oils

Fatty Acid	Structure
Palmitic (C16:0)	
Stearic (C18:0)	
Oleic (C18:1)	
Linoleic (C18:2)	
Linolenic (C18:3)	
Ricinoleic (C18:1 OH)	

3.2.1 Synthetic routes to vegetable oil-based polyols

Various synthetic routes to convert vegetable oils to polyols are described in the literature [6, 15]. Epoxidation of vegetable oils followed by ring opening of the epoxide rings to produce vegetable oil-based polyols is currently the most common commercial process. This route essentially consists of two steps, the first being the epoxidation of the double bonds present in the unsaturated fatty acids. The second step consists of a nucleophilic ring opening of epoxide groups using proton donors such as alcohols, water, acids or hydrogenation. The epoxidation of vegetable oils by generating a peracid in situ from hydrogen peroxide and acetic or formic acid is the mostly used commercial process and results in sufficient yields of epoxidised oil [16]. Various chemo-enzymatic epoxidation of vegetable oils are also reported in the literature [17-19]. The reaction scheme is shown in Figure 3.2, where R_2 and R_3 represent the unsaturated fatty acid residues.

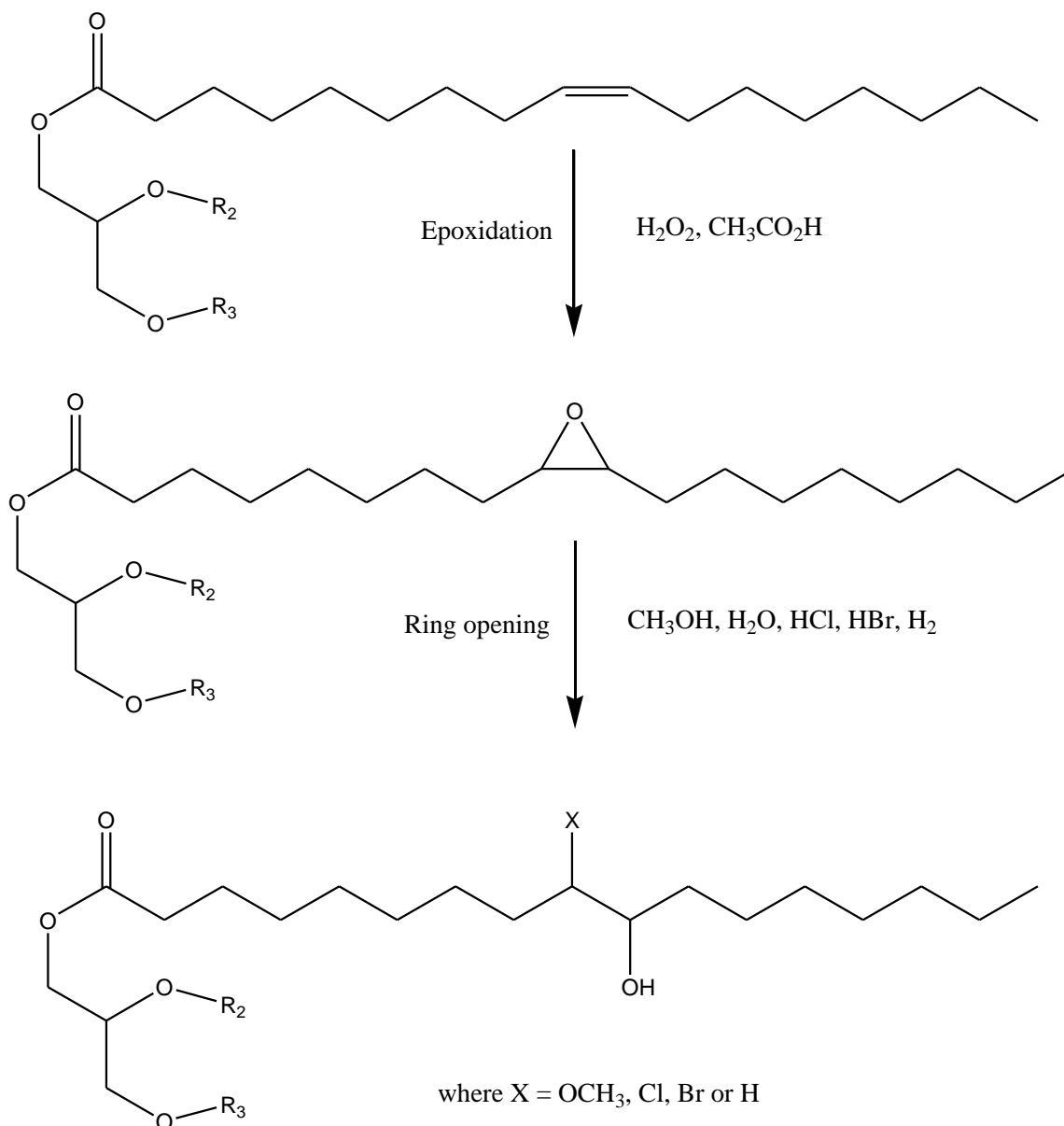


Figure 3.2: Polyol synthesis from epoxidized vegetable oils

Various mono-alcohols like methanol, diols like ethylene glycol and propylene glycol were used as the proton donors for the ring opening of the epoxides [20-25]. The use of diols results in obtaining two hydroxyl groups per epoxy group and therefore polyols with very high functionality are obtained. Moreover the use of diols like ethylene glycol results in primary hydroxyl groups which are more reactive than secondary hydroxyl

groups in polyurethane production. Apart from alcohols, various inorganic acids like hydrochloric acid, hydrobromic acid and organic acids like lactic acid have been used for the ring opening of epoxide groups [26, 27]. Furthermore, hydrogenation of the epoxidized oils with H₂ and Rany nickel as a catalyst were also reported. One of the significant drawbacks associated with these methods of obtaining polyols from epoxidized vegetable oils is the fact that the resultant polyols are a viscous grease and still have higher viscosity than the petroleum-based polyols [28, 29].

Ozonolysis is another method used to produce primary hydroxyl groups from vegetable oils [30-32]. In this method, the carbon-carbon double bonds present in the unsaturated fatty acid chains are cleaved to produce short-chain polyols. The ozonolysis of vegetable oils is shown in Figure 3.3. The application of ozonolysis to unsaturated vegetable oils results in a terminal aldehyde which is further reduced into primary alcohols, having at most three hydroxyl functional groups per molecule.

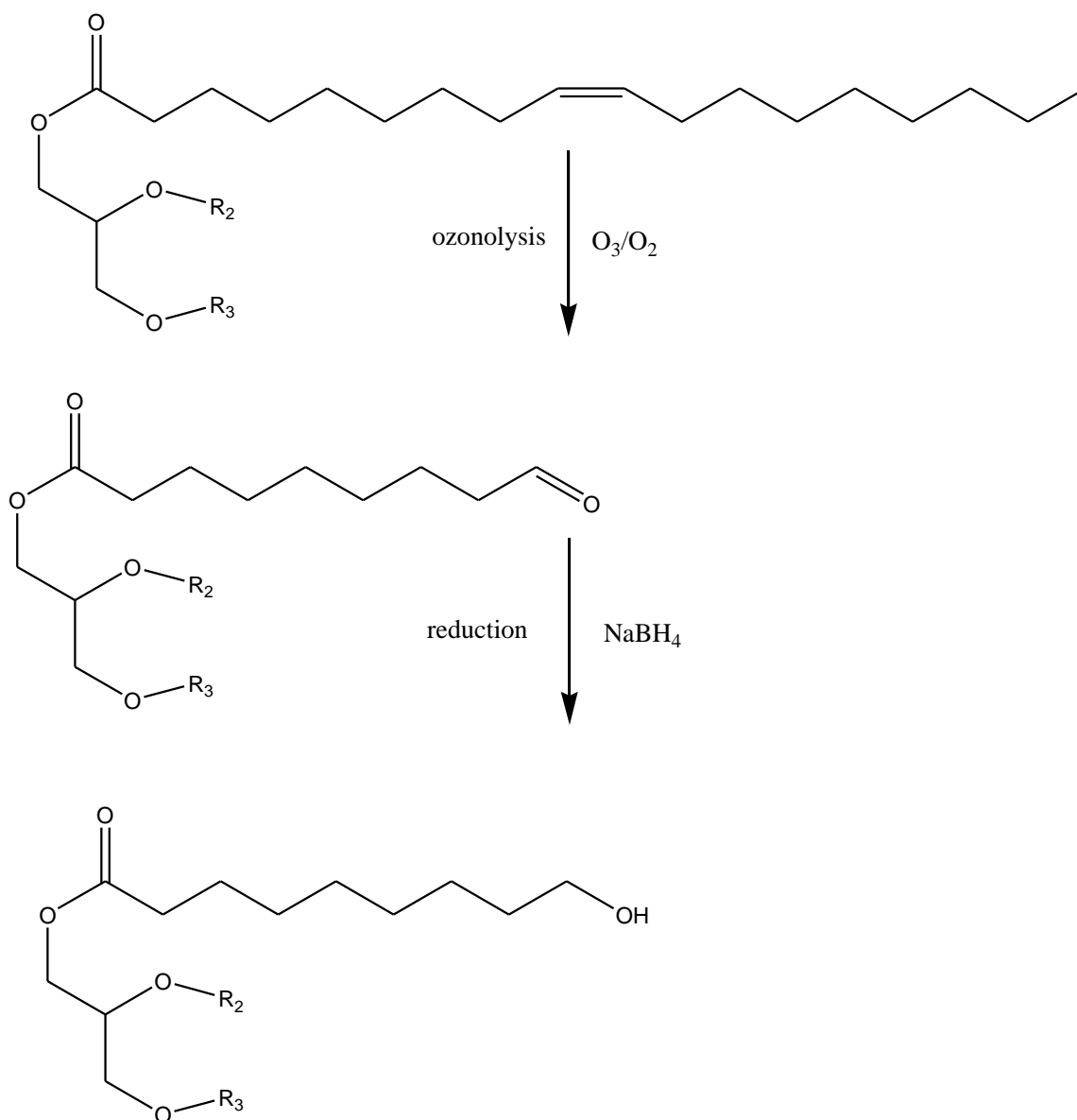


Figure 3.3: Ozonolysis route to synthesis of polyols from vegetable oil

Hydroformylation [33, 34] is another route to synthesize polyols from vegetable oils and involves the addition of hydroxymethyl groups to the carbon-carbon double bonds in the unsaturated fatty acid chains in a two step process as shown in Figure 3.4. In the first step, vegetable oils are treated with a mixture of CO and H₂ gas in the presence of catalysts to yield aldehydes, which are further reduced with H₂ in the second step to yield hydroxyl groups. This method yields vegetable oil-based polyols with primary

hydroxyl groups which are more reactive towards isocyanate in the polyurethane production.

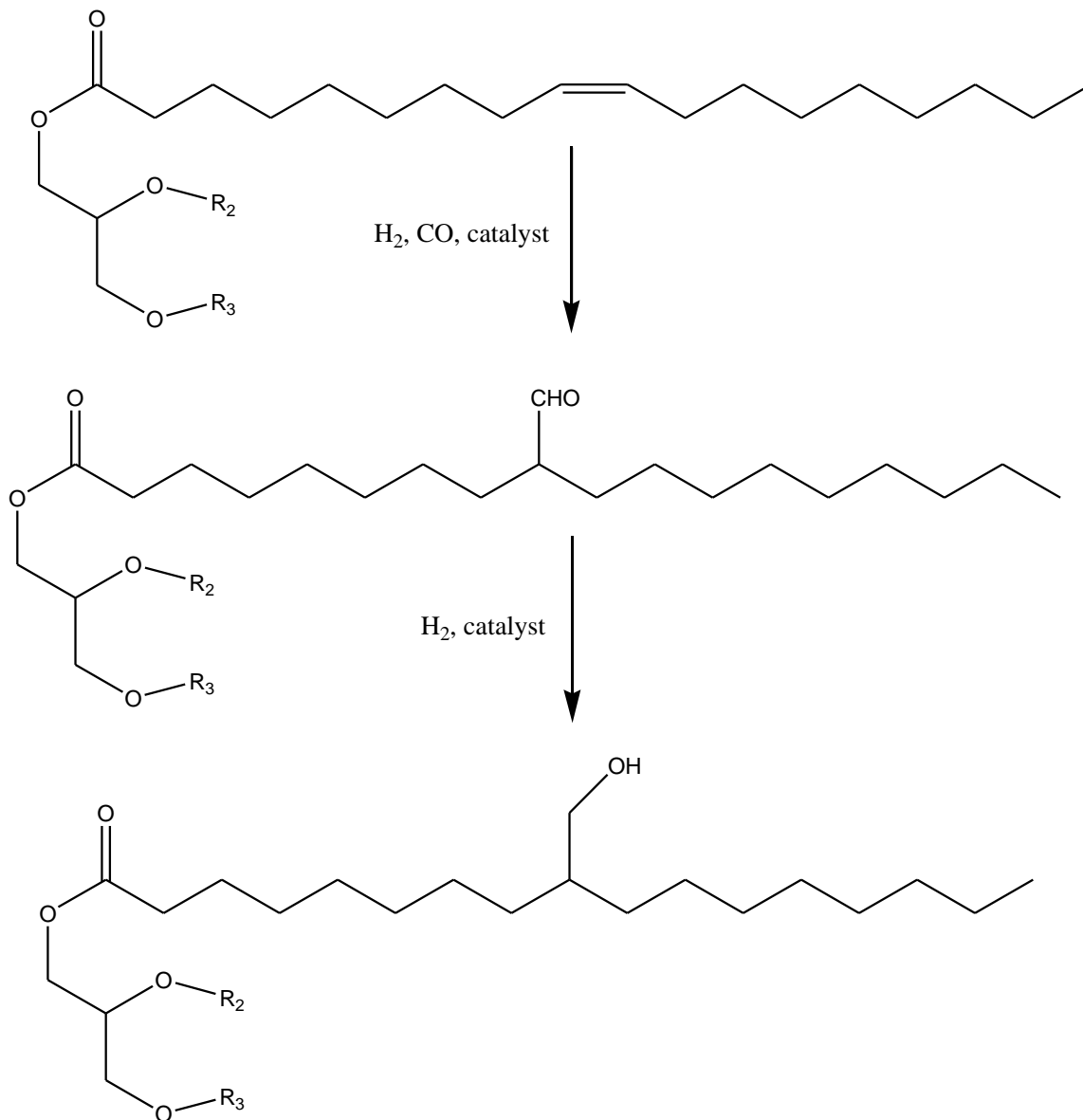


Figure 3.4: Synthesis of polyols from vegetable oils by hydroformylation

Transesterification of vegetable oils with various polyols is another route to synthesize polyols [35, 36]. Glycerol, sorbitol and trimethylolpropane are some of the

multifunctional alcohols used for the transesterification reactions. Similarly the amidation of vegetable oils with diethanolamine is also reported in the literature [37, 38].

3.2.2 Rigid polyurethane foams from vegetable oil-based polyols

Polyurethane rigid foams were prepared from hydroxymethylated castor oil, safflower oil, and polyol esters of castor oil, as early as 1974. The foams were observed to have satisfactory compressive strength and resistance to shrinkage on humid aging. Furthermore, rapeseed oil, and palm oil-based polyols were also used to make rigid PU foams [39, 40].

Guo et al. synthesized both HCFC and pentane-blown rigid PU foams with polyols derived from soybean oil. The soy polyols were prepared by the oxirane ring-opening reaction of epoxidized soybean oil with methanol to produce polyol with secondary OH groups [41]. The foam properties were studied by altering the types and amounts of catalyst, surfactant, water, crosslinker, blowing agent and isocyanate. The mechanical and thermal insulating properties of these foams were observed to be inferior to foams made from petro-based polyols. Further investigation was done by Guo et al on the effect of soy-based polyol structures on PU rigid foams [42]. The polyol synthesis involved the hydroformylation of the double bonds present in the soybean oil followed by hydrogenation resulting in primary OH groups. The reaction of the isocyanates with the primary alcohols was faster than the reaction with secondary alcohols and the resulting PU foams had properties comparable to petro-based foams. The rigidity of the PU foams made using primary OH group polyols was higher than the foams made previously using secondary OH groups.

Narine et al. synthesized rigid PU foams made from vegetable oils, canola oil, soy-based polyol and crude castor oil [43]. The polyols synthesized from canola oil by ozonolysis and hydrogenation based technology were found to be more highly reactive than the soybean oil and crude castor oil, as was indicated by the cream, rise time and gel times of the foams. Tu et al. investigated the properties of waterborne rigid PU foams by utilizing fifty vegetable oil-based polyols and evaluated their potential for replacing 50% of the petro-based polyols [44]. Density, compressive strength and thermal conductivity of the PU rigid foams were investigated and it was observed that the most of the foams made with 50% replacement of vegetable oil-based polyols were inferior to those made with 100% petro-based foams. However, the foams made using hydroxyl soybean oil, epoxidized soybean oil reacted with acetol, and oxidized epoxidized diglyceride of soybean oil had superior thermal conductivity, better density and compressive strength compared to foams made with 100% petro-based foams. Tan et al. investigated the properties of rigid PU foams by substituting a polypropylene-based polyol with a soybean oil-based polyol. The soy-based foams had a regular cell structure, smaller cell size and ultimately superior compressive strength than the petro-based foams [45].

Although various synthetic routes are described in the literature to convert vegetable oils to polyols and their applications in rigid polyurethane foam formulations no information was found describing the conversion of protein biomass that is left behind after extracting the oil to produce polyols for rigid polyurethane foams. The goal of this work is to synthesize polyols from defatted soymeal and investigate their utility in rigid PU foam formulations and compare the foam properties with those made from petro-based foams.

3.3 Experimental methods

Our approach is based on two basic principles: (1) protect the carboxylic acid in the amino acids by reacting it with ethylene diamine (or similar polyamines) to form an amide, and (2) react the resulting terminal amines with ethylene carbonate [46-52] to yield hydroxyl terminated urethane monomers that can be polycondensed to high molecular weight poly(amide-urethane)s. The use of ethylene diamine and ethylene carbonate has several advantages: these reactants are inexpensive compounds, their respective reactions are well known and proceed smoothly to high yields and both reactants are readily available .

Glycine and L-arginine amino acids were used as model compounds. Glycine was chosen as it is a simple amino acid containing one amine and one carboxylic acid. L-Arginine was chosen since it is present in the soy meal at relatively high concentrations and its structure is relatively complex (e.g. it contains two primary amines, one secondary amine and one imine group). Both of these amino acids exist as zwitterions, which could limit their reactivity. Thus, it was critical to determine if this zwitterionic structure would retard their reactivity. The following is a typical procedure that was used to prepare polyols from L-arginine (Figure 3.5):

In the first step, L-arginine (400 g, 2.3 moles), excess ethylenediamine (800 ml, 12.0 moles) and NaOH (8 g, 2 Wt.%) were added to a three-necked round bottom flask fitted with a dean-stark trap topped with a condenser, a thermal sensor for maintaining a constant temperature and a nitrogen inlet. The reaction mixture was refluxed at 113°C for 60 hours; then unreacted ethylene diamine was removed by distillation to yield L-arginine amido-amine.

In a second step, the intermediate L-arginine amido-amine was reacted with ethylene carbonate (Figure 3.5) to yield hydroxyl-terminated urethane monomer using the following procedure: arginine amido-amine (290.31g, 1.34 mole) and ethylene carbonate (293.72 g, 3.34 moles) were added to a 1000 ml three necked flask fitted with mechanical stirrer, thermometer and nitrogen inlet. The reaction mixture was continuously stirred while monitoring the C=O carbonate peak at 1800 cm^{-1} by FTIR.

A similar procedure was used to prepare a hydroxyl-terminated urethane monomer from glycine and the amino acid mixture from the hydrolysis of soy meal.

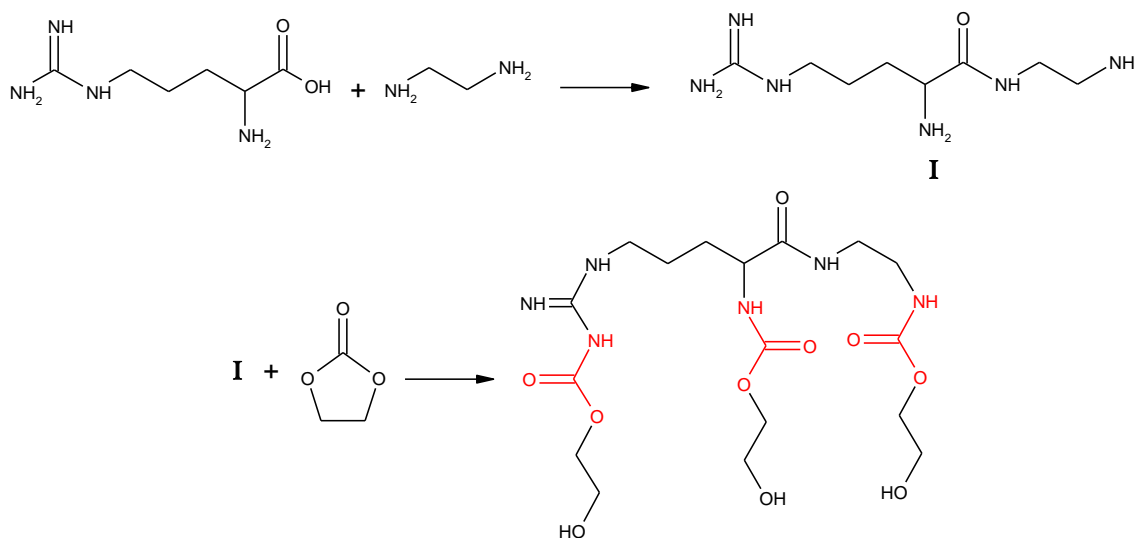


Figure 3.5: Preparation of hydroxyl-terminated urethane monomer

Polyols from soy meal required an additional hydrolysis step whereby the proteins in the meal were hydrolyzed to amino acids. In a typical hydrolysis reaction, soy meal (507 g) and 2500 ml of 3N HCl were added to a 5000 ml 3-necked round bottom flask fitted with a mechanical stirrer, condenser and nitrogen inlet. The reaction mixture was heated under reflux at 110°C for 36 hour while stirring. Then, the hydrolyzate was

filtered to remove any unreacted humin (105.26g) and treated with activated carbon to remove some of the dark brown color. The acidic hydrolyzate was neutralized using NaOH to pH 8 and then vacuum distilled to remove water. The amino acid mixture thus obtained was reacted with ethylene diamine and ethylene carbonate as before.

Since the soy meal also contains carbohydrates, it was possible to remove them before polymerization. However, it was found that these carbohydrates could be converted to active polyols by reacting them with propylene oxide (Figure 3.6). This propoxylation reaction is fairly fast and provided better economics since it eliminated the separation step and allowed higher yield polyols. In a typical procedure, 300 g of the polyol terminated urethane oligomers were placed in a glass reactor and pre-heated to 100°C. The reactor was purged by nitrogen three times. Each time, nitrogen was removed by vacuum. Finally, 60 g of propylene oxide was added dropwise to the reactor. The vacuum prior to the addition of propylene oxide was kept at -20 psi. Propylene oxide was added at a rate such that the temperature was kept below 100°C and the pressure of +10 psi. The addition was completed in 5 hours but mixing was continued for an additional 3 hours until the vacuum was close to the initial vacuum indicating complete reaction. It should be emphasized that no catalyst was needed in this process and the presence of the secondary and tertiary amines of the amino acids was sufficient to catalyze this propoxylation reaction.

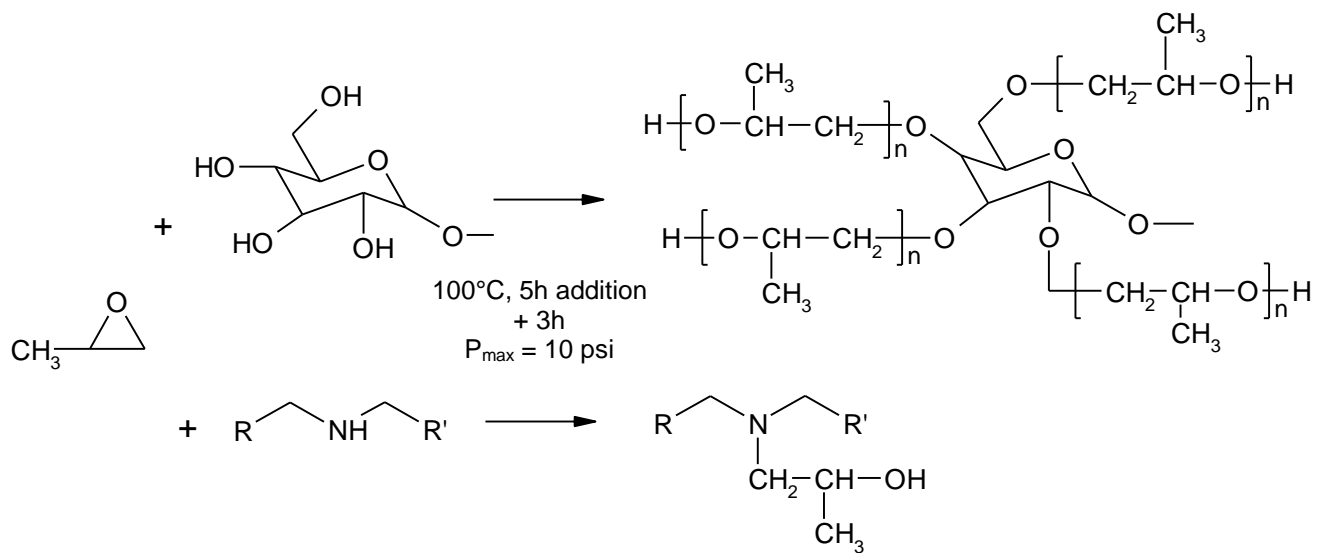


Figure 3.6: Propoxylation of soybean polyol

3.3.1 Preparation of rigid polyurethane foams

Water-blown pour-in-place rigid foams were prepared from the soy meal polyols targeting a foam density of 2 pcf (pounds per cubic foot). A commercial sucrose-based polyol having hydroxyl value in the range of 360 mg KOH/g was used as a reference polyol. Rigid polyurethane foams were prepared as a control using this polyol in the formulation described in Table 3.2 and the foams from the soy meal-based polyols were evaluated against this control foam. All rigid foams were prepared using a standard laboratory procedure using a high-torque mixer. Foams were prepared using water as a sole blowing agent as well as with a combination of water with Enovate 3000 (HFC-245fa) blowing agent. The polyol component of the polyurethane system was prepared by blending the polyol(s) with other formulation components and then the polyol component was mixed with the isocyanate and poured into the paper box. The foaming profile, including mixing time, cream time, gel time, rise time, and tack-free time were measured for all foams (Table 3.2). The foams were aged under room temperature conditions for one week before they were cut and tested. The ASTM test methods that were used to evaluate the properties of the foams are listed in Table 3.3.

Table 3.2: Typical formulation of rigid foams derived from propoxylated soymeal polyol

Sample	Control	Foam 1	Foam 2	Foam 3	Foam 4	Foam 5
Polyol system						
Poly - G 74-376	100	75	75	75	50	50
Propoxylated soymeal polyol	0	25	25	25	50	50
Water	4.5	4.5	4.5	4.5	4.5	4.5
Dabco DC193	2.0	2.0	2.0	2.0	2.0	2.0
Dabco 33LV	1.8	1.8	0.3	0.0	0.1	0.0
Niax A-1	0.1	0.1	0.05	0.05	0.05	0.0
Isocyanate System						
Rubinate M	168.59	179.05	176.99	176.59	187.18	187.01
Isocyanate Index	105	105	105	105	105	105
Reaction Profile						
Mix time, sec.	10	10	10	10	10	10
Cream time, sec.	13	8	13	24	19	32
Gel time, sec.	75	23	68	120	56	76
Rise time, sec.	110	45	68	120	56	76
Tack-free time, sec.	132	30	62	90	62	72

Table 3.3: Foam characterization methods

Description	Test method
Core Density	ASTM D 1622-03
Compressive Strength	ASTM D 1621-00
Compressive Strain at Yield	ASTM D 1621-00
Friability by mass loss	ASTM C 421-00
Burning Rate in a Horizontal Position	ASTM D 635-03
Aging Test at 70°C and Ambient Humidity	ASTM D 2126-99
Aging Test at -30°C and Ambient Humidity	ASTM D 2126-99
Water Absorption	ASTM D 2842-01
Insulation K-factor	ASTM C 518-02

3.4 Results and discussion

The soy meal-based polyols as well as the model polyols derived from L-arginine and glycine amino acids were viscous liquids at room temperature. These polyols were readily miscible with the other components of the foam formulation as well as many other polyols that are currently being used commercially in the production of rigid foams. Thus, the formulator can easily choose a blend of polyols to achieve specific foam properties. It should also be emphasized that in all cases a noticeable self catalytic reaction was noted when the soy meal polyols were used (as well as the polyols derived directly from the amino acids).

The hydrolysis reaction to break the proteins to the individual amino acids is well known and can be accomplished by acid catalysis, ion exchange or by enzymatic reactions. The rate of the hydrolysis is directly proportional to the temperature and the concentration of acid in the system. The temperature of the reaction can be increased above 100°C by running the hydrolysis under pressure. However, it is well known that excessive temperature (as well as excessive concentrations of acid) leads to degradation of the amino acids. We have used relatively mild conditions and, thus, long reaction time to ensure complete hydrolysis and minimum degradation of the resulting amino acids. The composition of the amino acids from the hydrolysis of the soy proteins is well known [53].

It was necessary to “protect” the carboxylic acids of the resulting amino acids in order to produce the urethane linkages. This was conveniently done by reacting with ethylene diamine to yield amido-amine derivatives containing terminal amines as shown in Figure 3.5. It should be noted, however, that excess ethylene diamine (or other

diamines) is required here, since otherwise both amines of the same molecule will react. Although this type of dimerization and increase in the molecular weight is not detrimental, it can lead to higher viscosity products. The use of a large excess of ethylene diamine minimized this side reaction. NMR analysis of the product clearly indicated that the amidation reaction proceeded as desired and these data are supported by FTIR spectra (shown in Chapter 2) that clearly showed a shift of the carbonyl groups from 1640 cm^{-1} to an amide at 1570 cm^{-1} .

End-group analyses (Table 3.4) provided further evidence to the successful sequence of these reactions. The experimental amine and acid values of the model amino acid compound L-arginine (Arg) are lower than the expected calculated values due to the zwitterion structure, the presence of imine and secondary amine groups. A significant increase in the amine value was observed after the reaction with ethylene diamine to convert the carboxylic acid groups to amides and produce the diamine derivative (Arg-ED) as shown in Figure 3.5. The subsequent reaction with ethylene carbonate led to the formation of the hydroxyl terminated urethane oligomers (Arg-ED-EC) as indicated by the significant drop in the amine value and the high hydroxyl value. The reaction of amine with carbonate to yield hydroxyl terminated urethanes is well known [46-54]. It should be noted here that the amine value did not decrease to zero due to the presence of the less reactive secondary amines and imine groups. However, further reduction in the amine value was obtained by propoxylation (Arg-ED-EC-PO). Similarly, the hydrolyzed mixture of amino acids from the soy meal (SMS) showed a marked increase in the amine value after similar reaction with ethylene diamine (SMS-ED) followed by high hydroxyl value after the reaction with ethylene carbonate (SMS-ED-EC). Since the meal also

contained carbohydrates [55], propoxylation led to a significant increase in the hydroxyl value as the propylene oxide reacted with the glucose. The propoxylation reaction also resulted in a lower viscosity product due to the insertion of short flexible propylene oxide chains that is particularly suitable for rigid polyurethane foams.

Table 3-4: End group analysis and viscosity of polyols

Sample	Amine value [mg KOH/g]		Acid value [mg KOH/g]		OH value [mg KOH/g]		Viscosity [cps]
	Calc.	Exp.	Calc.	Exp.	Calc.	Exp.	
Arg	644.1	336.6	322.0	-	0.0	-	-
Arg-ED	778.1	665.1	0.0	0.0	0.0	-	-
Arg-ED-EC	0.0	103.1	0.0	0.0	480.5	448.2	NA
Arg-ED-EC-PO	0.0	74.7	0.0	0.0	-	533.0	54174
SMS	483.7	33.7	549.4	64.9	0.0	-	-
SMS-ED	726.7	650.4	0.0	0.0	0.0	-	-
SMS-ED-EC	0.0	58.9	0.0	0.0	456.2	454.4	NA
SMS-ED-EC-PO	0.0	49.3	0.0	0.0	-	623.0	24500

3.4.1 Rigid polyurethane foams

The reaction of polymeric methylene diphenyl diisocyanate (Rubinate M, eq. wt.= 135.5) with the soy-meal polyols was noticeably faster than with the sucrose-based polyols. The presence of secondary amines and imines catalyzed this reaction. As can be seen from the data in Table 3.2, the cream time, gel time, rise time and tack-free time were all significantly shorter than the control polyol. It was noted that due to this self-catalytic reaction and the high reactivity of these polyols, no amine-based catalysts (Dabco 33LV and Niox A-1) were needed to produce the foams. Typical properties of rigid foams (Figure 3.7) prepared from soy-meal polyol with water as the blowing agent

as well as with 1,1,1,3,3-pentafluoropropane (HFC-245fa) blowing agent are listed in Table 3.5 and compared with a control foam prepared with Poly-G 74-376, sucrose/glycerin-based polyol. It is apparent that the two polyols are completely miscible. The physical properties (e.g. density, compressive strength, compressive strain and friability) of foams prepared with blends of these polyols are comparable. Similarly, results of the dimensional stability in aging tests at -30°C and 70°C up to 2 weeks are essentially identical to the control foams, and the flammability measured as burning rate (with no flame retardant additives) is very similar for all these foams.

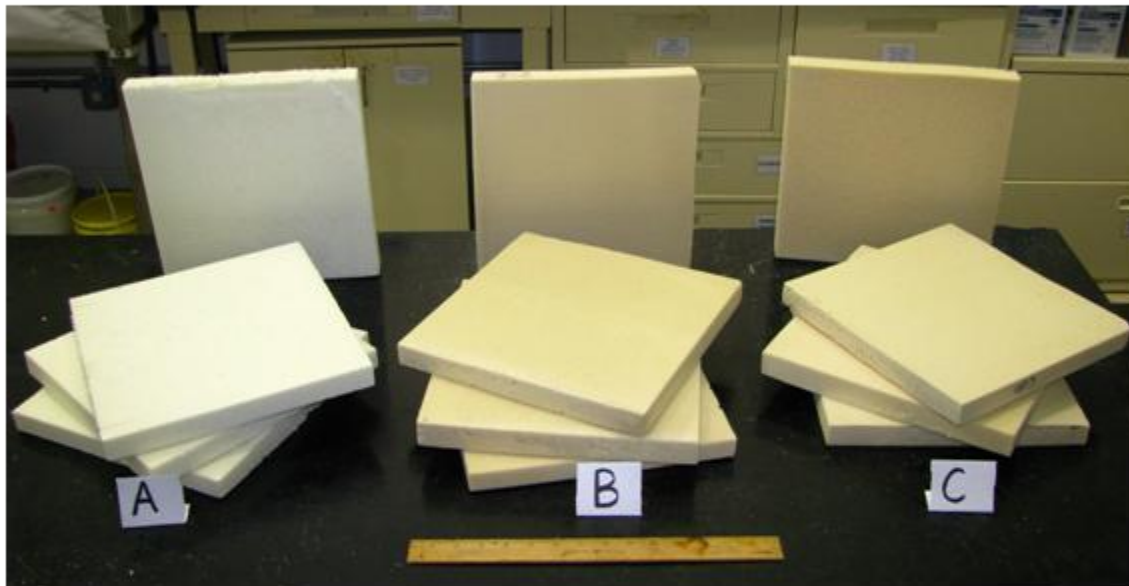


Figure 3.7: Samples of rigid polyurethane foams prepared with combination of water and Enovate 3000 blowing agent; A - reference formulations (0% soy meal polyol); B - formulations with 25% soy meal polyol; C - formulations with 50% soy meal polyol

Table 3.5: Properties of rigid PU foams prepared from propoxylated soy meal urethane polyols

Sample Designation	Control polyol*		Soy meal polyol		Control polyol*		Soy meal polyol	
Type of blowing agent	Water		Water		Water- HFC-245fa		Water- HFC-245fa	
Amount of soy meal polyol [%]	0		25		0		50	
Density, pcf	2.13 ± 0.19		1.62 ± 0.01		2.32 ± 0.03		2.03 ± 0.07	
Compressive Strength, psi	23.98 ± 2.11		17.84 ± 2.06		27.65 ± 2.1		23.40 ± 2.5	
Compressive Strain @ Yield [%]	6.06 ± 0.38		5.44 ± 0.31		5.83 ± 0.34		4.93 ± 0.71	
Friability, mass loss [%]	5.28 ± 0.03		12.99 ± 1.88		4.41 ± 0.73		8.02 ± 0.26	
Mass and Volume Change [%] with Aging and Water Immersion Tests								
	Mass	Vol.	Mass	Vol.	Mass	Vol.	Mass	Vol.
Aging Test @ -30°C								
after 1 day (24h)	0.61	0.66	-0.19	0.60	-0.42	0.43	-0.43	0.72
after 1 week (168 h)	1.69	0.88	0.93	0.17	0.98	0.11	-0.14	0.49
after 2 weeks (336 h)	1.53	-0.55	1.12	0.24	1.41	0.10	-0.14	-0.30
Aging Test @ 70°C								
after 1 day (24h)	-0.31	0.78	0.19	-0.29	-1.23	0.09	-1.04	-0.33
after 1 week (168 h)	-0.31	0.78	0.19	-0.29	-1.23	-0.29	-1.04	-0.32
after 2 weeks (336 h)	0.47	0.92	-0.19	-0.83	0.14	1.58	-1.19	-1.51
Water Absorption @ 25°C								
after 4 days (96 h)	217.49	0.39	304.46	2.17	165.44	-0.16	252.00	6.53
after 1 week (168 h)	229.73	0.73	325.84	2.14	162.04	0.14	300.15	2.44
Burning rate , mm/min	387 ± 55		380 ± 47		377 ± 35		242 ± 15	
K-factor, BTUs	-		-		0.170		-	
Density K-factor samples, pcf	-		-		2.62		-	
* Control polyol: Poly-G 74-376, Sucrose/glycerin-based polyol; Hydroxyl value = 361 from Arch Chemicals								

3.4.2 Soymeal rigid PU foams vs. commercial packaging PU foams

A comparison is made between the properties of soymeal rigid PU foams and commercially available PU foams (Unipaq, Inc., Chicago, USA) suitable for Foam-In-Place packaging applications [56] and shown in Table 3.6. It can be observed that the compression strength and densities of the soymeal polyol based rigid PU foams are comparable with the those of commercially made rigid PU foams. Soymeal polyol foams can therefore find potential applications in packaging, providing superior protection and material cost savings.

Table 3.6: Properties comparison between soymeal polyol foams and commercial packaging PU foams

Product	Compressive strength, psi	Density, pcf
Unipaq foam - 1	6.0	0.40
Unipaq foam - 2	9.2	0.62
Unipaq foam - 3	10.5	0.29
Unipaq foam - 4	17.4	1.19
Unipaq foam - 5	27.6	0.62
Soymeal polyol foams (25%)	17.84±2.06	1.62±0.01
Soymeal polyol foams (50%)	23.40±2.5	2.03±0.07

3.5 Conclusions

Soy meal polyols were prepared from a mixture of amino acids by amidation to protect the carboxylic acids followed by a reaction with ethylene carbonate. The carbohydrates in the meal as well as a portion of the secondary amines and imines were converted to hydroxyl groups by propoxylation. These multi-functional polyols having high hydroxyl values are suitable for rigid polyurethane foams. Some key advantages of these foams are:

- ◆ Low cost raw materials and relatively simple process.

- ◆ Readily available and stable source of domestic raw materials.
- ◆ Self catalytic (due to the presence of secondary amines).
- ◆ Partially biobased polyurethane – smaller carbon footprint than traditional rigid foams.
- ◆ High dimensional stability and chemical resistance derived from the amide linkages.
- ◆ Compatibility with other polyols, blowing agents and other foam additives.
- ◆ Low flammability (charring upon burning) in synergy with flame retardant additives.
- ◆ Potential applications for Foam-In-Place packaging applications.

REFERENCES

REFERENCES

1. Oertel G (1994) Polyurethane Handbook, 2nd ed. Hanser, New York.
2. Guo A, Javni I, Petrovic Z (2000) Rigid polyurethane foams based on soybean oil. *J Appl Polym Sci* 77:467-473
3. Harikrishnan G, Umasankar PT, Khakhar DV (2006) Polyurethane Foam - Clay Nanocomposites: Nanoclays as Cell Openers. *Ind Eng Chem Res* 45:7126-7134
4. Ghosh BS, Ghosh SB, Sain M (2010) Synthesis of Soy-Polyol By Two Step Continous Route and Development of Soy-Based Polyurethane Foam. *J Polym Environ* 18:437-442
5. Kong X, Yue J, Narine SS (2007) Physical Properties of Canola Oil Based Polyurethane Networks. *Biomacromolecule* 8:3584-3589
6. Pfister DP, Xia Y, Larock RC (2011) Recent advances in vegetable oil-based polyurethanes. *ChemSusChem* 4:703-717
7. Galia M, Lucas ME, Carles J, Gerard L, Virginia C (2010) Vegetable oil-based thermosetting polymers. *Eur J Lipid Sci Technol* 112:87-96
8. Petrovic ZS (2008) Polyurethanes from vegetable oils. *Polym Rev* 48:109-155
9. Lucas ME, Meier MAR (2011) Plant oils: The perfect renewable resource for polymer science?! *Eur Polym J* 47:837-852
10. Meier MAR, Metzger JO, Schubert US (2007) Plant oil renewable resources as green alternatives in polymer science. *Chem Soc Rev* 36:1788-1802
11. Srivastava A, Singh P (2002) Gel point prediction of metal-filled castor oil-based polyurethanes system. *Polym Adv Technol* 13:1055-1066
12. Mutlu H, Meier MAR (2010) Castor oil as a renewable resource for the chemical industry. *Eur J Lipid Sci Technol* 112:10-30
13. Mosiewicki MA, Dell'Arciprete GA, Aranguren MI, Marcovich NE (2009) Polyurethane foams obtained from castor oil-based polyol and filled with wood flour. *J Compos Mater* 43:3057-3072

14. Cardoso GT, Neto SC, Vecchia F (2012) Rigid foam polyurethane (PU) derived from castor oil (*Ricinus communis*) for thermal insulation in roof systems. *Frontiers of Architectural Research* 1:348-356
15. Desroches M, Escouvois M, Auvergne R, Caillol S, Boutevin B (2012) From vegetable oils to polyurethanes: synthetic routes to polyols and main industrial products. *Polymer Reviews* 52:38-79
16. Zlatanovic A, Petrovic Z S, Dusek K (2002) Structure and Properties of Triolein-Based Polyurethane Networks. *Biomacromolecules* 3:1048-1056
17. Piazza G, Foglia T (2005) Preparation of fatty amide polyols via epoxidation of vegetable oil amides by oat seed peroxygenase. *J Am Oil Chem Soc* 82:481-485
18. Biermann U, Friedt W, Lang S, Luhs W, Machmuller G, Metzger J O, gen M R, Hans K, Schafer J, Schneider M P (2000) New Synthesis with Oils and Fats as Renewable Raw Materials for the Chemical Industry. *Angew Chem Int Ed* 39:2206-2224
19. Klaas MRG, Warwel S (1999) Complete and partial epoxidation of plant oils by lipase - catalysed perhydrolysis. *Ind Crops Prod* 9:125-132
20. Petrovic Z, Javni I, Guo A, Zhang W (2002) Method of Making Natural Oil - based Polyols and Polyurethanes Therefrom. US Patent 6433121.
21. Petrovic Z, Guo A, Javni I (2000) Process for the preparation of vegetable oil - based polyols and electroninsulating casting compounds created from vegetable oil-based polyols. US Patent 6107433.
22. Ionescu M, Petrovic Z, WanX (2007) Ethoxylated Soybean Polyols for Polyurethanes, *J Polym Environ* 15:237-243
23. Lu Y, Larock RC (2008) Soybean Oil - Based Waterborne Polyurethane Dispersions : Effects of Polyol Functionality and Hard Segment Content on Properties. *Biomacromolecules* 9:3332-3340
24. Petrovic Z, Guo A, Javni I, Zhang W (2004) Method of Making natural oil-based polyols and polyurethanes therefrom. US Patent 6686435
25. Lozada z, Suppes GJ, Tu YC, Hsieh FH (2009) Preparation of polymerized soybean oil and soy-based polyols. *J Appl Polym Sci* 112(4):2127-2135
26. Guo A, Cho YJ, Petrovic ZS (2000) Structure and properties of halogenated and non halogenated soy based polyols. *J Polym Sci Pol Chem* 38:3900-3910

27. Miao S, Zhang S, Su Z, Wang P (2010) A novel vegetable oil-lactate hybrid monomer for synthesis of high - T_g polyurethanes. *J Polym Sci Pol Chem* 48(1):243-250
28. Guo A, Cho Y, Petrovic ZS (2000) Structure and properties of halogenated and non halogenated soy based polyols. *J Appl Polym Sci* 38:3900-3910
29. Petrovic Z S, Yang L, Zlatanic A, Zhang W, Javni I (2007) Network structure and properties of polyurethanes from soybean oil. *J Appl Polym Sci* 105 2717-2727
30. Narayan R, Graiver D, Farminer K, Tran PT (2010) Novel modified fatty acid esters and method of preparation thereof. US Patent 0084603.
31. Petrovic ZS, Zhang W, Javni I (2005) Structure and properties of polyurethanes prepared from triglyceride polyols by ozonolysis. *Biomacromolecules* 6:713-719
32. Petrovic ZS, Milic J, Xu Y, Cvetkovic I, (2010) A chemical route to high molecular weight vegetable oil-based polyhydroxyalkanoate. *Macromolecules* 43: 4120-4125
33. Guo A, Demydov D, Zhang W, Petrovic ZS (2002) Polyols and polyurethanes from hydroformylation of soybean oil. *J Polym Environ* 10:49.
34. Petrovic ZS, Guo A, Javni I, Cvetkovic I, Hong DP (2008) Polyurethane networks from polyols obtained by hydroformylation of soybean oil. *Polym Int* 57:275-281
35. Desai SD, Patel JV, Sinha VK (2003) Polyurethane adhesive system from biomaterial-based polyol for bonding wood. *Int. J. Adhes. Adhes.* 23:393-399
36. Kaushik A, Singh P (2005) Synthesis and Characterization of Castor Oil/Trimethylol Propane Polyol as Raw Materials for Polyurethanes Using Time-of-Flight Mass Spectroscopy. *Int. J. Polym. Anal. Charact.* 11:373-386
37. Dutta S, Karak N (2005) Synthesis, characterization of poly(urethane amide) resins from Nahar seed oil for surface coating applications. *Prog. Org. Coat.* 53:147-152
38. Lee CS, Ooi TL, Chuah CH, Ahmad S (2007) Rigid Polyurethane Foam Production from Palm Oil-Based Epoxidized Diethanolamides. *J Am Oil Chem Soc* 84:1161-1167
39. Lyon CK, Garrett VH, Franker EN (1974) Rigid urethane foams from hydroxymethylated castor oil, safflower oil, oleic safflower oil and polyol esters of castor acids. *J Am Oil Chem Soc* 51:331-334

40. Hu YH, Gao Y, Wang DN, Hu CP, Zu S, Vanoverloop L, Randall D (2002) Rigid polyurethane foam prepared from a rape seed oil based polyol. *J Appl Polym Sci* 84:591-597
41. Guo A, Javni I, Petrovic ZS (2000) Thermal stability of polyurethanes based on vegetable oils. *J Appl Polym Sci* 77, 1723-1734
42. Guo A, Zhang W, Petrovic ZS (2006) Structure - property relationships in polyurethanes derived from soybean oil. *J Mater Sci* 41:4914-4920
43. Narine SS, Kong X, Bouzidi L (2007) Physical Properties of Polyurethanes Produced from Polyols from Seed Oils: II. Foams. *J Am Oil Chem Soc* 84:65-72
44. Tu Y, Kiatsimkul P, Suppes G, Hsieh F (2006) Physical properties of water-blown rigid polyurethane foams from vegetable oil-based polyols. *J Appl Polym Sci* 105:453-459
45. Tan S, Abraham T, Ference D, Macosko CW (2011) Rigid polyurethane foams from a soybean oil-based Polyol. *Polymer* 52:2840-2846
46. Rokicki G, Piotrowska A (2002) A new route to polyurethanes from ethylene carbonate, diamines and diols. *Polymer* 43:2927-2935
47. Guan J, Song Y, Lin Y, Yin X, Zuo M, Zhao Y, Tao X, Zheng Q (2011) Progress in Study of Non-Isocyanate Polyurethane. *Ind Eng Chem Res* 50(11):6517-6527
48. Rokicki G, Lazinski R (1989) Polyamines containing β -hydroxyurethane linkages as curing agents for epoxy resin. *Angew Makromol Chem* 170:211-215
49. Kihara N, Kushida Y, Endo T (1996) Optically active poly(hydroxyurethane)s derived from cyclic carbonate and L-lysine derivatives. *J Polym Sci Part A: Polym Chem* 34:2173-2179
50. Kihara N, Endo T (1993) Synthesis and properties of poly(hydroxyurethanes). *J Polym Sci Part A: Polym Chem* 31(11): 2765-2773
51. Tomita H, Sanda F, Endo T (2001) Polyaddition of bis(seven-membered cyclic carbonate) with diamines: a novel and efficient synthetic method for polyhydroxyurethanes. *J Polym Sci Polymer Science Part A: Polym Chem* 39(23):860-867
52. Tomita H, Sanda F, Endo T (2001) Model reaction for the synthesis of polyhydroxyurethanes from cyclic carbonates with amines: substituent effect on the reactivity and selectivity of ring-opening direction in the reaction of five-membered cyclic carbonates with amine. *J Polym Sci Part A: Polym Chem* 9(21): 3678-3685

53. Tomita H, Sanda F, Endo T (2001) Self-Polyaddition of Six-Membered Cyclic Carbonate Having Fmoc-Protected Amino Group: Novel Synthetic Method of Polyhydroxyurethane. *Macromolecules* 34(22):7601-7607
54. Tomita H, Sanda F, Endo T (2001) Polyaddition behavior of bis(five- and six-membered cyclic carbonate)s with diamine. *J Polym Sci Part A: Polym Chem* 39(6): 860-867
55. Hancock JD, Lee DJ (1999) Evaluating the Ileal Digestibility of Amino Acids in Soybean Meal from Different Soy Processors. Kansas State University.
56. UNIPAQ (2014) <http://protectivepackaging.unipaq.com/item/all-categories/foam-in-place-packaging/item-1003>

Chapter 4 A spectroscopic method for hydroxyl value determination of polyols

A relatively simple method is described for routine determination of hydroxyl values for a wide range of hydroxyl containing compounds including soybean oil polyols, polyols derived from soy meal, polyether polyols and ethylene glycol as well as their blends. This method is based on reacting the hydroxyl compound with hexamethyldisilazane (HMDS) and determining the FTIR peak area of the silylated product at 1251 cm^{-1} . The method is simple, accurate and reproducible. It is not limited to a specific family of polyol compounds. It does not require any special equipment or hazardous chemicals and can be carried out by non-technical staff as a rapid and convenient method for quantitative determination of hydroxyl values. An excellent linear correlation was obtained between this spectroscopic method and conventional titration methods for different polyols over a wide range of hydroxyl values. Furthermore, unlike the titration methods the current method is not affected by the presence of acid, base or small amounts of water in the test sample.

4.1 Introduction

Recently, much attention has been directed toward the use of oleochemical polyols in the preparation of polyurethanes and unsaturated polyester resins for a wide range of applications ranging from flexible foams, flooring adhesives and coatings to thermoplastic materials. The use of domestic oleochemical polyols is advantageous from environmental and sustainability aspects as well as socio-economic issues over imported petroleum-based chemicals that are converted to polyols [1-3]. Precise determination of the hydroxyl functionality, commonly defined as hydroxyl value (OHV), is a critical parameter in the

analysis of the extent of the polycondensation reactions. It is also a critical parameter in the preparation of polyurethanes. OHV is usually determined by titration methods as specified by ASTM D1957-86(2001), ASTM E 1899-08, D6342-08 and the American Oil Chemists' Society (AOCS) method Cd 13–60.

The hydroxyl value is defined as the number of milligrams of KOH equivalent to the hydroxyl groups found in one gram of the sample and is expressed in mg of KOH/g. The titration methods are generally reliable and reproducible when conducted under standardized conditions. However, they require a relatively large sample size and hazardous reagents, some of which are irritant, highly toxic, or corrosive. Furthermore, the titration methods are inherently time-consuming, labor-intensive, largely dependent on the skills of the analyst and are susceptible to error due to contamination by acid, base or water in the sample. Thus, several other methods for hydroxyl group determination are described in the literature based on NMR, GC, GPC and IR spectroscopy.

IR spectroscopic methods are common due to their ease of operation, short analysis time, minimum sample preparation and the need for a relatively small sample size. Indeed, many routine quality control applications are based on IR spectroscopy and have been shown to be accurate and reliable [4-10]. FTIR coupled with horizontal attenuated total reflectance (ATR-FTIR) simplifies many of the sample handling problems commonly associated with infrared analysis. The ATR-FTIR method is notably rapid because it requires no weighing of the test sample or quantitative dilution in a solvent prior to the analysis.

Several methods have been published based on the near-infrared (NIR) region of the spectrum using one or a few selected wavelengths and different statistical approaches that

appear to yield a robust correlation with the titration methods [11]. In an early publication [12], the hydroxyl values of fatty alcohols were measured using carbon tetrachloride or tetrachloroethylene as solvent. Due to considerable overlap of the absorption bands in the NIR region, a partial least squares method or the second derivative of the spectra using univariate linear regressions were employed [13]. The advantages of these methods are the use of all the wavelengths in the calibration and the relatively high correlation of the data with the hydroxyl content of the polyol. However, as the number of variables increases, the proper variable selection becomes extremely time consuming. Furthermore, these methods are specific to a particular family of polyols having similar structure since the OH overtone band shifts to higher wavelengths in the order of primary-secondary-tertiary alcohols. Branching also affects the spectrum and a relatively wide variation in absorptivities was observed related to the appearance of nonsymmetrical absorption bands. It was concluded that a single calibration curve cannot be used for all hydroxyl containing systems [13]. Furthermore, this technique could only be used after suitable calibration data were obtained to determine the OHV of a family of essential oils in which the constituents were the same. As such, these NIR techniques cannot be calibrated for one type of polyol (e.g. soybean oil polyol) and applied to a different type of polyol (e.g. polyether polyol). Furthermore, it was found that when water was present, the correlation weakened when compared with the titration test measurements. It was therefore concluded that if water was present, a separate calibration was required for almost every combination of reactants [14]. Alternatively, anhydrous sodium sulphate had to be added and mixed thoroughly for 15 minutes to adsorb the water and then filtered out before acquiring the spectrum.

In this project, we report on a practical and rapid method to determine the OHV of polyols from different sources and their mixtures. This method is based on comparing the FTIR spectrum of the polyol sample and its silylated spectrum. Thus, subtracting the original spectrum from the silylated spectrum yields a well defined absorption peak of the methyl silyl group that has an area that is directly proportional to the concentration of the hydroxyl groups. Silylation is a well known technique that is frequently used to “protect” hydroxyl groups in analytical chemistry under mild conditions [15]. 1,1,1,3,3,3-hexamethyldisilazane (HMDS) is a common silylation reagent that yields silyl ethers with alcohols and phenols. It is a relatively inexpensive, readily available, stable compound and is non-hazardous. Its handling does not require special precautions other than storing it under moisture-free conditions. It is a preferred silylation agent since the by-product of its reaction with alcohols is ammonia, which is easily removed from the reaction medium.

4.2 Materials and methods

4.2.1 Materials

Soyol R2-052-C derived from soybean oil was manufactured by Urethane Soy System Company (South Dakota, USA). Refined castor oil was manufactured by G.R. O'Shea Company (Illinois, USA). Castor oil polyol derivatives CASPOL 1842 (OHV=145 mg KOH/g, CASPOL 5001 (OHV=285 mg KOH/g) and POLYCIN T-400 (OHV=403 mg KOH/g) were manufactured by Vertellus (Michigan, USA). Carbowax series polyethylene glycols (Carbowax PEG 200 (OHV=535-595 mg KOH/g), 300 (OHV=340-394 mg KOH/g) and 400 (OHV=264-300 mg KOH/g) were obtained from the Dow Chemical Company (Michigan, USA). Polyols derived from amino acids of hydrolyzed soy proteins were prepared in this laboratory. Ethylene glycol was purchased from J.T. Baker (New

Jersey, USA). When polyol blends were used, the mixtures were stirred for 2 hours at room temperature using a magnetic stirrer to ensure homogeneity. Hexamethyldisilazane, trifluoroacetic acid, p-toluenesulfonyl isocyanate (TSI) and tetrabutylammonium hydroxide (Bu₄NOH) were purchased from Sigma Aldrich (Missouri, USA). Reagent grade toluene and acetonitrile were purchased from Fisher Scientific (Massachusetts, USA). All reagents were used as received unless noted otherwise.

4.2.2 Instrumentation

The attenuated total reflection-Fourier transform infrared (ATR-FTIR) spectra were acquired on a Shimadzu IRAffinity-1 spectrometer (Tokyo, Japan) equipped with a single reflection ATR system (PIKE Technologies, Madison, USA, MIRacle ATR). All spectra were acquired using a resolution of 4 cm⁻¹ and a minimum of 32 scans. All the titration experiments were performed using a Metrohm titration device 857 Titrando (Florida, USA).

4.2.3 Silylation of polyols with HMDS

A typical procedure consisted of adding excess HMDS to the polyol (approximately, 3:1 molar ratio) with trifluoroacetic acid (14 mmol) as a catalyst to ensure complete reaction. The mixture was stirred at 60°C for 1 hour while ammonia was evolved and removed from the reaction mixture. Excess HMDS and the ammonia by-product were then removed under vacuum (Scheme 4.1).

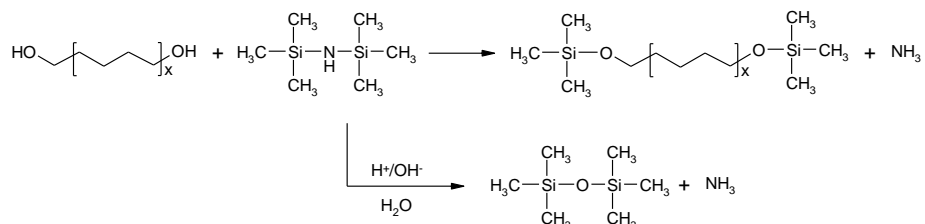


Figure 4.1: Silylation of polyols with HMDS

4.2.4 OHV determination by titration

OHVs were determined following ASTM E 1899-08. Briefly, a polyol sample was dissolved in toluene and acetonitrile. The sample was stirred until completely dissolved in the solvent mixture. Then, p-toluenesulfonyl isocyanate (TSI) solution in acetonitrile was added slowly to form the acidic carbamate. Then distilled water and acetonitrile were added to the reaction mixture. The product was then titrated with tetrabutylammonium hydroxide (Bu₄NOH). The OHV in mg KOH per gr. sample was then obtained according to Equation 1:

$$OHV = \frac{(V_2 - V_1) \times N \times 56.106}{w_{sample}} \quad \text{Eq. 1}$$

where V₁ is the first potentiometric end point in mL, V₂ is the second potentiometric end point in mL, N is the concentration of the titrant used in meq/mL, 56.106 is the molecular weight of KOH in g/mol, and w_{sample} is the mass of the sample in gram. The titration was repeated at least 3 times for each sample in order to obtain the mean and standard deviation of these measurements.

4.2.5 OHV determination by FTIR

The FTIR spectrum of the polyol was subtracted from the silylated polyol spectrum yielding a peak related to the well defined stretching vibration band of the methyl groups attached to the silicon atom at 1251 cm⁻¹. The baseline of this peak was determined from the minima on both sides of this peak and the peak area was calculated (Figure 4.2 insert).

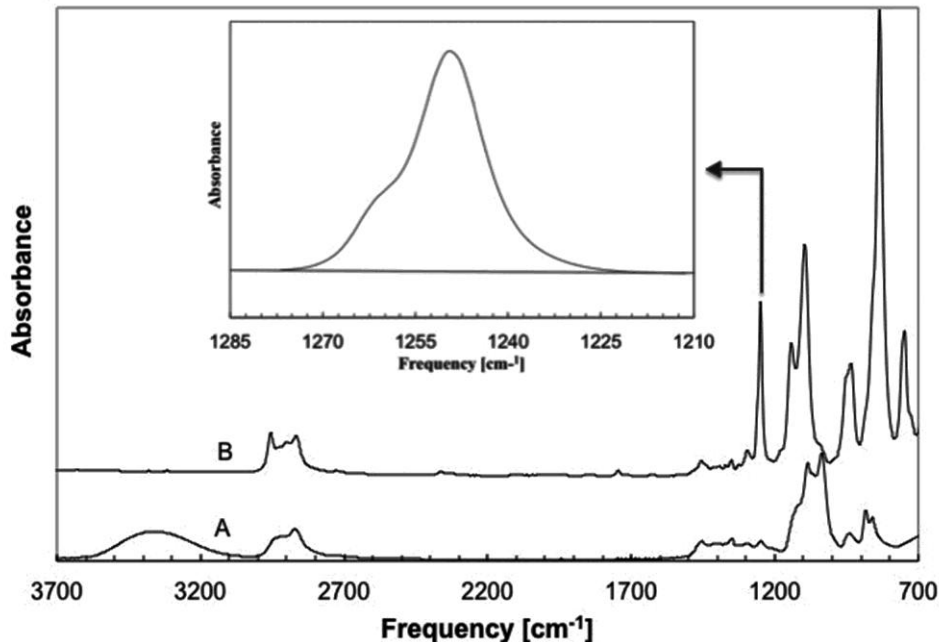


Figure 4.2: FTIR spectra of a sample polyol (A), the same sample after silylation (B) and after subtraction (insert)

4.3 Results and discussion

The FTIR method to determine the OHV of polyols is based on testing a large number of polyol samples including soybean oil polyols, castor oil, polyether polyols and ethylene glycol as well as blends of these polyols. The polyol samples varied in composition and OHV over a wide range from 20 to 1800 mg KOH/g.

The basis for quantitative analysis of absorption spectrometry is based on Beer's law which states that the absorbance at any frequency is given by Equation 2:

$$A = a \cdot b \cdot c \quad \text{Eq. 2}$$

Where A is the measured absorbance at a given frequency, a is the molecular absorptivity at this frequency, b is the path length of the source beam through the sample and c is the concentration (or thickness) of the sample. Since in ATR-FTIR the infra-red radiation is reflected at the surface/sample interface, the signal is not a simple variable of c and depends on the incident angle (e.g. penetration depth) as well as the refractive indexes of

the ATR crystal and the sample. Although Beer's law states that the intensity of any absorption band is additive and linearly proportional to the concentration of the absorbing group, small deviations may be present and can lead to a nonlinear relationship when plotting the absorbance (A) against the concentration (c). Such deviations from linearity, however, are negligible when the molecular absorptivity (a) is large and the path length (b) is small. Hence, linearity is best observed from a functional group having a high dipole moment that results in a narrow, sharp absorption band.

It would be most convenient to assess the hydroxyl content of a sample from direct evaluation of the area under the absorbance bands related to OH stretching vibrations. Although direct measurements of the spectra are fast and simple, the degree of hydrogen bond associations, and hence, the intensity of their absorption peaks varies markedly with the concentration and the nature of the sample making such measurements unreliable. It was suggested [16] that in very dilute solutions the degree of hydrogen bond association is negligible and under this condition, measurements of the intensity of the unassociated absorption peak could permit the determination of the OHV. Indeed, this method was used to determine the hydroxyl content of auto-oxidized fatty esters (e.g. methyl ricinoleate) which was then used to determine the hydroxyl content of other similar samples by comparison of the relative intensities of the unassociated hydroxyl absorption peaks. However, extremely dilute solutions had to be used and the spectrum of the pure solvent had to be subtracted from the spectrum of the solution containing the sample. More significantly, as mentioned above, this method is limited to a specific family of polyols having similar chemical structure and therefore cannot be used for different compounds other than the reference sample or for mixtures of different polyols.

We have used a different approach; each polyol sample was first reacted with HMDS yielding silyl ethers (Figure 4.1) that have exceptionally strong stretching vibration bands in the IR region. The FTIR spectra of the original polyol sample and the silylated sample were recorded and subtracted (Figure 4.2). It is apparent from these spectra that the O-H stretching band at 3300 cm^{-1} in the silylated spectrum disappeared indicating the reaction between the OH groups and HMDS had proceeded as expected. Additionally, new bands related to the methyl groups attached to the silyl ether products were observed, most notably at 1251 cm^{-1} and 835 cm^{-1} . Subtracting the original spectrum from the silylated spectrum gave rise to well defined peaks of the silylated products. The bands related to the symmetrical deformation vibration of the methyl groups attached to the silicon atom adjacent to the siloxy ethers are notably strong due to the high dipole moment and the partial ionic character of the C-O-Si linkage. Thus, this band is well defined, especially after subtracting the original polyol spectrum from the silylated spectrum. The areas under either of these peaks were then plotted against the OHV obtained by the titration method yielding excellent linear correlations (Table 4.1).

4.3.1 Method development

The statistical analysis from these absorbance bands is given in Table 4.1. Here, the root mean square error (RMSE) of each regression line was calculated according to Equation 3:

$$\text{RMSE} = \sqrt{\frac{\sum_{i=1}^n (Y' - Y)^2}{n}} \quad \text{Eq. 3}$$

where Y is the OHV obtained by titration, Y' is the predicted OHV from the subtracted FTIR peak area and n is the number of data points. The RMSE is particularly suited to

provide information of the spread of the y values about the predicted values. It was found that a slightly smaller RMSE was obtained from the correlation of the peak area at 1251 cm^{-1} compared with the peak area at 835 cm^{-1} (77.3 and 83.3, respectively in Table 4.1). Apparently the narrower absorption band at 1251 cm^{-1} is less susceptible to errors than the broader band at 835 cm^{-1} and provided more accurate results. Although both of these absorption bands can be used, only the band at 1251 cm^{-1} is considered here.

Table 4.1: Statistical analysis of the areas under the silylated FTIR bands

Model	Peak at 1251 [cm^{-1}]	Peak at 835 [cm^{-1}]
RMSEC	77.3±2.8	83.3±3.9
RMSEP	79.1±8.1	86.9±11.6
RMSEC/RMSEP	0.9771	0.9580
Calibration R^2	0.9783±0.0022	0.9731±0.0040
Prediction R^2	0.9732±0.0079	0.9647±0.0139
Slope	213.24±2.21	53.79±0.43

4.3.2 Precision and accuracy

The accuracy of the method was examined by determining how closely the measured (experimental) OHV agree with the calculated OHV (Figure 4.3). Calculated OHV can easily be obtained from the molecular structure of the polyol. Although it is possible in principle to determine the OHV of polyols blends knowing the relative concentration of each polyol in the blend, the accuracy of these calculations is less reliable. Thus, only the neat polyols were used in this analysis. It is apparent from the data that excellent linear correlation is obtained ($R^2=0.9554$) from plotting the experimental OHV against the calculated values, indicating a high degree of accuracy. For a perfect fit the diagonal line in this correlation has a slope of 1.00, whereas the slope of the correlation line is 0.9963 (Figure 4.3). The correlation of the Calculated OHV against the FTIR peak area from the

absorption band at 1251 cm^{-1} is shown in Figure 4.4. An excellent linear correlation is observed ($R^2=0.9603$) indicating a good fit of the calculated OHV with the FTIR peak areas.

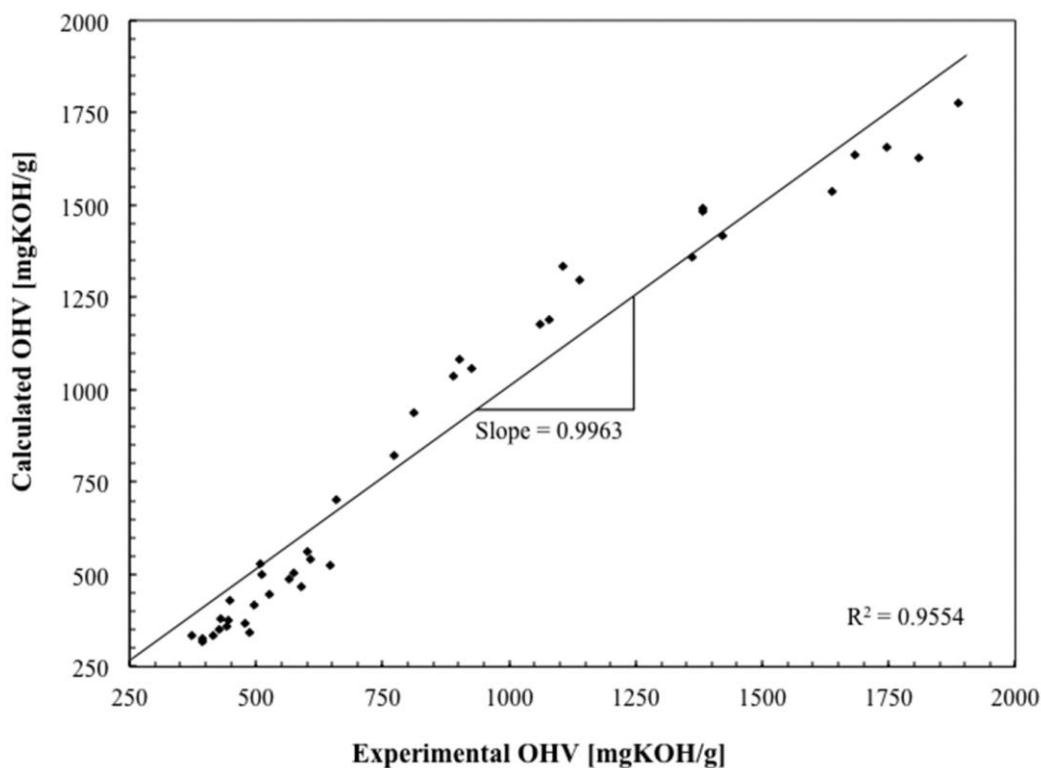


Figure 4.3: Accuracy of the method as determined by comparing the experimental to calculated OHVs

The precision (e.g. reproducibility) of the method was evaluated by examining how closely individual measurements agree with each other. Thus, representative polyol samples including polyols having different molecular structures, polyols containing different OHV and blends composed of different polyols were randomly selected and the FTIR spectra were examined repeatedly (Table 4.2). The statistical analysis of these data indicates excellent reproducibility with relatively small variations from the means.

Table 4.2: Reproducibility of FTIR peak areas of silylated polyols

OHV [mg KOH/g]	FTIR Peak area			Mean	Std. Dev.
	Run 1	Run 2	Run 3		
322.2	1.84	1.94	1.91	1.90	0.05
358.6	2.01	1.91	1.85	1.92	0.08
453.7	2.11	2.24	2.19	2.18	0.07
540.7	2.64	2.64	2.60	2.63	0.02
602.2	2.82	2.83	2.80	2.82	0.02
680.8	3.09	3.07	3.19	3.12	0.06
866.4	3.62	3.37	3.51	3.50	0.13
938.5	3.80	4.94	4.99	4.58	0.67
1046.1	4.34	4.15	4.18	4.22	0.10
1155.6	4.97	4.63	4.70	4.77	0.18
1298.7	5.34	5.49	5.28	5.37	0.11
1467.1	6.66	6.76	6.43	6.62	0.17
1527.7	7.68	8.18	7.89	7.92	0.25
1673.3	8.19	9.45	9.36	9.00	0.71
1776.0	8.84	8.85	8.87	8.86	0.02

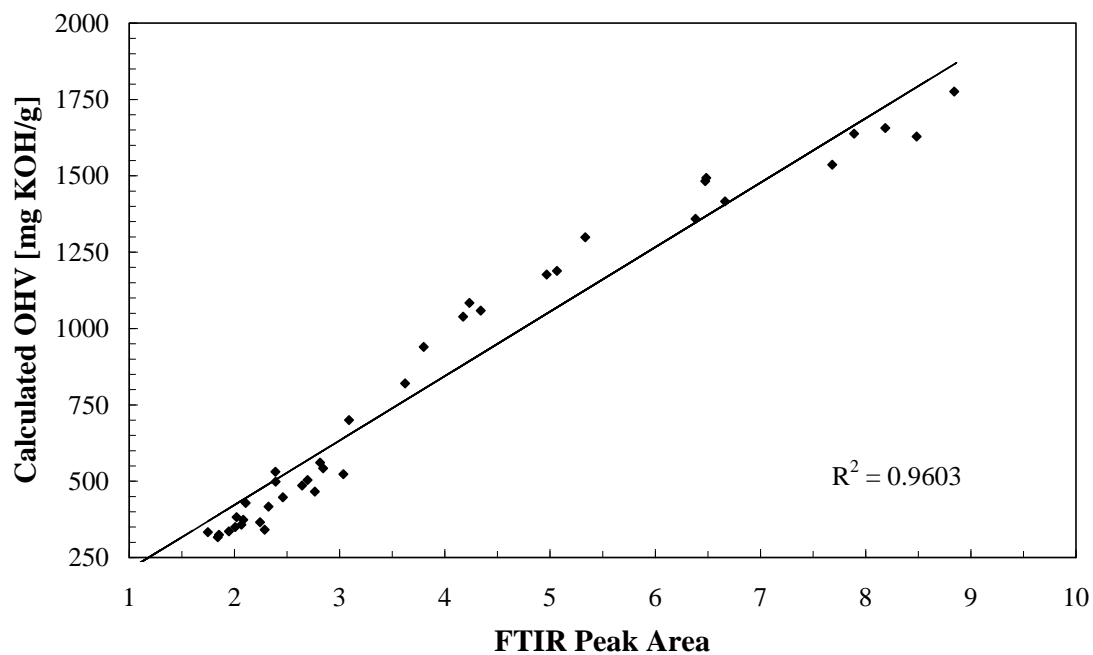


Figure 4.4: Correlation of the FTIR method with the calculated OHV

It is important to note that the current spectroscopic method is suitable for a wide range of polyols from very low to very high OHVs (20 - 1800 mg KOH/g). The only major limitation that we have noted is the requirement that the polyol has to be sufficiently reactive to produce the silyl ether derivative with HMDS. In our work all the selected polyols were sufficiently reactive and were successfully derivatized.

4.3.3 Structural considerations

It is noteworthy to mention that this correlation is general in nature as it does not depend on whether the polyol constitutes a terminal or secondary alcohol. Furthermore, it does not depend on the number of hydroxyls per molecule, the chemical composition of the backbone chain or the molecular weight of the polyol. The polyols in this work include primary alcohols attached to polyether chains, primary alcohols attached to hydrocarbon chains, secondary alcohols attached to triglycerides and polyols of low molecular weight polyurethanes derived from amino acids.

It is recognized that due to differences in the chemical environment of the hydroxyl groups in the various polyols, displacements of the infrared absorption band related to the angular deformations is to be expected. These variations are most significant in polyols derived from epoxidation of unsaturated fatty acids since the triglycerides in this case consist of distinct chains with double bonds at different positions [16]. As the double bonds are reacted and are converted to hydroxyls the absorption spectrum is affected. Indeed, in the ASTM method D6342-08, it is specifically mentioned that the spectra of all samples must be similar and if different types of polyols are used, separate calibrations are required. In this case, it is required to group the samples by chemistry and to develop a

separate calibration plot for each chemical grouping. The current method does not rely on calibration plots that are susceptible to these variations. Instead, we compare the original polyol spectrum to the same molecule after silylation such that variations related to the chemical structure are eliminated. Furthermore, the relatively large new absorption related to the Si-(CH₃)₃ vibration is essentially unaffected by the minor changes in the absorption of the neighbouring carbons. Consequently, the likelihood of interference problems is greatly reduced, thus, contributing to the robustness of the method. It should also be noted that the current method does not require pre-treatment of the spectral data. Most of the spectroscopic methods described in the literature require some pre-treatment of the data in order to obtain optimal calibrations. Such pre-treatments include baseline correction, path length correction or variable scaling. Also, this pre-treatment of the data can be greatly influenced by outlier samples and variables.

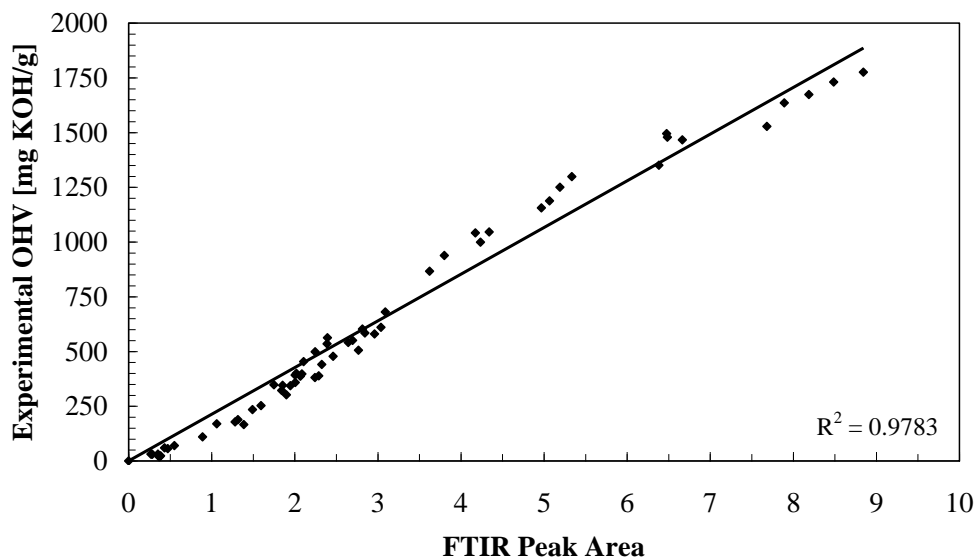


Figure 4.5: Correlation of the FTIR method with the titration method

4.3.4 Correlation with the titration method

The correlation of the OHVs determined by the FTIR peak area from the absorption band at 1251 cm^{-1} against the OHVs determined by the conventional ASTM titration method is shown in Figure 4.5. In order to ensure accuracy and determine the experimental error, the OHV of each sample was repeated by titration according to ASTM E 1899-08 at least 3 times and the mean value of these titrations was used. The standard deviations of the titrations varied between 0.4 to 5.1%. An excellent linear correlation is observed ($R^2=0.9783$) over a very wide range of OHVs for different polyols and their blends. Normal probability plots are often used to investigate whether the data exhibit the standard normal "bell curve" or Gaussian distribution. In our case the normal probability plot (Figure 4.6) follows a straight line indicating that indeed the data set is approximately normally distributed. The straight line plot with no apparent patterns indicates a good fit of the OHV data from the current method to the titration method with no obvious clusters or outliers.

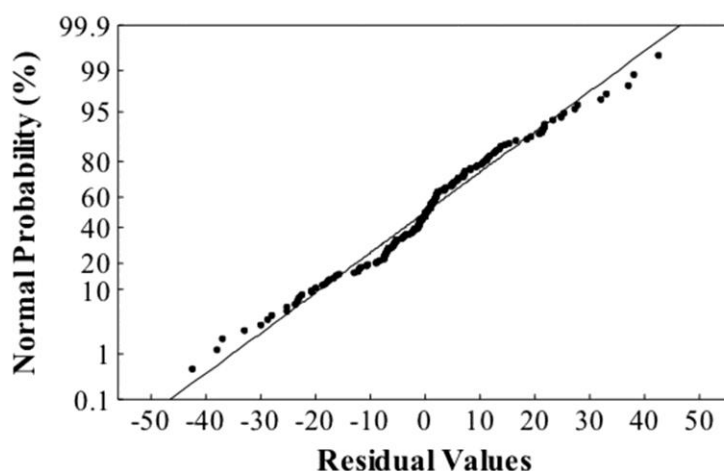


Figure 4.6: Normal probability plot

For further verification, a plot of the residuals versus the predicted OHV (Figure 4.7) yields a random scatter around the mean over the full range of the graph indicating no apparent outliers or trends related to a specific polyol or a mixture of polyols. The magnitude of the residuals is within the accepted experimental error although slightly higher residuals are observed at low OHVs. This relatively large error for the low OHVs is not surprising since even a small absolute experimental error is reflected as a relatively large number when presented in percents.

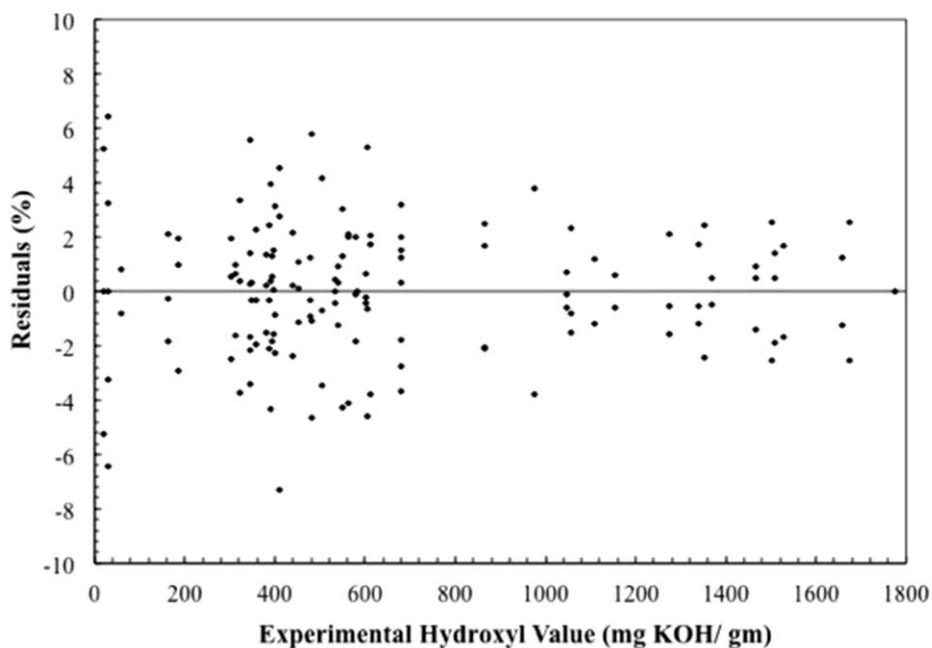


Figure 4.7: Residual plot of OHV

4.3.5 Interferences

It is known that the presence of acid, base or water contaminants in the sample can interfere with the titration. Thus, it is recommended that the samples be dried and contain no more than 0.2 wt% water as specified by the ASTM methods. Similarly, primary and secondary amines or excess base in a sample will react with the acidic carbamate to cause

low OHVs. Any acidic species with a pKa value close to that of the acidic carbamate can also react to form stable compounds that will skew the titration analysis and cause high OHVs. Consequently, all the ASTM titration test methods require that if a sample contains more than 0.05 milliequivalents of acidity or alkalinity, the test must first be corrected to determine the acid or alkaline number. The apparent OHVs by titration without corrections for the presence of these contaminants are listed in Table 4.3. It is apparent that 1-5 wt% water did not impact the test results as large excess of the TSI reagent is prescribed by the ASTM method. However, the presence of acetic acid contributed to a significant increase in the OHV whereas the presence of NaOH resulted in a decrease of the OHV. Contrary to these results, the analysis of OHV by the current FTIR method is not affected by such contaminants and the observed OHVs remained unchanged. Although HMDS will react with water, acid or a base to yield silanols, these silanols will further condense to yield hexamethyldisiloxane which will be removed from the reaction mixture and thus will not affect the analysis (Figure 4.1). The major limitation of this method is the requirement that the polyol has to be less volatile than HMDS. In case acid, base or water contaminants are present, the polyol also needs to be less volatile than the hexamethyldisiloxane byproduct.

It should be mentioned that the analysis of OHV by NIR spectra is also affected by water and 'catalyst'. Consequently, it is therefore required that any interactions of the sample with these factors need to be determined before a calibration procedure is initiated. Thus, the relationship between the NIR spectra and the OHV is generally evaluated during a separate feasibility study in order to identify such possible interferences before an adequate calibration model is constructed.

Table 4.3: Effect of acid, base and water on the OHV

	Polyol	Polyol+acid	Polyol+base	Polyol+water	Mean/Std. Dev.
FTIR peak Area	2.815	2.862	2.835	2.860	--
OHV by FTIR [mg KOH/g]	600.1	610.3	604.5	609.9	606.2 ± 4.8
OHV titration [mg KOH/g]	602.2 ±3.3	631.5 ±4.4	503.3 ±4.3	603.1 ±3.9	585.0 ±56.1

4.4 Conclusions

An excellent linear correlation was observed between the OHV and the absorbance band of silylated hydroxyl groups at 1251 cm^{-1} . This correlation was observed over a wide range of OHVs (20 - 1800 mg KOH/g) using polyols having different structures and different molecular weights as well as various mixtures of such polyol. The OHV is determined by simply reacting a small amount of polyol sample with HMDS, subtracting the original FTIR spectrum from the silylated spectrum and determining the area under the absorption band related to the silylated species. This method is simple and faster than conventional titration methods. It requires small samples, does not use toxic or hazardous reagents and is not susceptible to error due to the presence of water, acid/base or other functional groups containing active hydrogen contaminants. The statistical analysis of the data based on a relatively large number of different polyols clearly indicates that this method is accurate, robust and reproducible. Furthermore, this method is fairly simple such that it can be adopted for routine OHV analyses as well as quality control.

REFERENCES

REFERENCES

1. Huy H, Gao Y, Wang DN, Hu CP, Zu S, Vanoverloop L, Randall D (2002) Rigid polyurethane foam prepared from a rape seed oil based polyol. *J Appl Polym Sci* 84:591-597
2. Petrovic ZS, Guo A, Zhang W (2000) Structure and properties of polyurethanes based on halogenated and nonhalogenated soy-polyols. *J Polym Sci: Part A: Polym Chem* 38:4062-4069
3. Guo A, Javni I, Petrovic ZS (2000) Rigid polyurethane foams based on soybean oil. *J Appl Polym Sci* 77:467-473
4. Simone C, Godoy, Ferrao MF, Annelise E. Gerbase (2007) Determination of the Hydroxyl Value of Soybean Polyol by Attenuated Total Reflectance/Fourier Transform Infrared Spectroscopy. *J Am Oil Chem Soc* 84:503-508
5. Ratnayake WMN, Pelletier G (1996) Methyl esters from a partially hydrogenated vegetable oil is a better infrared external standard than methyl elaidate from the measurement of total trans content. *J Am Oil Chem Soc* 73:1165-1169
6. Russin TA, Van de Voort FR, Sedman J (2004) Rapid Determination of oxidative stability of edible oils by FTIR spectroscopy using disposable IR cards. *J Am Oil Chem Soc* 81:111-116
7. Seedman J, Van de Voort FR, Ismail AA (1997) Upgrading the AOCS infrared trans method for analysis of neat fats and oil by Fourier transform infrared spectroscopy. *J Am Oil Chem Soc* 74:907-913
8. Moh MH, Man YBC, Van de Voort FR, Abdullah WJW (1999) Determination of peroxide value in thermally oxidized crude palm oil by near infrared spectroscopy. *J Am Oil Chem Soc* 76:19-23
9. Seedman J, Van de Voort FR, Ismail AA, Maes P (1998) Industrial validation of Fourier transform infrared trans and iodine value analyses of fats and oils. *J Am Oil Chem Soc* 75:33-39
10. Parreira TF, Ferreira MMC, Sales HJS, Almeida WB (2002) Quantitative determination of epoxidized soybean oil using near infrared spectroscopy and multivariate calibration. *Appl Spectrosc* 56:1607-1614

11. Pastia L, Jouan-Rimbauda D, Massarta DL, de Noord ON (1998) Application of Fourier transform to multivariate calibration of near-infrared data. *Anal Chim Acta* 364:253-263
12. Crisler RO, Burrill AM, (1959) Determination of Hydroxyl Value of Alcohols by Near-Infrared Spectroscopy. *Anal Chem* 31(12):2055-2057
13. Miller KL, Curtin D (1994) On-line NIR monitoring of polyols, Instrumentation for the process industries, 49th annual symposium, College Station Tex
14. Heikka RA, Immonen KT, Minkkinen PO, Paatero EYO, Salmi TO (1997) Determination of acid value, hydroxyl value and water content in reactions between dicarboxylic acids and diols using near-infrared spectroscopy and non-linear partial least squares regression. *Anal Chim Acta* 349:287-294
15. Zareyee D, Karimi B (2007) A novel and highly efficient method for the silylation of alcohols with hexamethyldisilazane (HMDS) catalyzed by recyclable sulfonic acid-functionalized ordered nanoporous silica. *Tetrahedr, Lett.* 48:1277-1280
16. Ahlers NHE. McTaggart NG (1954) The Determination of Hydroxyl, Ketone and Ester Groups in Autoxidised Fatty Esters and Related Compounds by Infra-red Spectroscopy. *Analyst*, 79:70-76

Chapter - 5 Evaluation of PU coatings derived from soymeal polyol and castor oil

5.1 Introduction

Polyurethanes are one of the most versatile polymeric materials available today [1]. Polyurethanes are generally produced by the addition of two components, isocyanates and polyols. A wide variety of raw materials can be used for these components, resulting in polyurethanes with an enormous range of different property profiles. By proper selection of these reagents, polyurethanes with a wide range of applications from flexible foams in upholstered furniture, rigid insulation foams in walls and roofs, thermoplastic materials used in medical devices and footwear, coatings, adhesives, sealants and elastomers used on floors and automotive interiors can be synthesized [2]. However, conventional PU paints usually contain a significant amount of organic solvents and in certain cases even free isocyanate monomers [3]. Increased strict regulations on emissions to protect the environment and health have induced the PU manufacturers to increasingly eliminate solvents from PU formulations. Recently, waterborne dispersions have been developed where the water is a diluent and the binder is present in a dispersed phase. These environmentally friendly waterborne PUs have several advantages over conventional solventborne systems and are increasingly finding applications in inks, adhesives and various protective or decorative coatings [4].

In the PU industry, only a few polyisocyanates are commonly used, while a variety of polyols are available and therefore the choice of polyol typically determines the properties of the synthesized polyurethane [5]. Most of the polyols currently used for

the production of polyurethanes are based on polyethers derived from petro-fossil feedstock [6]. Due to increasing oil prices, global warming and other environmental concerns, there is an increasing need for change over from fossil feedstocks to biobased renewable resources. Furthermore, switching from the petro-fossil carbon feedstock to a bio-renewable carbon feedstock offers the “value proposition” of a reduced material carbon and environmental footprint [7, 8]. The increasing awareness about environmentally friendly materials produced from annually renewable biodegradable resources have led to intensified research on the production of chemicals and polymeric materials [9].

Vegetable oils are an important renewable source for producing polyols. Vegetable oils have a number of excellent properties and a wide variety of polymers such as alkyd resins [10], epoxys [11], polyamides [12], vinyl polymers [13-16] and PUs [17-23] are synthesized. In addition, various vegetable oils such as soybean oil [24], canola oil [25], palm oil[26,27], sunflower oil, corn oil, and linseed oil [28,29] have been extensively used as base materials for synthesizing polyols used to manufacture PUs with high thermal stability and mechanical properties. In comparison, only little attention has been directed towards utilization of biomass protein obtained after extraction of the oil for value-added polymeric materials. This raw material is rich in carboxylic acids and amines that can be utilized in the production of polyesters, polyamides, polyurea and polyurethanes. For example, soybean, which is abundantly available and low in cost, can provide a sustainable alternative source to petrochemicals. Soybean is composed of protein and oil that can open the door for a variety of uses. Soy oil, constituting about 18% of the bean has already been used in the polyol market, as mentioned above.

Soybean meal is the product remaining after extracting the oil from the soybeans. Soybean meal, which makes up to 80% of the soybean, is high in protein content and primarily serves as animal feed for swine, chickens, cattle, horse, sheep and fish. Currently, only a small percentage of the soybean meal is being utilized for industrial purposes, mainly for synthesis of adhesives, insecticides, paints, paper coatings, fire-resistant coatings, cosmetics, printing inks and emulsions. To the best of our knowledge, no other studies are available in the literature utilizing soybean meal as a renewable biomass resource for synthesizing polyols.

In this work, a novel route to the synthesis of biobased polyols from soymeal is reported. The overall process includes alcoholic treatment to remove the soluble carbohydrates from the meal, acid hydrolysis of soy proteins to individual amino acids or low molecular weight peptides, amination of the hydrolyzed product mixture with ethylene diamine followed by reacting the aminated hydrolyzate with cyclic ethylene carbonate. Waterborne PU dispersions were then prepared and their coatings were investigated and are reported here. Fourier transform infrared spectroscopy, end group analysis using amine, acid and OH values were used to characterize the polyols. In addition, the thermal properties, barrier properties against water vapor and oxygen permeation, contact angle and Cobb value tests of the PU coatings from the newly developed soymeal polyols and castor oil were compared.

5.2 Literature review

The important chemical reactions of isocyanates that can take place in the production of polyurethanes are:

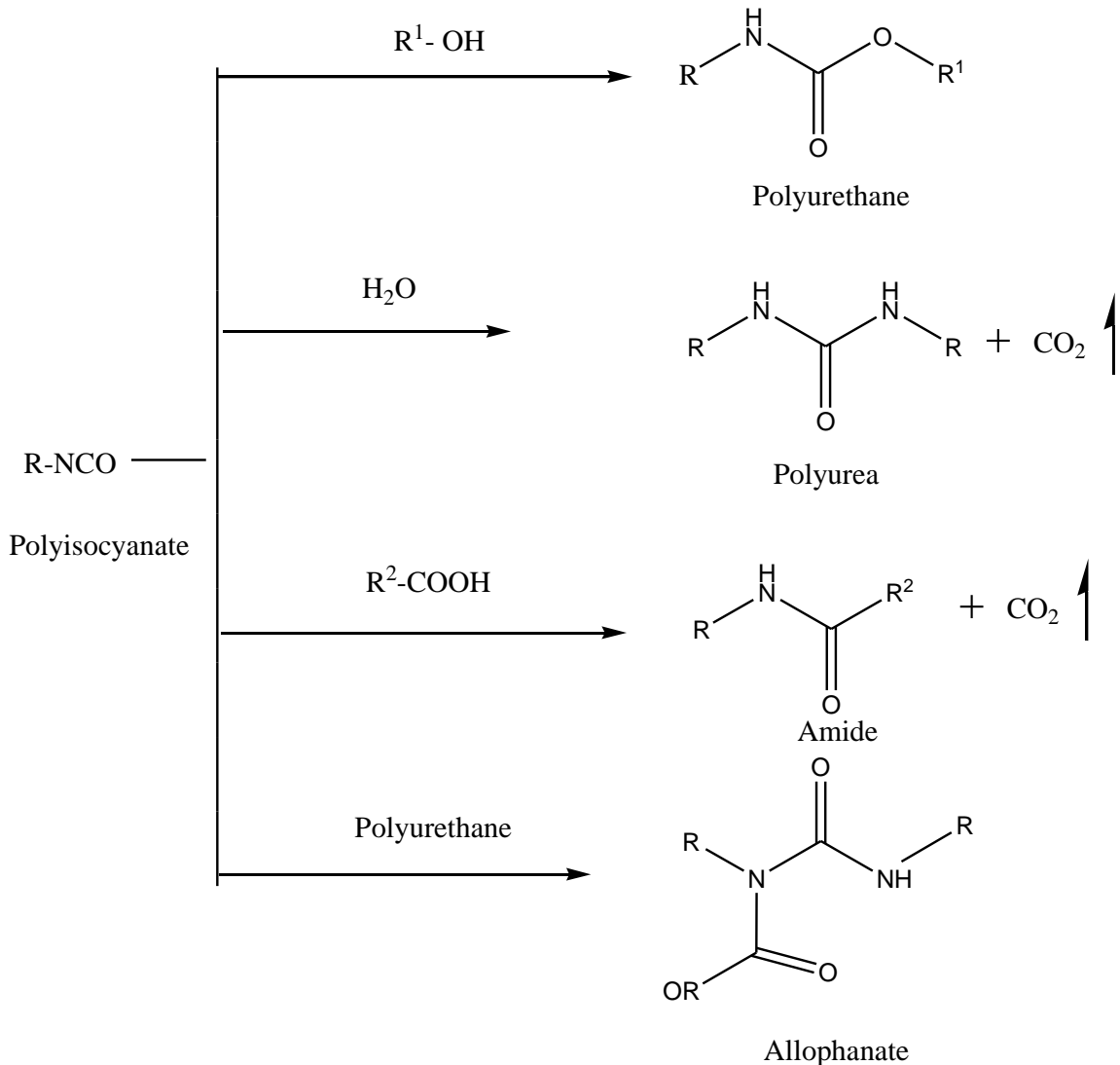


Figure 5.1: Reactions of polyisocyanates in PU coating systems

The basic reaction, which occurs in all PU coating systems is the NCO/OH reaction between the polyisocyanate and the polyol reaction (Figure 5.1). The main ancillary reaction takes place between the polyisocyanate and water and leads to the formation of polyurea. Other possible reactions, that can occur are the reactions between the carboxyl groups of the polyol and the polyisocyanate to form amide bonds and between the newly formed polyurethane and the polyisocyanate to form an allophanate reaction.

Polyurethane coatings can be commercially produced using a single component (1K) system or a two component (2K) system. In a 1K system, the prepolymer is prepared by reacting one or more polyols with a stoichiometric excess of isocyanate. The isocyanate functionality is retained in the pre-polymer but has an increased shelf life and lower volatility compared to pure isocyanates. The pre-polymer is then mixed with catalysts, plasticizers, fillers, antioxidants and adhesion promoters. In this system, when dispensed, the prepolymer reacts with ambient moisture to cure and a thermoset polyurethane film is left behind. In a 2K system, the polyols and additives are blended together to make up one of the two components and the isocyanate or prepolymer makes up the second component. The two components are then mixed on site to cure the system. The reaction begins immediately after mixing and continues for a time after the solvent has evaporated. The resultant films from the 2K systems are usually highly crosslinked but also requires the ability to mix separate components at the proper ratio. PU coatings have been classified by ASTM into six different groups in the ASTM D16 Standard [30]. The characteristics of the six ASTM PU coating types are summarized in Table 5.1.

Table 5.1: Different types of coatings by ASTM classification

ASTM description	Type I one package (pre-reacted)	Type II one package (moisture cured)	Type III one package (heat cured)	Type IV two package (catalyst)	Type V two package (polyol)	Type VI one package (non-reactive lacquer)
Characteristics	Unsaturated drying oil modified; no free isocyanate	Contains free isocyanate	Blocked isocyanate	Isocyanate prepolymer and catalyst	Part A: isocyanate rich, Part B: polyols or amines	Fully polymerized PUs dissolved in solvents
Curing mechanism	Oxidation of drying oil; solvent evaporation	Reaction with atmospheric moisture	Thermal release of blocking agent and then reaction	Reaction of isocyanate with moisture and or/components in catalysts	Reaction between Parts A and B; instant curing is possible	Solvent evaporation
Polymer	Alcoholysis products of drying oils reacted with isocyanate	Higher molecular weight diols and triols	Prepolymer forms an adduct with blocking agents	Prepolymer similar to type II but catalyst could contain polyol/amine	Relatively lower molecular weight	Thermoplastic polymer with relatively high molecular weight

5.2.1 Isocyanates, polyols and catalysts

Aromatic, aliphatic, cycloaliphatic or polycyclic structured isocyanates are used in the synthesis of PU coatings. Some of the commonly used isocyanates are toluene diisocyanate (TDI), methylene diphenyl diisocyanate (MDI), 4,4'-dicyclohexylmethane diisocyanate (H₁₂MDI), hexamethylene diisocyanate (HDI), isophorone diisocyanate (IPDI), xylene diisocyanate (XDI), tetramethyle-xylene diisocyanate (TMXDI), hydrogenated xylene diisocyanate (HXDI), naphthalene 1,5-diisocyanate (NDI), p-phenylene diisocyanate (PPDI), 3,3'-dimethyldiphenyl-4, 4'-diisocyanate (DDDI), 2,2,4-trimethyl-hexamethylene diisocyanate (TMDI), norbornane diisocyanate (NDI), 4,4'-dibenzyl diisocyanate (DBDI), etc. The reactivity of aromatic isocyanates is higher than the reactivity of aliphatic or cycloaliphatic diisocyanates. Aromatic diisocyanates produce more rigid PUs than the aliphatic ones, but also have lower oxidative and ultraviolet stability [31]. Thus the properties of the PUs vary with different diisocyanates.

Different polyols or a mixture of polyols can be used for the synthesis of PU coatings. Polyether polyols (polypropylene glycol, polyethylene glycol, polycaprolactone diol), polyester polyols, polycarbonate polyol and acrylic polyols are some of the petro-based polyols widely used. Simple polyols like glycols, such as ethylene glycol, 1,4-butane diol and 1,6-hexane diol are also used. Bio-based polyols synthesized from renewable resources are also increasingly finding their applications in PU coatings. Castor oils [32,33], chemically modified soybean oil [34,35,36,37], rapeseed oil based polyols [38,39] and Jatropha oil based polyols [40] are some of the vegetable oil based polyols, where the PUs derived therefrom exhibited excellent chemical and physical properties, including enhanced thermal and hydrolytic stability [41,42,43,44]. The

functionality of the hydroxyl-containing polyols can be adjusted, leading to a wide variety of branched or crosslinked polyurethanes. Low molecular weight polyols result in hard and stiff polymers, while the use of the higher molecular weight polyols produces polymer chains with fewer urethane groups and more flexible alkyl chains. Short-chain polyols of higher functionality (greater than 3) give more rigid, crosslinked products, while the long-chain polyols with low functionality (1.8-3.0) give soft, elastomeric PUs.

Catalysts are added to the PU formulations to increase the rate of reaction at lower temperatures and many effective urethane catalysts are available. The catalysts used most often are organo tin compounds like dibutyltin dilaurate (DBTDL), stannous octoate THORCAT [45], and tertiary amines like triethyl amine (TEA) and 1,4-diazabicyclo[2.2.2] octane (DABCO) [46].

5.2.2 Waterborne polyurethane dispersions

Polyurethanes are used commercially in the form of liquid solventborne and waterborne coatings. Increased strict regulations on emissions to protect the environment and health have induced coating manufacturers to increasingly eliminate solvents from coating systems. In the meantime, Water has proved to be the substitute solvent of choice, in which the binders are present in a dispersed phase, no longer as a solution, and marketed as waterborne dispersions. New types of resins for binder dispersions and additives are required for the waterborne coating technologies to fulfill high quality requirements [47,48]. The particle size of the PU in the aqueous dispersion tends to be about 20-200 nm, and the particles have high surface energy, which results in a strong driving force for film formation after water evaporation. PU polymers are usually not soluble in water and the particle size distributions in the polyurethane dispersions

(PUDs) are greatly influenced by the degree of hydrophilicity. Therefore structural modifications of the polymer are necessary for it to be dispersible in water. This can be achieved by incorporating hydrophilic groups such as ionomers into the polymer backbone which act as internal emulsifiers or by adding external emulsifiers. Therefore PU backbone with the PU ionomer consisting of a pendant acid or tertiary nitrogen groups are completely or partially neutralized to form salts, which form stable dispersions in aqueous medium (Figure 5.2).

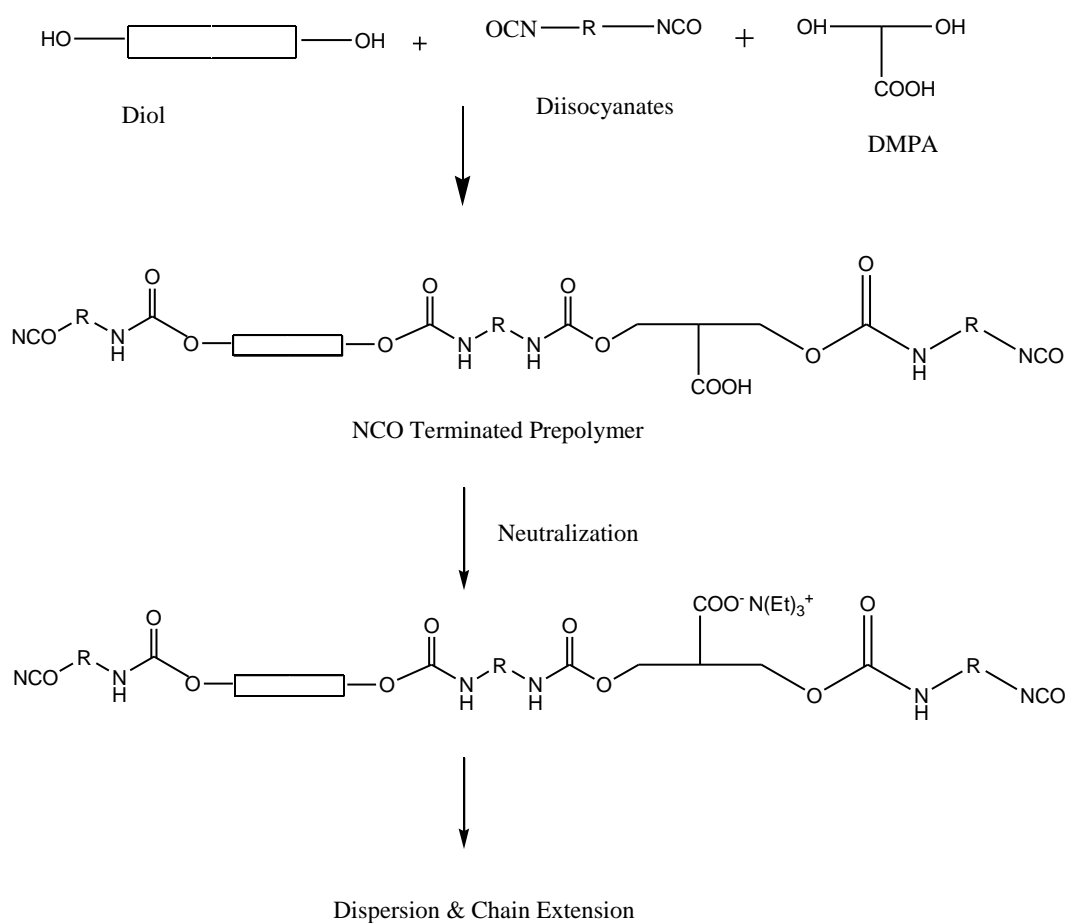


Figure 5.2: Synthesis of anionic waterborne PU dispersions

Waterborne PUDs can be broadly classified into two categories: anionic and cationic dispersions [49]. In the anionic PUDs, dimethylol propionic acid (DMPA) containing two hydroxyl groups and one free carboxylic group is commonly incorporated into the PU backbone. This intermediate is typically produced using an acetone process, a prepolymer mixing process, a ketamine/ketazine process or a hot melt process [53,54, 49]. The carboxylic groups in the prepolymer are subsequently neutralized with triethylamine for effective water dispersions [50,51,52,] (as in Figure 5.2). Cationic PU dispersions are synthesized by incorporating tertiary amines into the PU backbone and quarternized with a protonic acid or alkylating agent, which forms the water-soluble group in the polymer. Cationic dispersions, because of their application properties, are of lesser importance than anionic dispersions and are used in special applications [54].

Isocyanates are used as the cross-linkers in the synthesis of PU dispersions. They react readily with water and because of this reactivity it was assumed for many years that they could not be directly used in waterborne systems. However, in the last few years, hydrophilically modified polyisocyanates were developed and adopted commercially on a large scale [55,56]. The pioneering work in the production of hydrophilic polyisocyanates was done by Bayers. For the production of hydrophilic isocyanates, chemically binding emulsifying components (internal emulsification) were introduced to the polyisocyanate. This strategy suppresses the migration tendency of free emulsifiers in the coating (external emulsification) which can lead to problems with water resistance such as gloss decrease or blistering. Consequently, hydrophilic polyisocyanates can be produced by reacting a fraction of the $-NCO$ groups on a polyisocyanate (such as HDI or IPDI isocyanurate) with a polyglycol monoether [57, 58]. Figure 5.3 shows an

example of polyether modified hydrophilic polyisocyanate. However this reaction will lower the functionality of the polyisocyanates and can influence the final performance of the coatings. In order to increase the functionality, the allophanate structure had been introduced to the previous molecule as shown in Figure 5.4. The aminosulfonate modified polyisocyanates (Figure 5.5) represents the 3rd generation of hydrophilic polyisocyanate crosslinkers with significant advantages over polyether modified types, providing improved drying, hardness and chemical resistance [59].

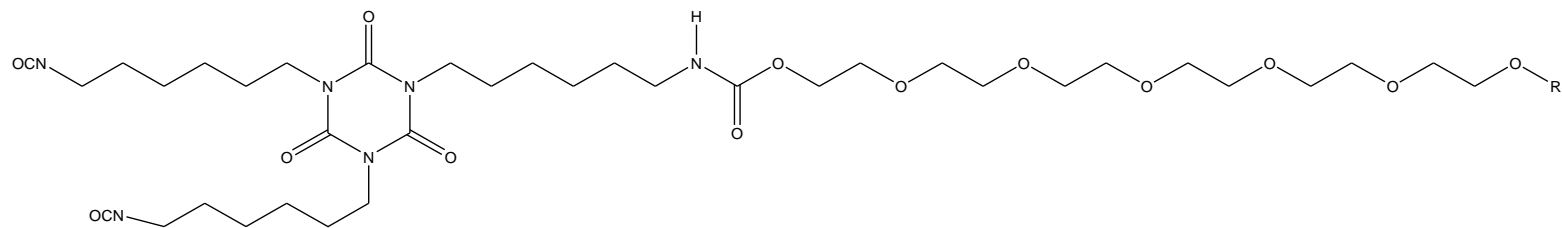


Figure 5.3: 1st generation, polyether modified hydrophilic polyisocyanate

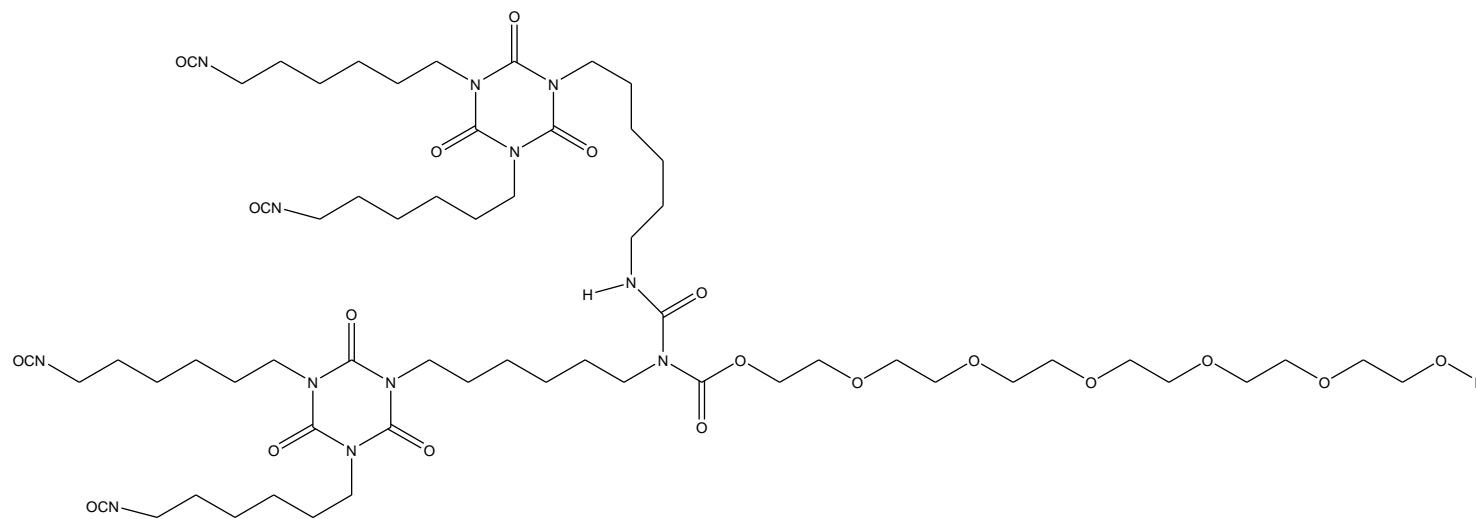


Figure 5.4: 2nd generation, polyether modified hydrophilic polyisocyanate (allophanate)

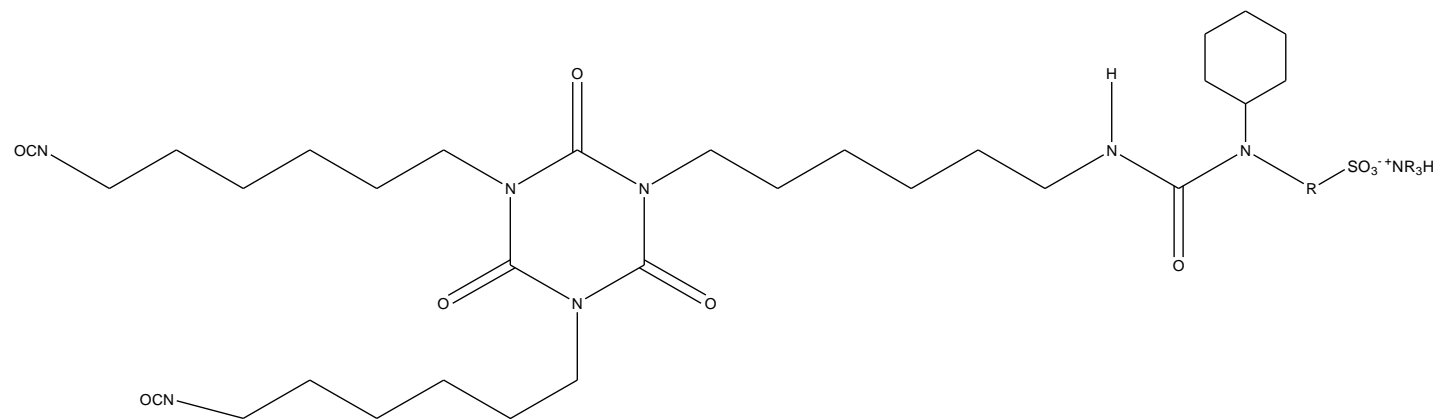


Figure 5.5: 3rd generation, aminosulfonate modified hydrophilic polyisocyanate

5.2.3 Application of PU dispersions

Figure 5.6 shows the various applications of polyurethane coatings. PU coatings have dominated the industrial finishes market for several decades because of their ability to create highly-crosslinked surface coatings.

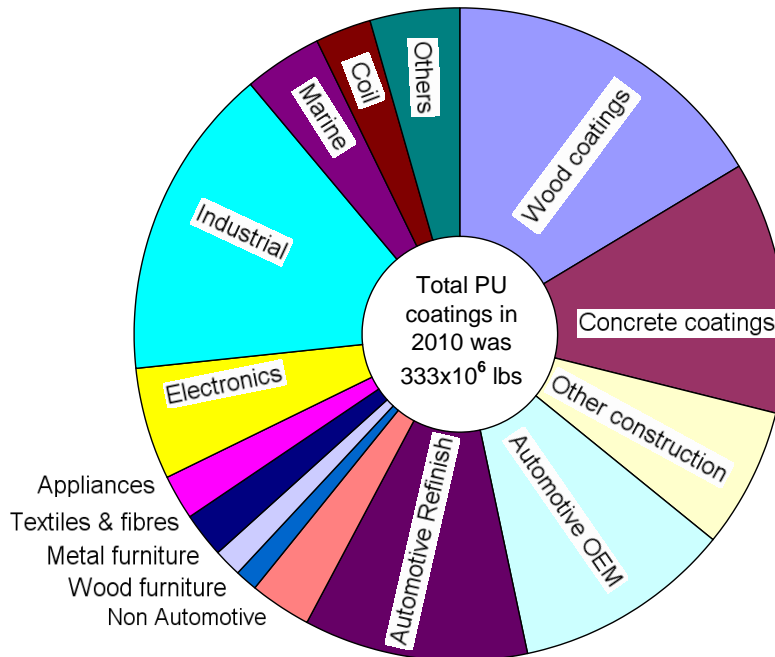


Figure 5.6: Breakdown of the US coating market in 2010

This crosslinking property results in desirable properties including high durability with excellent flexibility, superior gloss and protection from corrosion, humidity, wear and chemicals. Polyurethane coatings are widely used in the automotive refinish and large vehicle coating areas and in metal, wood, plastic, glass and textile coating. They are also widely used in ship paints and about about one in four cars produced worldwide today are coated with a polyurethane clear coat. They are also widely used in construction applications, such as floor and balcony coatings and increasingly gaining importance in pipeline coatings [60].

5.2.4 Castor oil based polyurethanes

Castor oil, like many other natural oils, is widely used in industry and is obtained from the seed of the castor plant (*Ricinus communis*). The primary sources of castor oil are from India, China and Brazil, with India being the world's largest exporter of castor oil with a 70% of the total exports. The major importing countries are the USA, Russia and Japan [61]. Castor oil is a triglyceride of fatty acids, with approximately 90% ricinoleic acid, an 18-carbon acid having a double bond in the 9-10 position and hydroxyl group on the 12th carbon (Figure 5.7). The composition of castor oil is shown in Table 5.2. Castor oil is the only natural oil with a unique combination of hydroxyl groups and unsaturation in its chemical structure. Scientific literature reveals that regardless of its country of origin or season in which it was grown, the chemical composition of the castor oil remains relatively constant [62].

Castor oil has certain characteristics like high lubricity, high viscosity over a wide range of temperatures, insolubility in aliphatic petrochemical fuels and solvents, and is used for many applications including base oil formulations for lubricants, functional fluids and process oils, feedstock for fuels and oleochemicals, reactive components for paints, coatings and inks, polymers and foams [63,64,65].

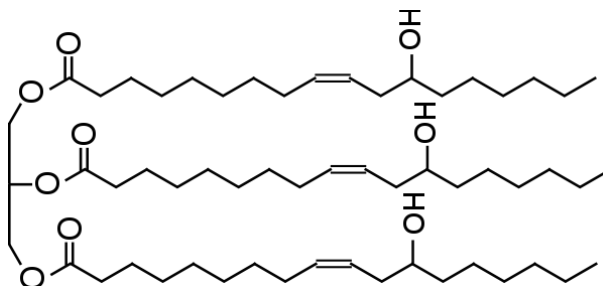


Figure 5.7: Structure of castor oil

Table 5.2: Castor oil composition. [62]

Fatty acid	Molecular formula	Percentage [%]
Palmitic	$C_{16}H_{32}O_2$	0.8 – 1.1
Stearic	$C_{18}H_{36}O_2$	0.7 – 1.0
Oleic	$C_{18}H_{34}O_2$	2.2 – 3.3
Linoleic	$C_{18}H_{32}O_2$	4.1 – 3.3
Linolenic	$C_{18}H_{30}O_2$	0.5 – 0.7
Ricinoleic	$C_{18}H_{34}O_3$	87.7 – 90.4

Petro-based hydrocarbon feedstocks are being increasingly replaced by renewable vegetable oils for polyols in the synthesis of polyurethanes as they are cost competitive and offer environmentally friendly alternatives [66]. Castor oil has an average functionality of 2.7 and is the only commercially available naturally occurring polyol produced directly by nature. Thus, castor oil is being used for synthesizing a variety of polyurethane products ranging from coatings, cast elastomers, thermoplastic elastomers, rigid foams, semi-rigid foams, flexible foams, adhesives and sealants.

There are advantages as well as disadvantages of directly utilizing the castor oil as a polyol in rigid polyurethane formulations. The advantages are water resistance and flexibility, while low functionality and low reactivity due to the secondary hydroxyl groups are some of the disadvantages [67]. These disadvantages can be overcome by reacting the castor oil with polyols such as glycerol, resulting in a higher hydroxyl number which can be utilized for synthesizing rigid PU foams with good physico-mechanical properties. Compared to PU prepared from pure

castor oils, glycerol modified PU products clearly exhibit higher tensile strength, lower elongation at break and chemical resistance. However glycerol is unstable at higher temperatures and can lead to formation of unsaturated compounds at elevated temperatures by elimination of water. This problem can be solved by replacing glycerol with other alcohols such as trimethylolpropane [68] or pentaerythritol [69, 70], which unlike glycerol do not contain β -hydrogen atoms. Valero et al. [71] reacted pentaerythritol-modified castor oil with yucca starch derived glycosides to generate polyol glycosides which were later reacted with isophorone diisocyanate to obtain polyurethanes. These polyurethanes showed excellent chemical resistance, hardness and tensile strength compared to the polyurethanes synthesized from unmodified castor oil. Petrovic et al. [72] investigated transesterification of substantially pure polyricinoleic acid methyl esters with trimethylol propane to obtain new non-crystallizing triols with varying molecular weights and low viscosity. These polyols were further reacted with methylene diphenyl diisocyanate (MDI) to obtain elastomers having glass transition temperatures, T_g , below -60°C . Karak et al. [73] reported the synthesis of hyperbranched thermoplastic PU, derived from castor oil, a macroglycol [e.g. poly(ϵ -caprolactone) (PCL)-diol or PEG], and MDI, with or without chain extender. The hard-segment content, the nature of the macroglycol and the composition of the polymers had prominent effects on thermal and crystallization properties. Higher crystallinity and higher thermal stability were resulted from a higher hard segment content, while PUs with PEG as soft segments have higher melting points, in comparison to PCL-diol (58.8°C for PEG based and 48.3°C for PCL-diol, respectively). A novel green poly(ether-ester urethane) insulating coating based on polyols derived from glycolized poly-ethylene terephthalate (PET), castor oil, adipic acid and a blocked isocyanate

made from trimethylol propane, toluene diisocyanate (TDI) and N-methyl aniline were also reported [74]. It was observed that excellent mechanical properties, 326.1% elongation at break, 16.88 MPa tensile strength, as well as superior electrical insulation characteristics were observed in the cases of PU based on the lowest-molecular weight polyols. Furthermore, phenyl diisocyanate-modified difunctional castor oil or its blends with poly(propylene glycol) with two different ratios of 1,4-butane diol as chain extender and TDI were used for synthesizing PU elastomers [75].

Composites prepared from oil-based polymers are gaining prominence in recent years. A graphite composite used as an electrode material was made by a PU resin made from castor oil [76]. Good mechanical properties, appropriate electric resistance, ease of preparation and surface reformation were observed in these composites synthesized using castor oil based PUs. Metal filled castor oil based PUs were synthesized and their gel points were predicted [77]. The gelation time depended on the process temperature, OH content, functionality of polyol and also the amount of filler used. Furthermore, the synthesis of biodegradable PU based on castor oil and PEG through the reaction of epoxy-terminated PU prepolymers (EPU) with 1,6-hexamethylene diamine (HMDA) as the curing agent was also reported in the literature[78]. The introduction of hydrophilic polyols into the backbone of vegetable oil based PU increased the degradation rate due to enhancement in water permeability and increase in the surface and bulk hydrophilicities. In addition, utilization of castor oil or modified castor oil in the synthesis of interpenetrating polymer networks (IPN) was reviewed and extensively reported in the literature [79-87].

5.3 Materials and methods

Ethylenediamine (ED), ethylene carbonate (EC), Dimethylolpropionic acid (DMPA), isophorone diisocyanate (IPDI), methyl ethyl ketone (MEK), triethylamine (TEA) and dibutyltin dilaurate (DBTL), as well as all the reagents required for the titrations (e.g. butanol, pyridine, acetic anhydride, hydrochloric acid, hydroxide potassium, phenolphthalein and bromophenol blue) were purchased from Sigma Aldrich. Defatted soymeal was obtained from Zeeland farms, Michigan. All chemicals were used as received unless otherwise noted.

5.3.1 Measurements

5.3.1.1 Attenuated total reflection-fourier transform infrared (ATR-FTIR)

The ATR-FTIR spectra were acquired on a FT-IR (Shimadzu Co., Tokyo, Japan, IRAffinity-1) equipped with a single reflection ATR system (PIKE Technologies, Madison, USA, MIRacle ATR).

5.3.1.2 End group analysis

Acid values (mgKOH/g) were determined in accordance with ASTM D1980-87. Samples were dissolved in water and were then titrated with 0.2N KOH in water in the presence of phenolphthalein as indicator. Amine values (mgKOH/g) were determined in accordance with ASTM D2073-92. Samples were dissolved in water and were then titrated with freshly standardized 0.2N HCl in water by using bromophenol blue solution as indicator. Hydroxyl values were determined according to ASTM D1957-86 . Samples were dissolved in pyridine containing acetic anhydride solution and boiled using a steambath of 2 hours. The solution was then cooled down with distilled water. The remaining acetic anhydride was thus transformed into

acetic acid. Butanol was added to the solution and the remaining acetic acid was titrated with freshly standardized 0.2N KOH in methanol using phenolphthalein as indicator.

5.3.1.3 Differential scanning calorimetry (DSC)

DSC measurements were performed using DSC Q2000 TA Instruments under nitrogen flow. To determine the thermal properties profile, a sample (5-10 mg placed in an aluminium pan) was heated up to 100 °C at 10 °C/min, held at this temperature for 3 min to remove the thermal history, then cooled to -70 °C at 10 °C/min and finally heated again to 100 °C at 10 °C/min. The glass transition temperature T_g was determined from the inflection point. This value was determined from the second heating scan.

5.3.1.4 Thermogravimetric analysis (TGA)

TGA measurements were conducted under nitrogen flow using a Hi-Res TGA 2950 apparatus from TA Instruments. In a typical experiment, a sample (10-20 mg placed in an aluminium pan) was heated up to 550 °C at 10 °C/min. The characteristic degradation temperatures were taken as the temperature at the maximum of the derivative thermogram (DTG) curve (T_{dmax}) for each degradation step and at which the sample weight equaled 95% ($T_{95\%}$).

5.3.1.5 Barrier properties against water vapor and oxygen permeation

Permatran - W 3/31 Water vapor permeability instrument from Mocon, Inc., Minneapolis was used for testing the WVTR of various polyurethane coatings made on a standard paper substrate (Form WB, from Lenetta) at a temperature of 23 °C, barometric pressure 760 mm Hg, and relative humidity (100%). An OX-TRAN Model 2/21 Mocon instrument was used for testing the oxygen transmission rates at a temperature of 23 °C, barometric pressure 1 atm, relative

humidity (0-5%) and a permeant concentration of 100%. The thickness of the coatings was measured using a digital micrometer and recorded. The coated samples were masked using aluminium foil with a surface area exposure of 3.14 cm².

5.3.1.6 Water absorption resistance test of coatings (Cobb test)

Cobb test samples were cut into 12.5 cm x 12.5 cm square sizes and weighed. The samples were then placed on a neoprene mat and held tightly by clamping on a 100 cm² Cobb cylinder. 100 ml of water was poured on the sample surface and the timer was commenced at the same time. After 1 minute 45 seconds (for the 2 minute test and after 29 minutes 45 seconds for the 30 minute test), the water was poured from the Cobb cylinder, taking care not to drop any water on the portion of the sample outside of the 100 cm² ring. The sample was then removed, placed on a sheet of blotting paper with the wetted side up, covered with a second blotting paper on the top and rolled once forward and once backward using a 10 kg roller to remove any excess water. The sample was then re-weighed again and the Cobb value was measured according to the following equation.

$$\text{Cobb Value (gsm)} = \frac{\text{Paper mass (Final)} - \text{Paper mass (initial)}}{0.01 \text{ m}^2}$$

5.3.1.7 Scanning electron microscopy

The morphology of the cross-section and the surface of the PU coated sheets was observed by scanning electron microscopy (JEOL 6610LV SEM, JEOL Ltd., Tokyo, Japan). The sheets were fractured in liquid nitrogen to preserve the cross-section and then sputter coated with osmium (\approx 20 nm thickness) in an NEOC-AT osmium coater (Meiwafosis Co., Ltd., Osaka, Japan) prior to being viewed under the microscope.

5.4 Experimental procedures

5.4.1 Soymeal-based polyurethane dispersions

5.4.1.1 Aqueous alcoholic treatment of soymeal

Defatted soymeal (880 g) was added to a 5000 ml three necked round bottom flask fitted with a mechanical stirrer and washed with 2000 ml of 60% ethanol water solution under continuous stirring for 3 hours. The soymeal was then allowed to settle down and the supernatant alcoholic mixture is drained out. This procedure was repeated twice to remove soluble carbohydrates and dried in a oven at 80°C overnight. The alcohol treated soymeal (700 g) was then hydrolyzed with HCl, followed by neutralization with NaOH, amination with Ethylenediamine, and reacted with ethylene carbonate to synthesize soymeal polyol similar to the procedures mentioned in Chapter 2.

5.4.1.2 Synthesis of soymeal polyurethane dispersions

Soymeal polyol (15.1 g, 0.12 equivalents of OH), DMPA (8.4 g, 0.12 equivalents of OH), IPDI (28.5 g, 0.26 equivalents of NCO), 1 drop of dibutyltin dilaurate and 50 ml of MEK solvent were added to a 500 ml three necked round bottom flask fitted with a mechanical stirrer, nitrogen inlet, condenser and heated in an oil bath. The ratio of the NCO groups to the OH groups present in the soymeal polyol, DMPA as well as the secondary amines present in the soymeal polyol is taken to be 1.03. The reaction was carried out at 78°C for 3 hours under continuous stirring. The reaction mixture was then cooled down to 60°C and triethylamine (6.3 g, 1.0 equivalent of DMPA) was added to neutralize the free carboxylic groups present in the PU chains and stirred for another 30 minutes. Then water (158 g) was added to the pre-polymer and it was vigorously

agitated for 1 hour to obtain a stable dispersion of 20% solid content. The polyurethane dispersions were then applied on coating paper (Form - WB, purchased from Leneta) using a wire-wound coating rod (0.5 mil guage, BYK instruments) and then dried under ambient conditions for 72 hours.

5.4.2 Synthesis of castor oil based polyurethane dispersions (CO-PUDs)

Castor oil (83.97 g, 0.24 OH molar equivalents), DMPA (18.28 g, 0.26 OH molar equivalents), IPDI (57.32 g, 0.51 NCO molar equivalents) and 3 drops of dibutyltin dilaurate along with methyl ethyl ketone (106 g) were added to a 1000 ml three necked round bottom flask and stirred continuously for 3 hours at a temperature of 78°C by heating using an oil bath. The ratio of the NCO/OH groups used in the reaction was 1.03/1.0. After 3 hours of reaction, the reaction mixture was cooled down to 60°C and the carboxylic groups present in the polymer backbone were neutralized by adding triethylamine (13.79 g; 0.14 moles; 1.0 equiv. for DMPA) and it was stirred for another 30 minutes. After cooling down the mixture to room temperature, water (414 g) was added to the reaction mixture and it was stirred vigorously for another 1 hour to obtain a waterborne polyurethane dispersions with approximately 25% solid content. The PU dispersions were coated on a cellophane substrate using a wire-wound coating rod (0.5 mil guage, BYK instruments) and then dried under ambient conditions for 72 hours.

5.5 Results and discussion

5.5.1 Soymeal polyol PUDs

The flow chart for the synthesis of polyurethane dispersions from soymeal is shown in Figure 5.8. The carbohydrate content in the soymeal before and after the alcoholic treatment were determined according to ASTM E1758-95 (Standard Test Method for Determination of

Carbohydrates in Biomass by High Performance Liquid Chromatography). Papyrus wood samples were taken as the control for determining the accuracy of the method and the soymeal samples before and after alcoholic treatment were analyzed in duplicate and the results are reported on a dry weight basis as given in Table 5.3.

Table 5.3: Carbohydrate content analysis in soymeal

Samples	% Glucan	% Xylan	% Galactan
Wood	45.10±0.39	17.47±0.27	9.05±0.12
Soymeal	10.99±0.43	2.36±0.00	8.16±0.00
Alcohol treated soymeal	6.33±0.02	1.47±0.07	6.63±0.34

This method requires the soymeal samples to be finely ground, followed by two stage hydrolysis using concentrated sulphuric acid (74%) in the first stage for 1 hour, and hydrolysis using diluted sulphuric acid (4%) in the second stage (2 hours). Then the hydrolyzate was diluted using calcium carbonate, and the carbohydrate content analyzed using HPLC. The carbohydrate content in the papyrus wood was taken as the control for determining the accuracy of the test method. The carbohydrate content in the soymeal was 10.99% glucan, 2.36 % zylan, 8.16% galactan. The carbohydrate content in the ethanol-water treated soymeal was 6.33% glucan, 1.46% xylan, 6.6% galactan on a dry weight basis. Generally, there are three major methods for extracting the carbohydrates from the defatted soymeal to synthesize soy protein concentrates; the aqueous alcohol wash process, acid wash process, and the water wash process. These methods are commonly used to synthesize soy protein concentrates without solubilizing the major protein fractions. These are not different methods for manufacturing the same product, but each method produces a different type of concentrate, with distinct characteristics and specific

uses [88]. The aqueous alcoholic treatment using 60% ethanol-water solution was employed in our case to remove the carbohydrates from the defatted soymeal. The ethanol/water extraction process allows the removal of soy oligosaccharides and soluble non-starch polysaccharides. Ethanol extraction achieves a 90% reduction in the oligosaccharides in the soybean meal [89]. The carbohydrate composition of the soybean varies according to the geographical locations where the soybean was grown, harvest conditions and post-harvest processing [90]. Besides the variation due to genotype and origin of the soybean, the carbohydrate content may also be related to the method of analysis [91]. According to Elridge et. al (1979) [92], the carbohydrate content in the defatted soy flour was 10.9% glucan, 0.97% xylan, 7.6% galactan and the carbohydrate content in the soy protein concentrate was 5.06% glucan, 0.92% xylan, 5.69% galactan. The carbohydrate content for the defatted soymeal and alcohol treated soymeal obtained by our analysis closely matches with the results mentioned in the literature.

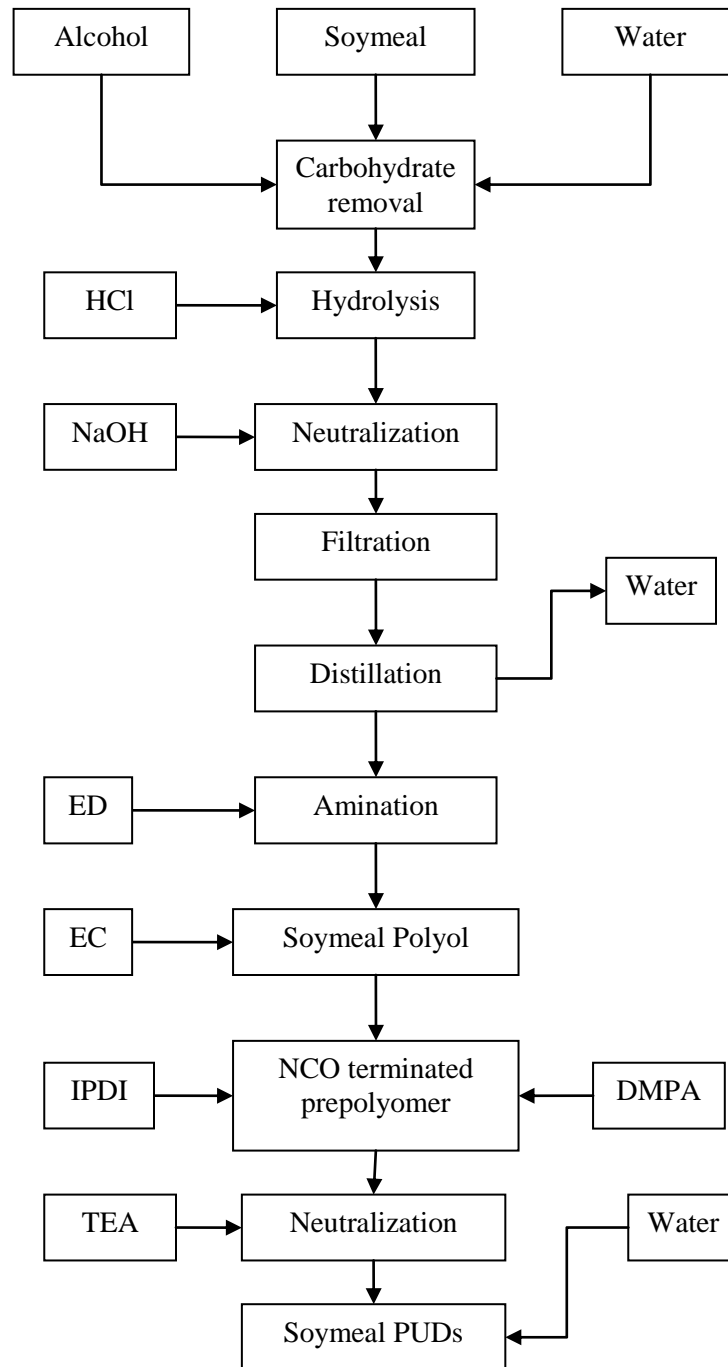


Figure 5.8: Flow chart for the synthesis of PUDs from soymeal

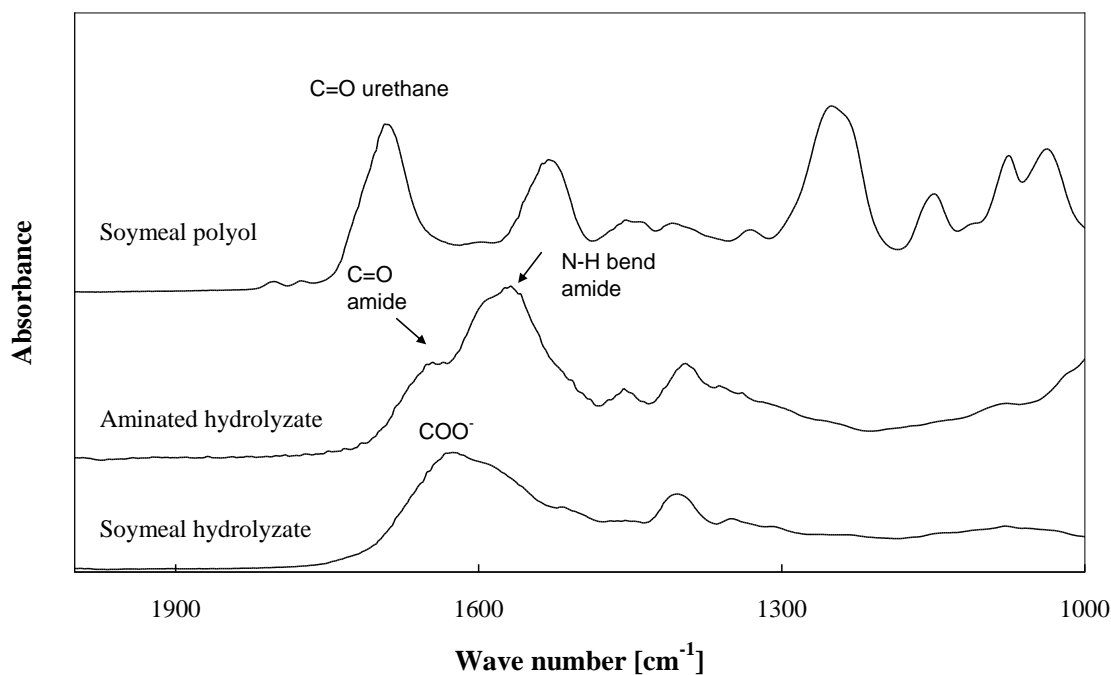


Figure 5.9: FTIR of soymeal polyol and its intermediates

The soymeal hydrolyzate as analysed by FTIR in Figure 5.9 shows a peak at 1625 cm^{-1} which was typical of C=O stretch of carboxylic acids in the amino acid mixture. The protection of carboxylic groups in the hydrolyzate by ethylene diamine to yield the aminated hydrolyzate was confirmed by FTIR. Significant changes observed from soymeal hydrolyzate to aminated hydrolyzate spectrum was the shift in the C=O stretch from 1625 cm^{-1} to 1656 cm^{-1} , typical of C=O stretch of amides. In the next step, after the reaction of aminated hydrolyzate with ethylene carbonate to synthesize hydroxy-terminated soymeal polyols, the formation of urethane groups in this reaction was confirmed by the appearance of a peak corresponding to C=O stretch of urethane groups at 1697 cm^{-1} . The end group analysis of soymeal polyol and its intermediates is given in Table 5.4.

Table 5.4: End group analysis of soymeal polyol

	Amine value (mgKOH/g)		Acid value (mgKOH/g)		Hydroxyl value (mgKOH/g)	
	Calc.	Exp.	Cal.	Exp.	Calc.	Exp.
Soy hydrolyzate	483.7	33.7± 0.8	549.4	64.9± 1.2	-	-
Aminated hydrolyzate	726.7	517.8± 9.5	0	6.1± 3.1	-	-
Soymeal polyol	0	50.1± 4.9	0	-	456.23	435.74± 6.2

The amine and acid values of soymeal hydrolyzate do not match with the calculated values due to the zwitterionic nature of the amino acids. A significant increase in the amine value of aminated hydrolyzate (517.8 mgKOH/g) was observed, followed by a decrease in the acid value (6.1 mgKOH/g), indicating the protection of carboxylic groups followed by the addition of ethylene diamine upon amidation. The decrease in the amine value (50.1 mgKOH/g) followed by the hydroxyl value (435.74 mgKOH/g) signifies the conversion of amines to hydroxyl-terminated soymeal polyols.

The FTIR spectra of soymeal polyol based PU films are shown in Figure 5.10. The peak at 2958 cm^{-1} was assigned to C-H symmetric bending vibration of $-\text{CH}_3$, N-H stretching vibration at 3329 cm^{-1} , N-H bending vibration at 1543 cm^{-1} , C=O stretch of urethanes at 1697 cm^{-1} and the $-\text{NCO}$ group at 2273 cm^{-1} did not appear, implying that a complete reaction of $-\text{NCO}$ of IPDI with $-\text{OH}$ of soymeal polyol had occurred.

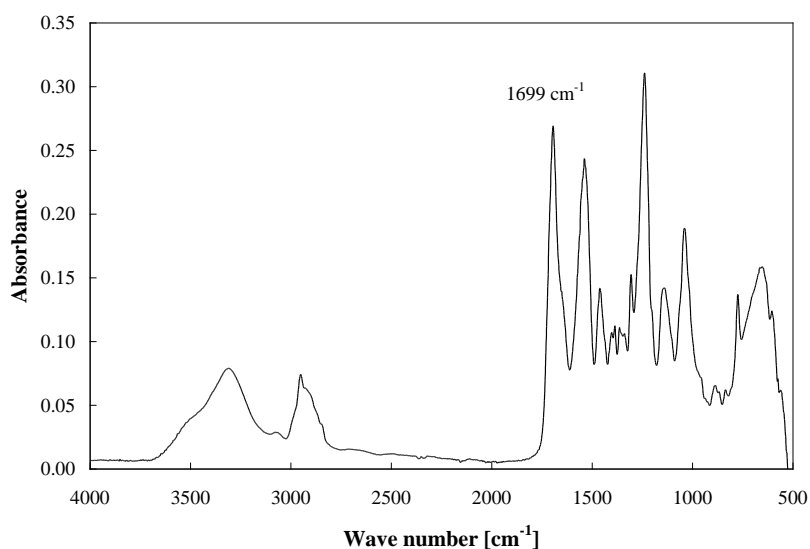


Figure 5.10: FTIR spectra of coatings made using soymeal polyol PUDs

TGA and its derivative thermograms of soymeal polyol PUD films under nitrogen atmosphere are shown in Figure 5.11, T_g , $T_{98\%}$, T_{dmax} and $T_{5\%}$ data are listed in Table 5.5. A small and monotonous weight loss was observed from 70 °C to 174°C, most probably related to methyl ethyl ketone and water evaporation. The first stage of degradation involved minor degradation at 174 °C and then the main degradation at 228 °C. Urethane bonds are known to dissociate and re-associate simultaneously starting around 160 °C with irreversible degradation above 200 °C. Two different mechanisms of degradation of urethane bonds were proposed in the literature; one relates to the formation of primary amines and olefins and the other involves the formation of secondary amines [93]. The second stage of degradation started at an onset temperature of 272°C with the maximum degradation at 335°C, which could possibly be the degradation of amide groups derived from soymeal polyol [94], followed by dehydrogenation and depolycondensation of alkyl groups of polyol [95].

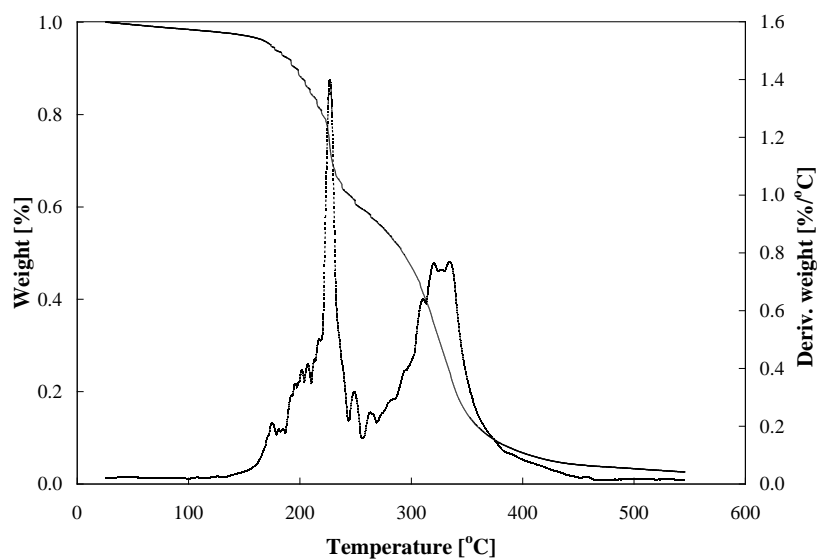


Figure 5.11: TGA and its derivative curve for soymeal polyol PUD films.

Table 5.5: Glass transition and degrading temperatures of soymeal polyol PUD films

Sample	DSC	TGA		
	T _g (°C)	T _{5%} (°C)	T _{dmax} (°C)	T _{98%} (°C)
Soymeal polyol PUD films	87.7	174°C	228°C	545.5

Figure 5.12 shows the DSC thermogram of the soymeal polyol PUD films. The polymer had a glass transition temperature of 87.7°C and is brittle at room temperature. No melting peaks are observed, indicating an amorphous film.

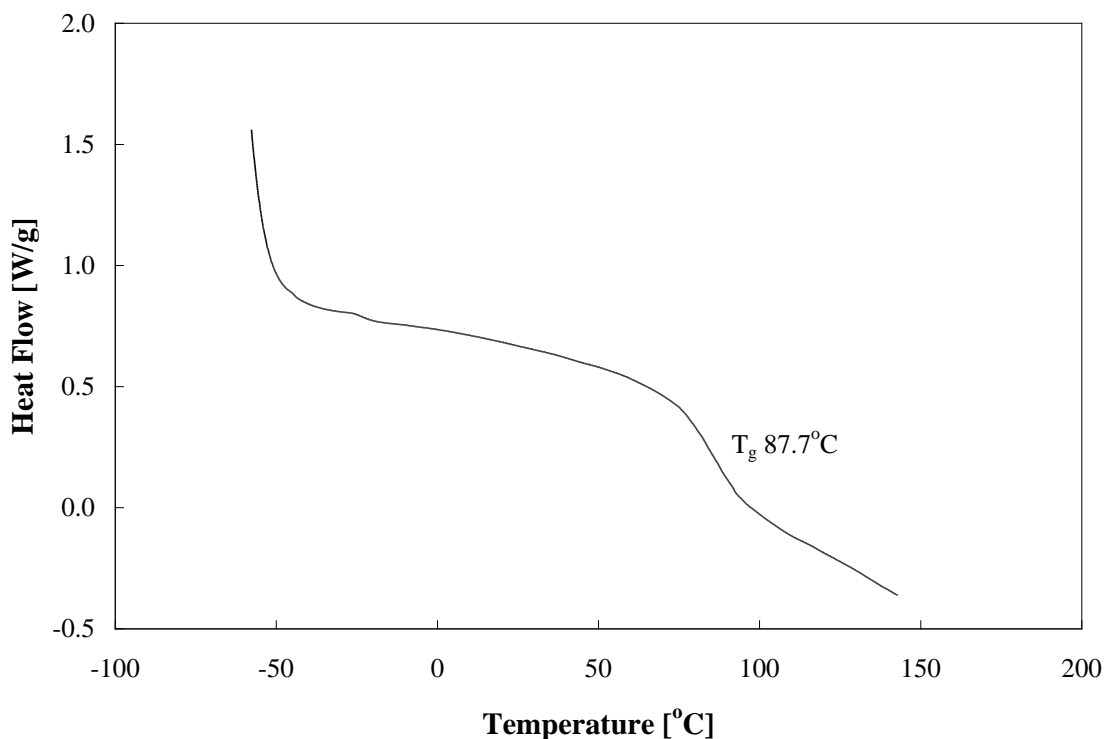


Figure 5.12: DSC scan for the soymeal polyol based PUD film

The surface and cross-sectional SEM images of the blank uncoated Form-WB substrates and soymeal polyol PUD coatings are shown in Figure 5.13 and 5.14, respectively. The surface

and cross-sectional images of the PUD coatings shown from Figure 5.14 indicate that the adhesion between the polyurethane matrix and the surface of the substrate was good as was indicated by the cross-sectional image. The surface morphology of the coatings indicated no presence of any pinholes.

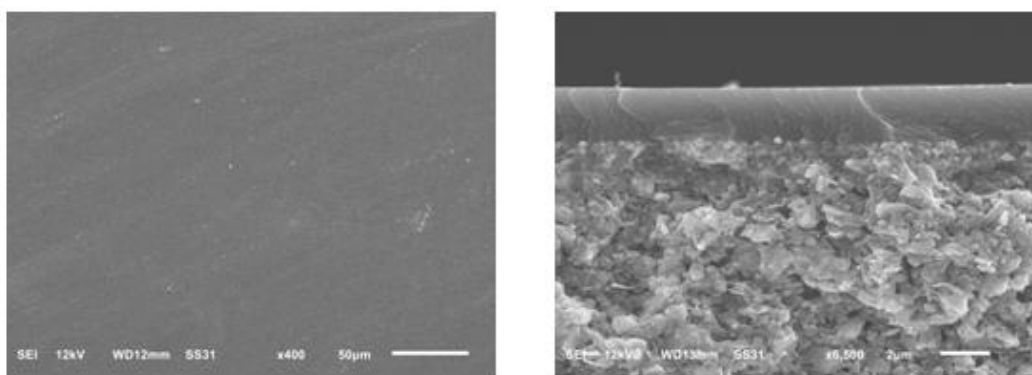


Figure 5.13: Surface (left) and cross-sectional (right) SEM images of Form-WB uncoated substrate

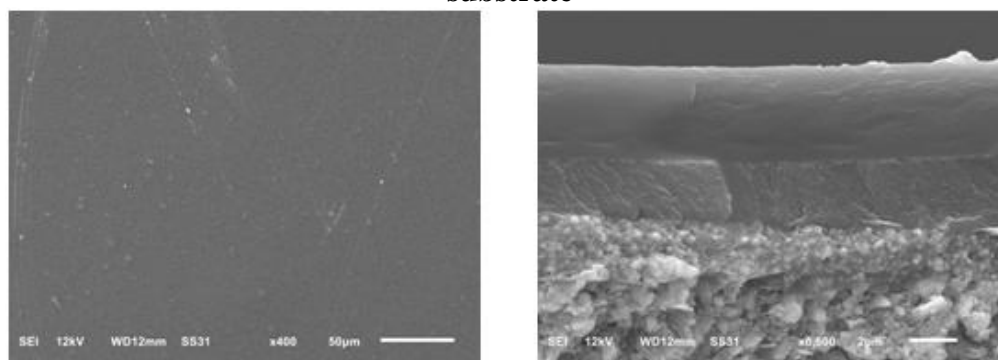


Figure 5.14: Surface (left) and cross-sectional (right) SEM images of soymeal polyol PUD coatings

Table 5.6: Cobb values, WVTR and contact angles of soymeal polyol PUD coatings

Coating sample	Cobb values, gm	WVTR, (gm/m ² .day)	Contact angle, (°)
Form WB- Blank	0.35±0.07	937.8±27.1	85.2±0.7
Soymeal polyol-PUD	4.35±0.35	314.1±12.7	33.0±1.4

Table 5.6 shows the Cobb values, water vapor transmission rates (WVTR) and contact angles of the soymeal polyol PUD coatings. The uncoated substrate had a Cobb value (2 min test) of 0.35 gsm, while the substrates coated with soymeal polyol PUD coating had a higher Cobb value of 4.35 gsm, indicating poor resistance against water absorption by the coatings. The contact angle analysis done using water on the PUD coated substrates to determine the wettability of the surface of the coatings indicated that the soymeal PUD coatings had a contact angle of 33.0° . The wetting tendency is larger when the contact angle is smaller. A non wetting surface is usually characterized by a contact angle greater than 90° . From the results obtained, it is further confirmed that the coatings were hydrophilic. However, the coated substrates had a significant decrease in water vapor transmission rates compared to the uncoated substrates. The WVTR of soymeal polyol PUD coated substrate and uncoated substrate were $314.1 \text{ gm/m}^2\cdot\text{day}$ and $937.8 \text{ gm/m}^2\cdot\text{day}$, respectively. This variation in the results between Cobb tests, contact angle analysis and water vapor transmission rates could be better explained by understanding the phenomena behind them. Cobb tests and contact angle analysis is more of a surface phenomenon, whereas permeation of water vapor is a multi-step process which involves absorbance of the permeant in the polymer, diffusion of the permeant through the polymer matrix and ultimately desorption from the polymer matrix towards the lower concentration side. As the permeation is a function of both the solubility coefficient (S) and diffusion coefficient (D), a polymer can have a lower permeability if it has a low value of D or a low value of S or both. The diffusion coefficient is affected by the properties of the polymer such as molecular packing, amorphous content, cross linking density and amount of crystallinity. The soymeal polyurethane dispersions have a highly crosslinked structure due to their multifunctionality,

which could limit the movement of the permeant through the free volume available in the polymer. The higher the cross linking density, the lower the free volume available in the polymer for the permeant to pass through, and perhaps this could be the reason why the coated dispersions have barrier properties inspite of their hydrophilicity as indicated by contact angle analysis. Polydimethylsiloxane is a class of silicon based polymers, which was observed to display such contrasting behaviour, originally hydrophobic in nature and yet highly permeable to water vapour [96-97].

5.5.2 Castor oil PUDs

Figure 5.15 shows the flow chart for the synthesis of PUDs from castor oil. The castor oil based PUDs were characterized for experimental solid content by running samples using TGA under isothermal conditions at 120°C for 45 minutes. The experimental solid content of the castor oil PUDs as shown in Table 5.7 was 25.2%. The stability of the dispersions was ascertained by monitoring the viscosity using a Brookfield viscometer at different RPMs under regular time intervals. The dispersions were found to be stable with no significant changes in the viscosity over a period of time as shown in Figure 5.16. The coat weight of the PUD coatings was 3.27 gsm with a thickness of 0.3 mil.

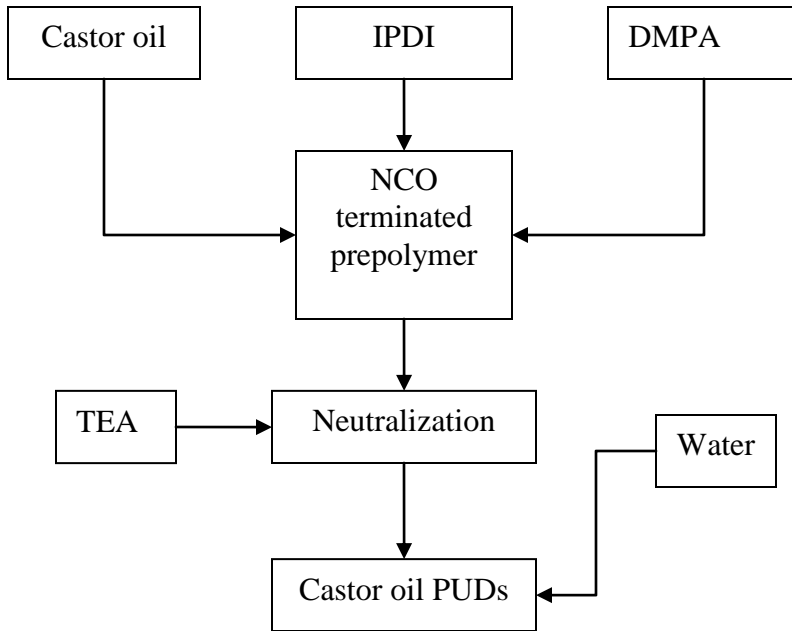


Figure 5.15: Flow chart for the synthesis of PUDs from castor oil

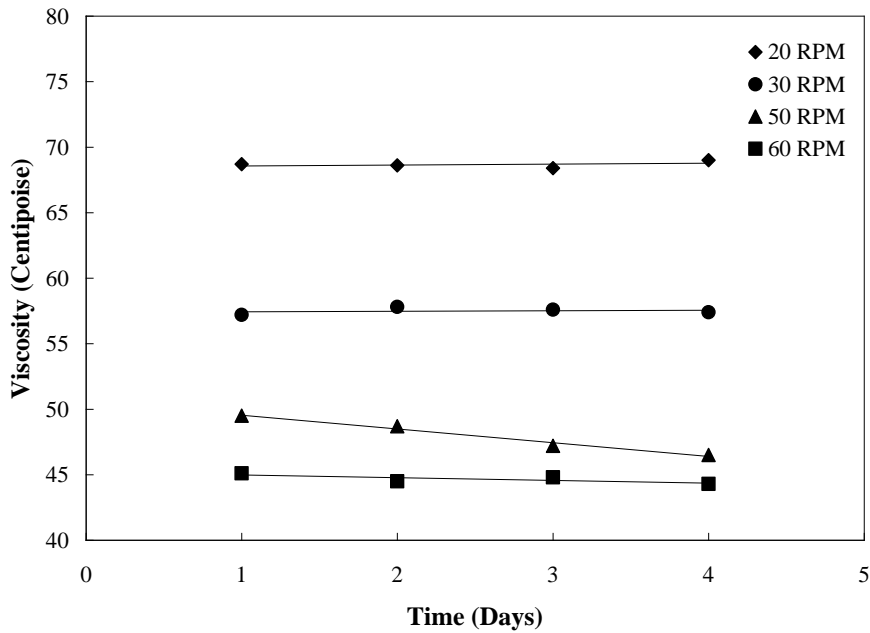


Figure 5.16: Viscosity of the castor oil PUDs as a function of time at different RPMs

Table 5.7: Properties of castor oil PUDs & coatings

Sample	Experimental solid content, %	Viscosity, cP, @60 RPM	Coat weight, gsm	Coating Thickness, mil
Castor oil PUDs	25.2	44 - 46	3.27±0.24	0.3±0.05

The FTIR spectrum of castor oil based PU coated film is shown in Figure 5.17. The peak at 2900 cm^{-1} was assigned to the C-H symmetric bending vibration of $-\text{CH}_3$, N-H stretching vibration at 3340 cm^{-1} , C=O stretch of urethanes at 1705 cm^{-1} and the absence of the $-\text{NCO}$ group at 2273 cm^{-1} , implying that a complete reaction of $-\text{NCO}$ of IPDI with $-\text{OH}$ of castor oil had occurred.

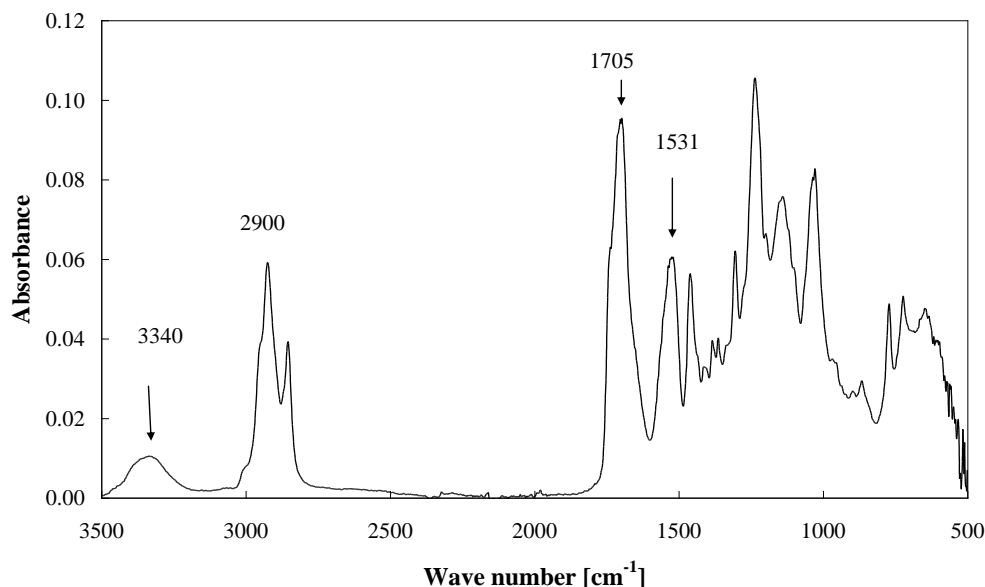


Figure 5.17: FTIR spectrum of castor oil PUD coated film

Figure 5.18 shows the TGA curve and the derivative curve for the castor oil based PUD film and the $T_{5\%}$, T_{dmax} , and $T_{98\%}$ are listed in Table 5.8. The first stage of degradation involved

minor degradation at 160.7 °C and then the main degradation at 305.7 °C. The degradation of the samples in the temperature range 150 - 300°C can be attributed to the dissociation of the urethane bonds to form isocyanates, alcohols, primary and secondary amines, olefins and carbon dioxide. The second stage of degradation occurring above 300°C is due to the chain scission of the castor oil, while the last stage degradation above 500°C corresponds to the thermo-oxidative degradation of the alkyl groups of the polyurethanes. Figure 5.19 shows the DSC thermograms of the castor oil PUDs and the T_g of the samples is shown in Table 5.8. The T_g of the film is around 22.8°C and no melting peak is observed, indicating an amorphous polymer.

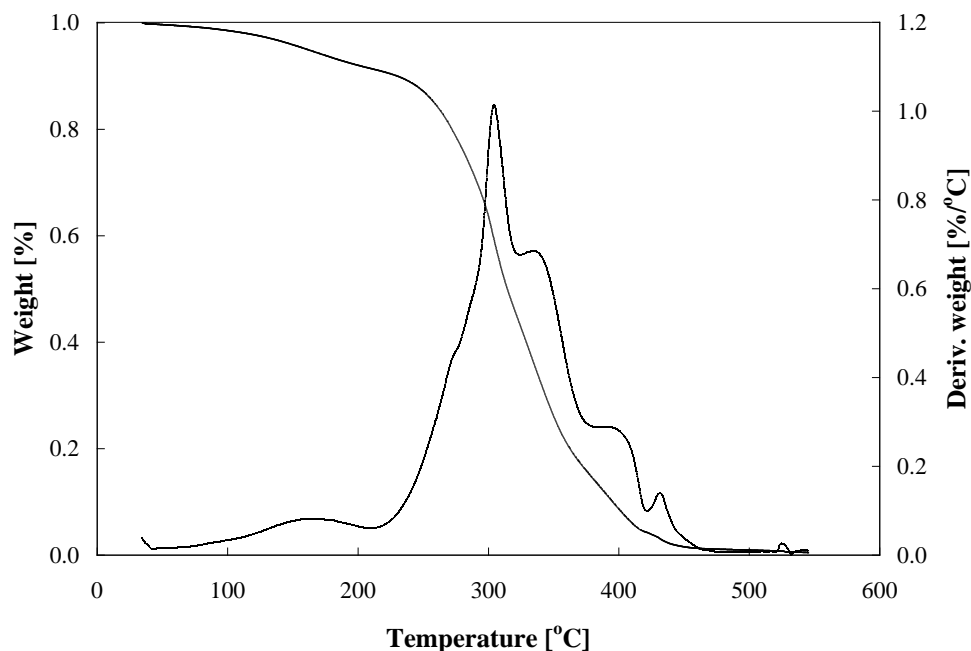


Figure 5.18: TGA and its derivative curve for castor oil PUD film.

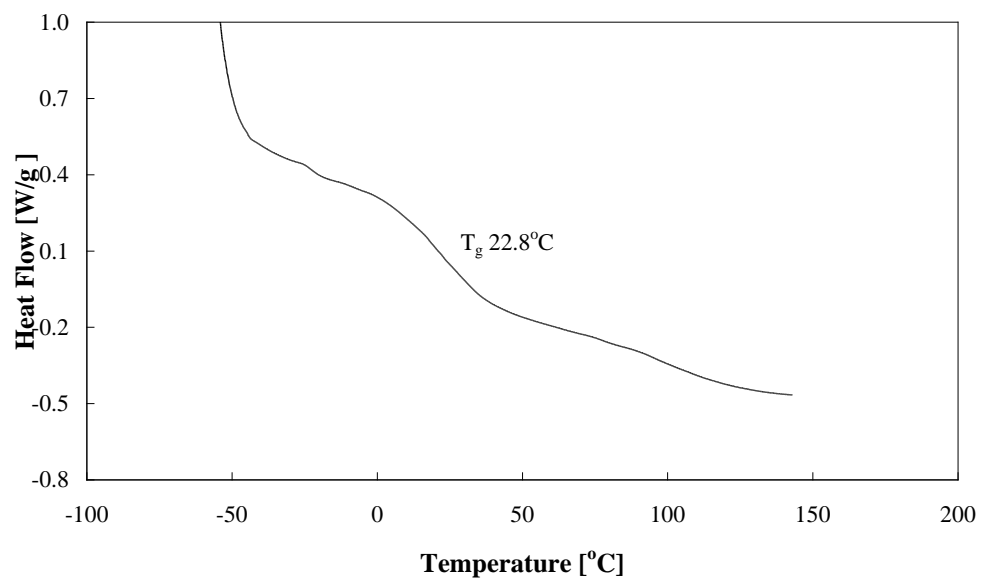


Figure 5.19: DSC scan for the castor oil PUD film

Table 5.8: Glass transition and degrading temperatures of castor oil PUD films

Sample	DSC	TGA		
	T _g (°C)	T _{5%} (°C)	T _{dmax} (°C)	T _{98%} (°C)
Castor oil PUD films	22.8	160.7	305.7	440.9

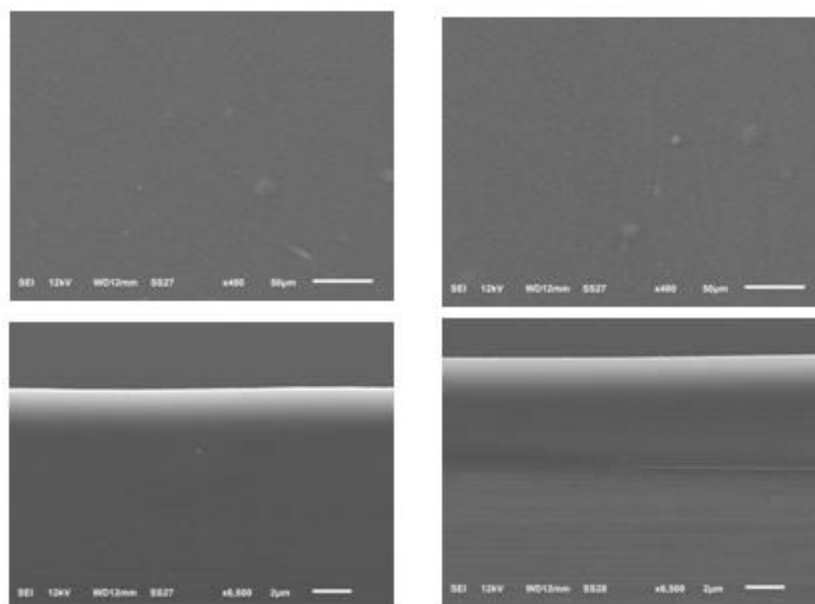


Figure 5.20: SEM photographs of uncoated (left) and coated (right) cellophane substrate (top): SEM photographs showing the cross-sections of the uncoated (left) and coated (right) cellophane substrates (bottom)

The surface and cross-sectional SEM images of the blank uncoated Cellophane and castor oil PUD coated substrates are shown in Figure 5.20. The cross-sectional images of the coated substrates indicate good adhesion between the polymer matrix and the surface of the substrate. The surface morphology of the coatings indicated no presence of any pinholes.

Table 5.9: Cobb values, contact angles, WVTR and OTR results of castor oil PUD coatings

sample	Cobb values (2 min), gsm	Cobb values (30 min), gsm	Contact angle, (°)	WVTR, (gm/m².day)	OTR, (cc/ m².day)
Cellophane	35.44±0.88	41.16±1.62	30.16±1.38	-	0.10±0.001
CO-PUD	1.78±0.19	18.86±1.31	93.25±2.67	1354.15±8.15	-

Table 5.9 shows the Cobb values, water vapor transmission rates (WVTR), Oxygen transmission rates (OTR) and contact angles of the castor oil PUD coatings. The uncoated cellophane substrate had Cobb values of 35.44 gsm and 41.16 gsm for the 2 minute and 30 minute tests respectively. The castor oil PUD coated cellophane substrate had showed significant resistance to water absorption as indicated by the Cobb values, 1.78 gsm (2 min test) and 18.86 gsm (30 min test). This increase in resistance to moisture absorption is attributed to the non polar hydrocarbons present in the castor oil polyurethane dispersions. These results are further confirmed by an increased contact angle of the coated substrate (93.25°) compared to the cellophane (30.16°). The coated substrate had a contact angle greater than 90° indicating the hydrophobic nature of the coating, while the uncoated cellophane had a smaller contact angle indicating its sensitivity to moisture. A significant resistance to water vapor transmission rates is further observed in the case of coated substrates. The WVTR of the cellophane is so high that the values could not be obtained as they are far beyond the limitations of the permeability testing equipment. The castor oil PUD coated cellophane showed significant resistance to water vapor transmission and a WVTR value of $1354.15 \text{ gm/m}^2\cdot\text{day}$ was obtained. Cellophane had good oxygen barrier properties as indicated by the OTR values of $0.01 \text{ cc/m}^2\cdot\text{day}$. However, in contrast to WVTR, the coated cellophane substrate did not show any significant resistance to oxygen; the values are so high they are beyond the limitations of the oxygen permeability testing equipment and no readings could be obtained. Water molecules are known to associate and build clusters during their diffusion through polymer matrices [98]. The clusters of water molecules are larger in size than the oxygen molecules and probably cannot travel through the thin gaps between

the polymer matrix. This offers a possible explanation for the difference observed in the oxygen and water vapor transmission rates of the coated substrates. Cellophane is highly sensitive to moisture and the probability of intermolecular hydrogen bonding forces being disrupted upon exposure to moisture is very high. This could be the possible reason for the low barrier properties of the aqueous polyurethane dispersion coatings.

5.5.3 Comparison between soymeal polyol and castor oil based PUDs

Significant differences were observed between the properties of soymeal polyol and castor oil based polyurethane dispersions. The differences in the properties are primarily attributed to the differences in the nature of the polyol component used in the dispersions. Soymeal polyol had a hydroxyl value of 435.74 mgKOH/g, which resulted in a highly crosslinked rigid polyurethane film upon reaction with the isocyanate component. In comparison, castor oil had a lower hydroxyl value of 163 mgKOH/g and resulted in a flexible film with fewer cross links between the polymer chains on reaction with isocyanate. These differences could be clearly observed by comparing the thermal properties of both the PUDs. Soymeal polyol PUDs had a higher T_g of 87.7°C compared to the castor oil based PUDs (22.8 °C). Soymeal polyol synthesized from amino acids exhibited hydrophilicity due to the short alkyl chain between the amide and urethane linkages, while the castor oil composed of non-polar hydrocarbons exhibited a hydrophobic nature. As a result, soymeal polyol PUDs exhibited lower Cobb values and contact angles compared to the castor oil based PUDs.

5.6 Conclusions

In this work, aqueous polyurethane dispersions were synthesized using soymeal polyol and castor oil as the polyol components and applied as coatings on different substrates. A systematic investigation of the thermal properties, Cobb tests, contact angle analysis, barrier properties against water vapor and oxygen permeation enabled the study of the contribution of the polyol component to the properties of the PUDs. Soymeal polyol based PUD coatings were more rigid having a higher glass transition temperatures as a result of the higher degree of crosslinking compared to the castor oil PUDs which were more rubbery and flexible. Castor oil based PUD coatings exhibited significant resistance to water absorption compared to the soymeal based PUDs as indicated by the Cobb values, contact angle and water vapor transmission rates. The differences in these properties are attributed to the differences in the polarity of the molecular chains. Furthermore, the barrier properties of the coatings on cellophane were influenced by the aqueous nature of the polyurethane dispersions, which could disrupt the intermolecular hydrogen bonding forces inherent in the substrate.

REFERENCES

REFERENCES

1. SZycher, (1999) M. Szycher's Handbook of Polyurethanes; CRC: Boca Raton, FL.
2. Zhang L, Jeon HK, Malsam J, Herrington R, Macosko C W (2007) Substituting soybean oil - based polyols into polyurethane flexible foams. *Polymer* 48: 6656-6667
3. Kim BS, Kim BK (2005) Enhancement of hydrolytic stability and adhesion of waterborne polyurethanes. *J Appl Polym Sci* 97:1961-1969
4. Athawale VD, Nimbalkar RV (2011) Waterborne Coatings Based on Renewable Oil Resources: an Overview. *J Am Oil.Chem Soc* 88:159-185
5. Pfister DP, Xia Y, Larock RC (2011) Recent Advances in Vegetable Oil Based Polyurethanes. *ChemSusChem* 4:703-717
6. Velayutham TS, Abd Majid WH, Ahmad AB, Kang GY, Gan SN (2009) Synthesis and characterization of polyurethane coatings derived from polyols synthesized with glycerol. *Progress in Organic Coatings* 66:367-371
7. Narayan R (2000) Reactive Extrusion Process Produces Biodegradable Films & Injection Molded Products Based on Soy Protein-Polyester. *MRS (Materials Research Society) Bulletin*, Vol. 28:10
8. Narayan R (2006) Rationale, Drivers, Standards, and Technology for Biobased Materials in Renewable Resources and Renewable Energy, CRC Press, Ed Mauro Graziani & Paolo Fornasiero.
9. Williams CK, Hillmyer MA (2008) Polymers from renewable resources: a perspective for a special issue of polymer reviews. *Poly Rev* 48:1-10
10. Igwe IO, Ogbob O (2000) Studies on the properties of polysters and polyster blends of selected vegetable oils. *J Appl Polym Sci* 75:1441-1446
11. Uyama H, Kuwabara M, Tsujimoto T, Kobayashi S (2003) Enzymatic synthesis and curing of biodegradable epoxide - containing polysters from renewable resources. *Biomacromolecules* 4:211-215
12. Oldring PKT, Turk N, (2001) Eds. Resins for Surface Coatings: Polyurethanes, Polyamides, Phenoplasts, Aminoplasts, Maleic Resins.; Wiley: New York, Vol. 3.

13. Li FK, Larock RC (2003) Synthesis, structure and properties of new tung oil - styrene - divinylbenzene copolymers prepared by thermal polymerization. *Biomacromolecules* 4:1018-1025
14. Andjelkovic DD, Valverde M, Henna P, Li F, Larock RC(2005) Novel thermosets prepared by cationic copolymerization of various vegetable oils - synthesis and their structure - property relationships. *Polymer* 46:9674-9685
15. Lascala J, Wool RP (2005) Property analysis of triglyceride - based thermosets. *Polymer* 46: 61-69
16. Khot SN, Lascala J, Can C, Morye SS, Williams GL, Palmese G R, Kusefoglou SH, Wool RP (2001) Development and application of triglyceride - based polymers and composites. *J Appl Polym Sci* 82:703-723
17. Petrovic ZS, Zhang W, Javni I (2005) Structure and properties of polyurethanes prepared from triglyceride polyols by ozonolysis. *Biomacromolecules* 6:713-719
18. Guo A, Cho Y, Petrovic ZS (2000) Structure and properties of polyurethanes based on halogenated and nonhalogenated soy-polyols. *J Polym Sci Part A: Polym Chem* 38:4062-4069
19. Petrovic ZS, Guo A, Zhang W (2000) Structure and properties of polyurethanes based on halogenated and nonhalogenated soy-polyols. *J Polym Sci Part A: Polym Chem* 38:4062-4069
20. Lligadas G, Ronda JC, Galia M, Biermann U, Metzger JO (2006) Synthesis and characterization of polyurethanes from epoxidized methyl oleate based polyether polyols as renewable resources. *J Polym Sci Part A: Polym Chem* 44: 634-645
21. Lligadas G, Ronda JC, Galia M, Cadiz V (2007) Poly(ether urethane) Networks from Renewable Resources as Candidate Biomaterials: Synthesis and Characterization. *Biomacromolecules* 8:686-692
22. Lligadas G, Ronda JC, Galia M, Cadiz V (2007) Polyurethane Networks from Fatty-acid-based Aromatic Triols: Synthesis and Characterization. *Biomacromolecules* 8:1858-1864
23. Kong ZH, Narine SS (2007) Physical Properties of Polyurethane Plastic Sheets Prepared from Polyols from Canola Oil. *Biomacromolecules* 8:2203-2209
24. Campanella A, Bonnaillie LM, Wool RP (2009) Polyurethane Foams from Soyoil-based Polyols. *J Appl Polym Sci* 112:2567-2578

25. Kong XH, Yue J, Narine SS (2007) Physical Properties of Canola Oil Based Polyurethane Networks. *Biomacromolecules* 8:3584-3589
26. Chian KS, Gan LH (1998) Development of a polyurethane rigid foam from palm oil. *J Appl Polym Sci* 68:509-515
27. Tanaka R, Hirose S, Hatakeyama H (2008) Preparation and characterization of polyurethane foams using a palm oil-based polyols. *Bioresour Technol* 99:3810-3816
28. Sharma V, Banait JS, Kundu PP (2009) Swelling kinetics of linseed oil-based polymers. *J Appl Polym Sci* 111:1816-1827
29. De Souza VHR, Silva SA, Ramos LP, Zawadzki SF (2012) Synthesis and Characterization of Polyols Derived from Corn Oil by Epoxidation and Ozonolysis. *J Am Oil Chem Soc* 89:1723-1731
30. ASTM Standard D16-00. Technology for paint, related coatings, materials and applications. ASTM, West Conshohocken, PA.
31. Saunders JH, Frisch KC (1962) Polyurethanes: Chemistry and technology, vol. XVI. High polymers, Part I. New York: Wiley.
32. Xia Y, Larock RC (2011) Castor-Oil Based Waterborne Polyurethane Dispersions Cured with an Aziridine-Based Crosslinker. *Macromol Mater Eng* 296:703-709
33. Madbouly SA, Xia Y, Kessler MR (2013) Rheological Behaviour of Environmentally Friendly Castor Oil-Based Waterborne Polyurethane Dispersions. *Macromolecules* 46:4606-4616
34. Lu Y, Larock RC (2010) Soybean oil - based, aqueous cationic polyurethane dispersions: Synthesis and properties. *Prog Org Coat* 69:31-37
35. Lu Y, Larock RC (2008) Soybean oil - Based Waterborne Polyurethane Dispersions: Effects of Polyol Functionality and Hard Segment Content on Properties. *Biomacromolecules* 9:3332-3340
36. Lu Y, Larock RC (2007) New Hybrid Latexes from a Soybean Oil - Based Waterborne Polyurethane and Acrylics via Emulsion Polymerization. *Biomacromolecules* 8:3108-3114
37. Petrovic ZS, Guo A, Zhang W (2000) Structure and properties of polyurethanes based on halogenated and nonhalogenated soy - polyols. *J Polym Sci Part A: Polym Chem* 38:4062-4069

38. Lu Y, Tighzert L, Dole P, Erre D (2005) Preparation and properties of starch thermoplastics modified with waterborne polyurethane from renewable resources. *Polymer* 46:9863-9870
39. Lu Y, Tighzert L, Berzin F, Rondot S (2005) Innovative plasticized starch films modified with waterborne polyurethane from renewable resources. *Carbohydr Polym* 61:174-182
40. Harjono, Sugita P, Mas'ud ZA (2012) Synthesis and Application of Jatropha Oil based Polyurethane as Paint Coating Material. *Makara J Sci* 16(2):134-140
41. Lligadas G, Ronda JC, Galia M, Cadiz V (2007) Poly(ether urethane) Networks from Renewable Resources as Candidate Biomaterials: Synthesis and Characterization. *Biomacromolecules* 8:686-692
42. Lligadas G, Ronda J C, Galia M, Cadiz V (2007) Polyurethane Networks from Fatty Acid - Based Aromatic Triols: Synthesis and Characterization. *Biomacromolecules* 8:1858-1864
43. Kong XH, Narine SS (2007) Physical Properties of Polyurethane Plastic Sheets Produced from Polyols from Canola Oil. *Biomacromolecules* 8:2203-2209
44. Petrovic ZS, Guo A, Javni I, Cvetkovic I, Hong DP (2008) Polyurethane networks from polyols obtained by hydroformylation of soybean oil. *Polym Int* 57:275-281
45. Roy S, Majumdar KK (2004) Preparation of organo-tin catalyst useful for preparation of polyurethanes. Indian patent 194604.
46. Burdeniuc JJ, Kamzelski AZ (2006) Blowing catalyst compositions containing hydroxyl and surface active groups for the production of polyurethane foams. European patent 1702913.
47. Krajnik JM, Olesen KR, Vandezande GA (2005) Waterborne casting having improved Chemicals resistance. US patent 6869996.
48. Hart RE (1997) Water-based, solvent free or low VOC, two-component polyurethane coatings. US patent 5693703.
49. Zeno W. Wicks, Jr., Douglas A. Wicks, James W. Rosthauser (2002) Two package waterborne urethane systems. *Progress in Organic Coatings* 44:161-183
50. Kim BK, Kim TK, Jeong HM (1994) Aqueous dispersion of polyurethane anionomers from H12MDI/IPDI, PCL, BD and DMPA. *J Appl Polym Sci* 53:371-378

51. Chen Y, Chen YL (1992) Aqueous dispersions of polyurethane anionomers: effects of counteraction. *J Appl Polym Sci* 46:435-43
52. Narayan R, Chattopadhyay DK, Sreedhar B, Raju KVS, Mallikarjuna NN, Aminabhavi TM (2006) Synthesis and characterization of crosslinked polyurethane dispersions based on hydroxylated polyesters. *J Appl Polym Sci* 99:368-80
53. Weiss KD (1997) Paint and coatings, a mature industry in transition. *Prog Polym Sci* 22:203-245
54. Noble KL (1997) Waterborne polyurethanes. *Prog Org Coat* 32:131-136
55. Melchior M, Casselmann H, Kobusch C, Noble KL, Sonntag M (2000) Designing coatings to cover high performance applications. *Polym Paint Colour J* 190 (4426):24-28
56. Melchior M, Sonntag M, Kobusch C, Jurgens E (2000) Recent developments in aqueous two-component polyurethane (2K-PUR) coatings. *Prog. Org. Coat.* 40:99-109.
57. Hegedus CR, Gilinski AG, Haney RJ (1996) Film formation mechanism of two - component waterborne polyurethane coatings. *J Coat Technol* 68(852):51-61
58. Renk CA, Schwartz AJ (1995) in: *Proceedings of the Waterborne High-solids Powder Coating Symposium, New Orleans, LA*, p.266.
59. Prashant Gangwar (2013) Two component waterborne polyurethanes for construction coatings. *paintindia* 118-123
60. American Chemistry Council (2012) *CPI 2010 End-Use Market Survey on the Polyurethane Industry*
61. Mutlu H, Meier MAR (2010) Castor oil as a renewable resource for the chemical industry. *Eur J Lipid Sci Tech* 112(1)10-30
62. Binder RG, Applewhite TH, Kohler GO, Goldblatt LA (1962) Chromatographic analysis of seed oils. Fatty acid composition of castor oil. *J Am Oil Chem Soc* 39: 513-517
63. Belgacem MN, Gandini A (2008) Materials from vegetable oils: Major sources, properties and applications. In: *Monomers, Polymers and Composites from Renewable Resources*. Eds. M. N. Belgacem, A. Gandini, Elsevier, Amsterdam (The Netherlands) pp.39-66.

64. Brink M, Belay G (2006) Alphabetical treatment of vegetable oils. In: Plant Resources of Tropical Africa. 1. Cereals and Pulses. Eds. M. Brink, G. Belay, Backhuys Publishers, Leiden (The Netherlands) p.144
65. Dwivedi MC, Sapre S (2002) Total vegetable-oil based greases prepared from castor oil. *J Syn Lubrication* 19:229-241
66. Hoffer P, Daute P, Grutzmacher R, Westfechtel A (1997). Oleochemical Polyols-A New Raw Material Source for Polyurethane Coatings and Floorings. *Journal Coatings and Technology* 69 (869): 65-72
67. Petrovic ZS (2008) Polyurethanes from vegetable oils. *Polym Rev* 48:109-155
68. Petrovic ZS, Ionescu M, Javni I (2009) Polyglycerol based polyols and polyurethanes and methods for producing polyols and polyurethanes. US Patent Application 20090082483
69. Valero MF, Pulido JE, Ramirez A, Cheng Z (2008) Polyurethanes synthesized of polyols obtained from castor oil modified by transesterification with pentaerythritol. *Quim Nova* 31:2076-2082
70. Valero MF, Pulido JE, Ramirez A, Cheng Z (2009) Simultaneous interpenetrating polymer networks with pentaerythritol-modified castor oil and polystyrene: Structure-property relationship. *J Am Oil Chem Soc* 86:383-392
71. Valero MF, Pulido JE, Hernandez JC, Posada JA, Ramirez A, Cheng Z (2009) Preparation and properties of polyurethanes base don chemically modified with yucca Storch glycoside. *J Elastomers Plast* 41:223-244
72. Petrovic ZS, Cvetkovic I, Hong DP, Wan X, Zhang W, Abraham T, Malsam J (2008) Polyester polyols and polyurethanes from ricinoleic acid. *J Appl Polym Sci* 108:1184-1190
73. Karak N, Rana S, Cho JW (2009) Synthesis and characterization of castor-oil modified hyperbranched polyurethanes. *J Appl Polym Sci* 112:736-743
74. Moeini HR (2007) Preparation and properties of novel green poly(ether-ester urethane)s insulating coatings based on polyols derived from glycolyzed PET, castor oil, and adipic acid and blocked isocyanate. *J Appl Polym Sci* 106:1853-1859
75. Yeganeh H, Mehdizadeh MR (2004) Synthesis and properties of isocyanate curable millable polyurethane elastomers based on castor oil as a renewable resource polyol. *Eur Polym J* 40:1233-1238

76. Mendes RK, Claro-Neto, Cavalheiro ETG (2002) Evaluation of a new rigid carbon-castor oil polyurethane composite as an electrode material. *Talanta* 57:909-917
77. Srivastava A, Singh P (2002) Gel point prediction of metal-filled castor oil-based polyurethanes system. *Polym Adv Technol* 13:1055-1066
78. Yeganeh H, Hojati-Talemi P (2007) Preparation and properties of novel biodegradable polyurethane networks based on castor oil and poly(ethylene glycol). *Polym Degrad Stab* 92:480-489
79. Sperling LH, Manson JA, Yenwo GM, Devia-Manjarres N, Pulido J, Conde A (1977) Novel plastics and elastomers from simultaneous interpenetrating networks from castor oil based IPNs – a review of an international program. *Polym Sci Technol* 10:113-140
80. Nayak PL (2000) Natural oil-based polymers: Opportunities and challenges. *J Macromol Sci Rev Macromol Chem Phys.* 40:1-21
81. Yin Y, Yao S, Zhou X (2003) Synthesis and dynamic mechanical behavior of crosslinked copolymers and IPNs from vegetable oils. *J Appl Polym Sci* 88:1840-1842
82. Guner FS, Yagci Y, Erciyes AT (2006) Polymers from triglyceride oils. *Prog Polym Sci* 31:633-670
83. Devia-Manjarres N, Conde A, Yenwo GM, Pulido J, Manson JA, Sperling LH (1977) Castor oil based interpenetrating polymer Networks, II. Synthesis and properties of emulsion polymerized products. *Polym Eng Sci* 17:294-299
84. Zhang L, Ding H (1997) Study on the properties, morphology, and applications of castor oil polyurethane – poly(methyl methacrylate) IPNs. *J Appl Polym Sci* 64:1393-1401
85. Sanmathi CS, Prasannakumar S, Sherigara BS (2004) Interpenetrating polymer networks based on polyol modified castor oil polyurethane and poly(2-ethoxyethyl methacrylate) synthesis, chemical, mechanical, thermal properties, and morphology. *J Appl Polym Sci* 94:1029-1034
86. Cunha FOV, Melo DHR, Veronese VB, Forte MMC (2004) Study of castor oil polyurethane-poly(methyl methacrylate) semi-interpenetrating polymer network (SIPN) reaction parameters using a 2³ factorial experimental design. *Mater Res* 7:539-543
87. Prashantha K, Pai KVK, Sherigara BS, Prasannakumar S (2001) Interpenetrating polymer networks based on polyol modified castor oil polyurethane and poly(2-

- hydroxy-ethylmethacrylate): Synthesis, chemical, mechanical and thermal properties. *Bull Mater Sci* 24:535-538
88. Campbell MF, Kraut CW, Yackel WC, Yang HS (1985). "Soy Protein Concentrates". in "New Protein Foods", A. M. Altschul and H. L. Wilke, Editors. Vol. 5, p. 301. Academic Press, Inc. Orlando, Florida.
 89. Veldman A, Veen WAG, Barug D, van Paridon PA (1993) Effect of α -galactosides and α -galactosidase in feed on ileal piglet digestive physiology. *J Animal Physiol Anim Nutr* 69:57-65
 90. Karr-Lilienthal LK, Kadzere CT, Grieshop CM, Fahey Jr. GC (2005) Chemical and nutritional properties of soybean carbohydrates as related to nonruminants. A review *Livest Prod Sci* 97:1-12
 91. Choct M, Li YD, McLeish J, Peisker M (2010) Soy Oligosaccharides and Soluble Non-starch Polysaccharides: A Review of Digestion, Nutritive and Anti-nutritive Effects in Pigs and Poultry. *Asian-Aust J Anim Sci* 23(10):1386-1398
 92. Eldrige AC, Black LT, Wolf WJ (1979) Carbohydrate Composition of Soybean Flours, Protein Concentrates, and Isolates. *J Agric Food Chem* 27(4):799-802
 93. Javni I, Petrvic ZS, Guo A, Fuller R (2000) Thermal stability of polyurethanes based on vegetable oils. *J Appl Polym Sci* 77:1723-1734
 94. Hablot E, Zheng D, Bouquey M, Averous L (2008) Polyurethanes Based on Castor Oil: Kinetics, Chemical, Mechanical and Thermal Properties. *Macromol. Mater. Eng.* 293:922-929
 95. Gaboriaud F, Vantelon JP (1982) Mechanism of thermal degradation of polyurethane based on MDI and propoxylated trimethylol propane. *J Polym Sci Polym Chem Ed* 20:2063-2071
 96. Andriot M, Chao S H, Colas A (2009) Silicones in Industrial Applications: Organo-Functional Silanes, In *Silicon-Based Inorganic Polymers*, De Jaeger, R. & Gleria, M., Eds., Nova, 142-146
 97. Finzel WA, Vincent HL (1996) Silicones in Coatings, In: *Federation Series on Coatings*, Federation of Societies for Coatings Technologies, Blue Bell, PA, 18-20
 98. George SC, Thomas S (2001) Transport Phenomena Through Polymeric Systems. *Prog Polym Sci* 26:985-1017

Chapter - 6 Biodegradability studies

6.1 Introduction

Plastics are long chain polymeric molecules and are used extensively in packaging of products like food, pharmaceuticals, cosmetics, detergents and chemicals. Plastics have good physical, chemical, mechanical and thermal properties such as light weight, high strength, good stability, durability, as well as high resistance to water and most water-borne microorganisms. Therefore they have replaced most of the paper and cellulose based products in packaging applications. A consequence of this phenomenal use of plastic materials is their increasing presence in municipal solid waste (MSW) throw away products. In the USA, plastics waste accounted for approximately 31.75 million tons (12.7% of the total MSW) in 2011[1]. The most common methods available for treating waste disposal are landfills, recycling, incineration and composting. However, most plastic materials are resistant to microbial attack and tend to accumulate in the environment. Furthermore, they may represent an undesired pollutant in many ecosystems like soil, freshwater and marine habitats. However due to current limitations with landfills, new environmental regulations, discussions about renewable versus fossil resources have led to an increasing research in synthesis of biodegradable materials. Biodegradable polymers can be composted as a waste disposable option which may be a viable solution for some plastic materials, especially those materials that are litter-prone and not easily collected nor easily recycled such as those used in agriculture. This composting option has led to a need for standard evaluating procedures for these biodegradable polymers in solid waste treatment and in aquatic environments. Various

standards have been developed by ASTM (American Society for Testing and Materials) and ISO (International Standards Organization) for assessment of the biodegradability of polymers under various conditions such as composting, anaerobic degradation and waste water treatment. In this project, the biodegradability of polyvinyl alcohol, soy meal polyol and castor oil based polyurethane films were assessed according to various ISO and ASTM standards and the results are analyzed and reported.

6.2 Literature review

Biodegradation is the natural and complex process of decomposition of materials facilitated by microorganisms, and each standards organization gives its own definition for a biodegradable polymer. According to ASTM, a biodegradable plastic is "a plastic that degrades because of the action of naturally occurring microorganisms such as bacteria, fungi and algae"[2]. Standard organizations such as ASTM and ISO have published their own series of standards to assess the biodegradability of plastics in different environments such as composting (ASTM D5338, ISO 14885), anaerobic digestion (ASTM D5511, D5526 and ISO 15985) and wastewater treatment (ASTM D5210, ISO 14853) [3].

6.2.1 Various factors affecting the biodegradability of polymers

Biodegradation is predominantly a series of biological activities, however, in nature biotic and abiotic factors act synergistically to decompose organic matter. Several studies show that plastics are degraded by several interacting mechanisms like:

- photodegradation by natural daylight
- chemical degradation like oxidation by chemical additives

- thermal degradation by heat
- mechanical degradation by mechanical stress
- biodegradation by microorganisms (e.g. bacteria, fungi)

Plastics exposed to outdoor conditions (weather, ageing) undergo transformations in their structure due to abiotic factors (mechanical, light, thermal and chemical) and this affects the ability of the polymeric materials to be biodegraded [4-8]. The abiotic parameters in most of the cases are useful either as a synergistic factor or to initiate the biodegradation process. Figure 6.1 shows the various factors which affect the rate and extent of biodegradation.

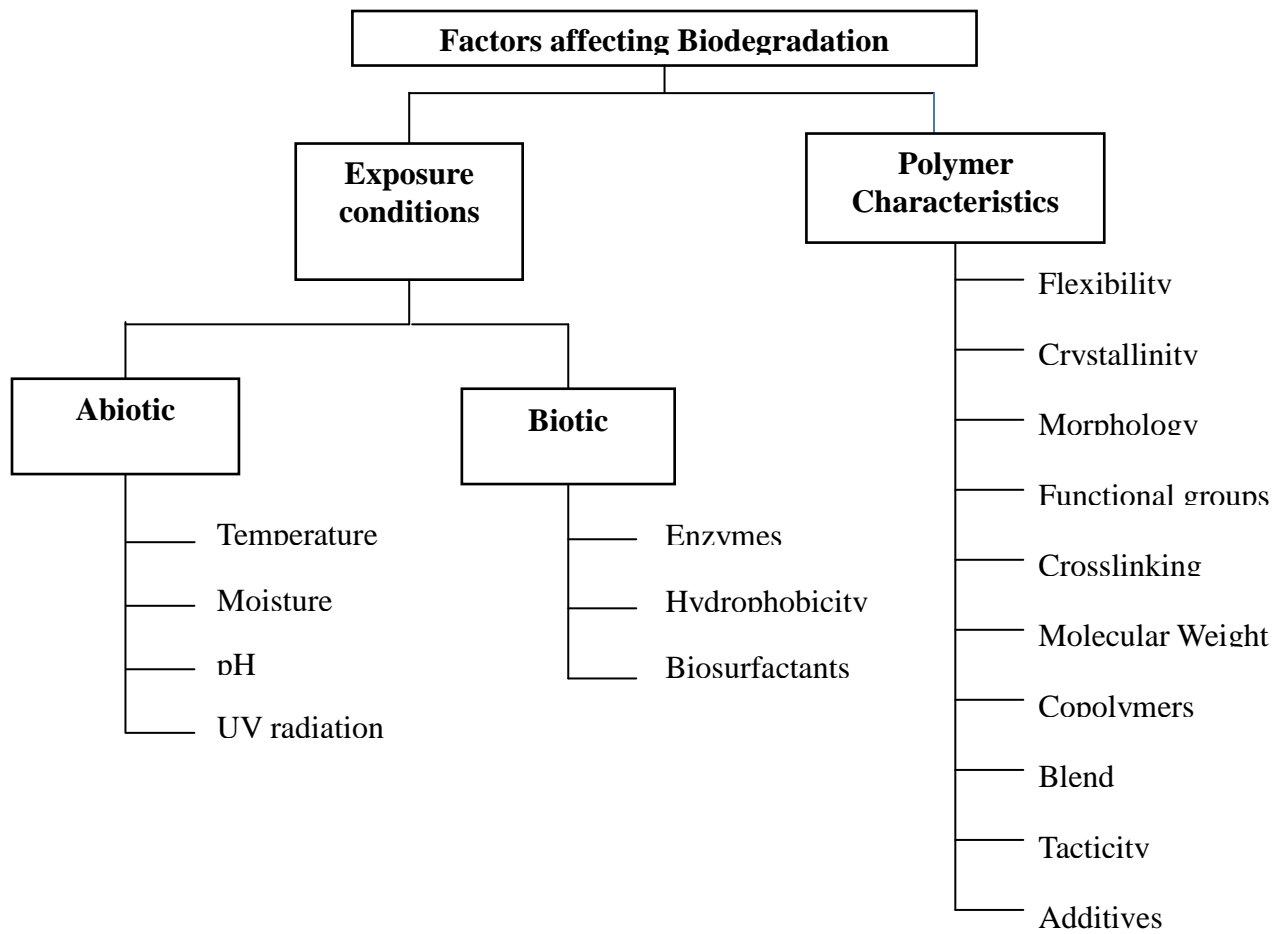


Figure 6.1: Various factors that affect biodegradation

Biodegradation is influenced by different factors like the type of microorganisms, exposure conditions and the characteristics of the polymer. Microorganisms like bacteria and fungi are involved in the biodegradation of both natural and synthetic plastics [9, 10]. Different soil conditions have their own optimal microbial growth conditions, thus varying the extent of biodegradability of the polymers. For example, a compost pile has higher moisture content and temperature conditions suitable for a variety of microbes to live and reproduce. Figure 6.2 shows the general mechanism of biodegradation of plastics by the enzymatic action of microorganisms. Bacteria can be broadly classified into two categories, aerobic and anaerobic. In aerobic biodegradation, the microbes utilize oxygen in the air and consume carbon from the polymer as a food source, producing carbon dioxide and water. This enzymatic biological oxidation reaction predominates in the presence of a high oxygen concentration (not less than 6% as described in ASTM D5338) and any depletion of oxygen supply can affect the metabolism rate of aerobic microorganisms, thus affecting the biodegradation rate. In anaerobic biodegradation, anaerobic bacteria consume carbon from the polymer source, producing methane and carbon dioxide. Each type of microorganisms consumes carbon at different rates and therefore the biodegradation of plastics under aerobic conditions may not be the same as in anaerobic conditions [11]. In both these cases, it is important to note that a small portion of the biodegradable polymer will be incorporated into microbial biomass, humus and other natural products. The growth of many fungi happens under aerobic conditions, and can cause small-scale swelling and bursting as the fungi penetrate the surface of the polymer solids [12]. The biodegradation reaction involves the production of enzymes that break down complex polymers to yield smaller molecules of short chains, e.g., oligomers,

dimers and monomers that can be easily assimilated by the microorganisms. Enzymes are essentially biological catalysts and can affect the rate of biodegradation reactions. There are two categories of enzymatic reactions: enzymatic oxidation (by aerobic microorganisms) and enzymatic hydrolysis (by either aerobic or anaerobic microbes)[13].

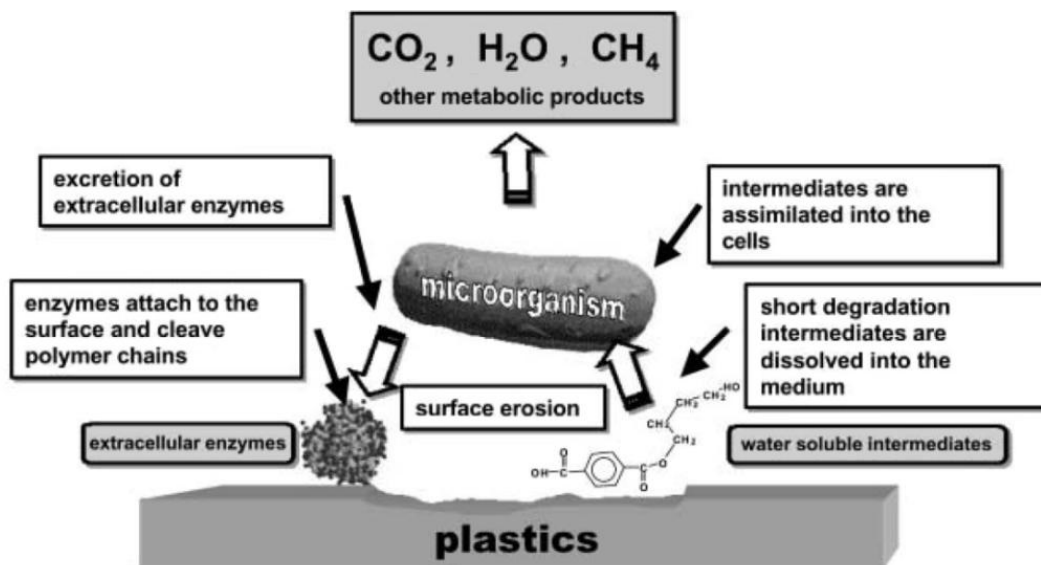


Figure 6.2: General mechanism for the biodegradation of plastics by microorganisms

6.2.2 Influence of environmental conditions on biodegradability

Biodegradation of plastics also depends on environmental factors like moisture, temperature, oxygen and pH of the surroundings. Water or moisture can affect the biodegradation of polymers in two ways. First, microorganisms need water to grow and reproduce. Therefore, under conditions where moisture content is suitable there should be more microbial activity and the rate of biodegradation would be faster. Second, hydrolysis plays an important role in the biodegradation of some polymers in moisture rich environments, resulting in the cleavage of polymers and increasing the available sites for microorganisms to attack. It can be therefore expected that the polymers will degrade faster in moisture rich environments than in dry conditions [14]. Hydrolysis reactions can

be catalyzed under both acidic and base conditions. The pH of the environment affects bacterial growth. Most bacteria grow best in pH from 6-8. However, there are also many acid tolerant bacteria as well as alkaline tolerant bacterial strains. Furthermore, the pH of the environment also significantly affects the biodegradation of plastics[15]. The temperature in many natural environments changes drastically over the seasons. Most of the well characterized bacteria live best at temperatures from 25°-40°C (mesophiles) although many bacteria thrive at high temperatures above 45°C (thermophiles) and others grow best at 0°-15°C (psychrophiles). In general, the rate of biodegradation increases with increase in the temperature as long as it is not beyond the optimum temperature for growth of the microorganisms [16]. The rate and the extent of the hydrolysis of many polymers are also affected by changes in the temperature.

6.2.3 Affects of polymers properties on their biodegradability

The characteristics of the polymer such as its mobility, tacticity, crystallinity, molecular weight, type of functional groups and additives all play an important role in its biodegradability[17]. The higher the flexibility of a polymer, the higher is the probability of more active sites available for assimilation by the enzymatic action of the microorganisms and higher is the biodegradation rate[18]. Amorphous regions of the polymers are more susceptible to biodegradation than crystalline regions due to the easy accessibility to microorganisms. Polymers with different degrees of crystallinity tend to have different rates of biodegradation [19,20]. Generally, an increase in the molecular weight of a polymer results in a decrease in the degradability of the polymer by microorganisms. Thus monomers, dimers and oligomers are more easily degraded than

the high molecular weight polymer. Furthermore, high molecular weight results in a decrease in the solubility, increase in the Tg making the polymer less flexible, and increases the number of bonds that must be cleaved, making them unfavorable for microbial attack [13, 15]. The type of comonomers introduced into a polymer structure also affects its biodegradability. The crystallinity of the polymer could be decreased by the presence of comonomer thus increasing its biodegradability. Similarly the presence of comonomers with hydrolyzable groups can increase biodegradability. On the contrary, comonomers containing aromatic structures which impart rigidity to the polymer can reduce its biodegradability. Therefore the biodegradability of the polymer depends on the type of comonomer introduced and its effect on the properties of the polymer [22,23]. The size and shape of the polymer also influences the rate of biodegradation. The smaller the size of the polymer, higher is the surface area that is in contact with the microorganisms and thus degrades faster [24].

6.2.4 Standard test methods

Several standard tests have been developed by standards organizations around the world to determine the biodegradability of packaging materials in different environments. Most commonly, these standards describe terminology and definitions, testing guidelines, procedures, conditions, significance, limits and interpretation of the results. In this review, only the standards prescribed by ASTM and ISO dealing with the aerobic biodegradation of polymers in composting and aqueous medium are included and discussed.

ASTM D6400 [2] addresses the compostability of plastic materials, standard specifications, terminologies as well as guidelines for using test method ASTM D5338. The test method ASTM D5338 [25] is used to ascertain the biodegradability of plastics exposed to a compost mixture under controlled laboratory conditions. The test prescribes a minimum of 12 test vessels: 3 blanks, 3 negative controls, 3 positive controls and 3 for the test material. Carbon dioxide free humidified air is supplied for a test period of no less than 45 or more than 180 days at a constant temperature of 58°C or a desired temperature depending on the properties of the test material. The carbon dioxide gas produced is trapped by using a sodium hydroxide (NaOH) or barium hydroxide (Ba(OH)₂) solution and its concentration is determined by titration using hydrochloric acid. Carbon dioxide production can also be alternatively determined by using a carbon dioxide analyzer (either infrared or chromatographic). For a test material to be certified as biodegradable, a 60% or higher mineralization value must be attained for a material containing a single polymer (homopolymer or random copolymer) and 90% for a material containing a block copolymer, segmented copolymer, blend or low molecular weight additives. Further ecotoxicity tests are carried out in accordance with ASTM D6400.

The ISO 14855-1[24] biodegradation test is similar to the test method in ASTM D5338, with a few differences. The ISO test method does not require negative control vessels, prescribes using inert materials such as sea sand or vermiculite with the compost for providing better aeration and moisture retention, and the mineralization of the test material should be 90% of the value obtained for a reference material to prove its biodegradability. ISO 14855-2[26] is another standard test method which measures

mineralization of a polymer by a gravimetric method. It is similar to 14855-1 except for the method of carbon dioxide measurement and the amount of compost and sample used.

For aqueous biodegradation standard tests, a liquid environment is used to assess the biodegradability of materials. The general principle of the tests is the same except for aerobic fermentation of polymers in an aquatic environment, regardless of the other parameters used to estimate the biodegradability. Generally the source of microorganisms is activated sludge from a well operated municipal sewage treatment plant. The material to be tested is the sole organic carbon source in the medium. Through the action of microorganisms and in the presence of oxygen, this carbon is converted into biomass, carbon dioxide, residual polymer or oligomers and inorganic dissolved carbon.

6.3 Biodegradability testing of polyvinyl alcohol in aqueous medium

6.3.1 Introduction

Poly(vinyl alcohol) (PVA) is a water soluble synthetic polymer that is widely used in adhesive, paper-coating, textile-industries and for packing pharmaceutical products [27,28]. Various grades of this polymer are generally synthesized by the saponification reaction of polyvinyl acetate using sodium hydroxide as the catalyst. The percentage of the residual acetate groups present in the product varies depending on the extent of the saponification reaction and significantly influences the solubility of the PVA. With increased acetate groups, the polymer becomes less soluble in water and more soluble in aromatic hydrocarbons and aliphatic esters [29]. Due to its increased applicability, PVA is very likely to enter the environment without entering any integrated

system of waste treatment. Therefore, ascertaining the biodegradability of PVA is of utmost importance. PVA is difficult to be degraded in natural environments, however microorganisms and enzymes that degrade PVA have been identified and reported [30-32]. However, the properties of these materials very much depend upon the degree of polymerization, distribution of hydroxyl groups, stereoregularity and crystallinity of PVA. Therefore, it is of utmost importance to assess the relationship between biodegradability and structure of the polymer.

In this work, the degradation behavior of two types of PVA with different degrees of hydrolysis were considered and investigated for their biodegradability under different environmental conditions. Biodegradability tests were conducted in aqueous medium according to ISO standard 14852 [33] using both acclimatized and non-acclimatized inoculum and the results were analyzed and reported.

6.3.2 Experimental methods

6.3.2.1 Materials

Commercial PVA samples PVA-88 (Partially hydrolysed, 86.7 – 88.7 mol.-% hydrolysis) and PVA-99 (Fully hydrolysed, 99.0 – 99.8 mol.-% hydrolysis) were purchased from Kuraray Specialities Europe GmbH. The organic content of the PVA samples, PVA-88 & PVA-99 were 55.4% & 54.5% as determined from the chemical formula (Figure 6.3.1). Cellulose and Starch (Food starch – unmodified) were utilized as positive controls in respirometric biodegradation tests and were purchased from Fluka, and Cargill Gel respectively. Antifoam 204 used as an anti-foaming agent during the tests was purchased from Sigma – Aldrich.

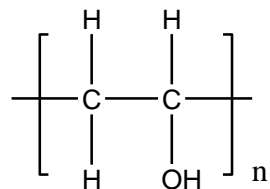


Figure 6.3.1: Chemical structure of poly(vinyl alcohol)

6.3.2.2 Microbial source

The microbial inoculum was a sample of activated sludge collected from a well-operated waste water treatment plant based handling predominantly domestic sewage at East Lansing, MI, USA.

A PVA acclimated culture was obtained by adopting a common enrichment procedure. The activated sludge from the waste water plant was added in 1% by weight ratio to 100 ml of the mineral medium having the following composition: 2.2 g K₂HPO₄, 0.8 g KH₂PO₄, 0.7 g MgSO₄·7H₂O, 1.0 g NH₄NO₃, 0.1 g NaCl, 0.01 g FeSO₄·7H₂O, 0.05 g yeast extract (Bacto Yeast Extract, Difco), 1000 ml distilled water, with a pH 7.1 ± 0.1. The liquid culture was then added with PVA at a concentration of 0.1 – 10 g/L and then incubated at 25°C under reciprocal shaking (120 rpm) for three weeks. The liquid cultures were further enriched by filtering 5 ml sample on 1.2 µm cellulose acetate filter and transferring the filtrate into the fresh mineral medium containing increasing PVA concentrations from 0.1 – 10 g/L. The microbial culture resulting from the repeated sequential transfers was used as the acclimated inoculum in the biodegradation tests.

6.3.2.3 Biodegradation tests in aqueous medium

A respirometric mineralization test system based on International Standard ISO 14852 was built. This system was designed to yield the percentage of carbon dioxide from the organic carbon content of the sample in aqueous medium. An optimized test medium which was highly buffered and contained more inorganic nutrients was prepared as mentioned in the ISO standard and given below.

a. *Solution A* - dissolve 37.5 g of anhydrous potassium dihydrogen phosphate (KH_2PO_4), 87.3 g of disodium hydrogen phosphate dihydrate ($\text{Na}_2\text{HPO}_4 \cdot 2\text{H}_2\text{O}$), 2 g of ammonium chloride (NH_4Cl) in water and diluted to 1 L.

b. *Solution B* - dissolve 22.5 g of magnesium sulfate heptahydrate ($\text{MgSO}_4 \cdot 7\text{H}_2\text{O}$) in water and diluted to 1 L.

c. *Solution C* - dissolve 36.4 g of calcium chloride dihydrate ($\text{CaCl}_2 \cdot 2\text{H}_2\text{O}$) in water and diluted to 1 L.

d. *Solution D* - dissolve 0.25 g of iron (III) chloride hexahydrate ($\text{FeCl}_3 \cdot 6\text{H}_2\text{O}$) in water and diluted to 1 L.

The test medium was then prepared by using the above stock solutions. For preparing a liter of test medium, to about 800 ml of water was added 100 ml of solution A, 1 ml of solution B, 1 ml of solution C, 1 ml of solution D and made up to 1000 ml with water, the pH of which was measured to be 7.0 ± 0.2 . The PVA samples taken for respirometric tests were such that the concentrations of organic carbon content in the test flasks was 2000 mg/liter of test medium. The PVA samples were dissolved in test flasks by adding 500 ml of water and refluxed at 95°C for 3 hours under constant stirring using a magnetic stirrer. Cellulose, starch and glucose were used as positive reference

materials. PVA acclimatized microbial inoculum was introduced to the test flasks at a concentration of 5% (V/V) in the test medium.

The current test system was comprised of two test flasks for each PVA sample, two flasks for the blank and two flasks for each of the positive reference materials placed in a dark temperature controlled system – an environmentally controlled room manufactured by Lab-Line Instruments Inc. (Melrose Park, IL) maintained at 25°C with an accuracy of $\pm 1^\circ\text{C}$. The test flasks were agitated throughout the test with a magnetic stirrer. The test flasks were connected to a CO₂ free air production system as shown in Figure 6.3.2. Frothing problems encountered were dealt with by adding 1 ml of 2% Antifoam 204 (Sigma Aldrich) solution in all the flasks including the blanks. The air was divided and passed through flow meters for each bioreactor at a flow rate of 60 mL/min.

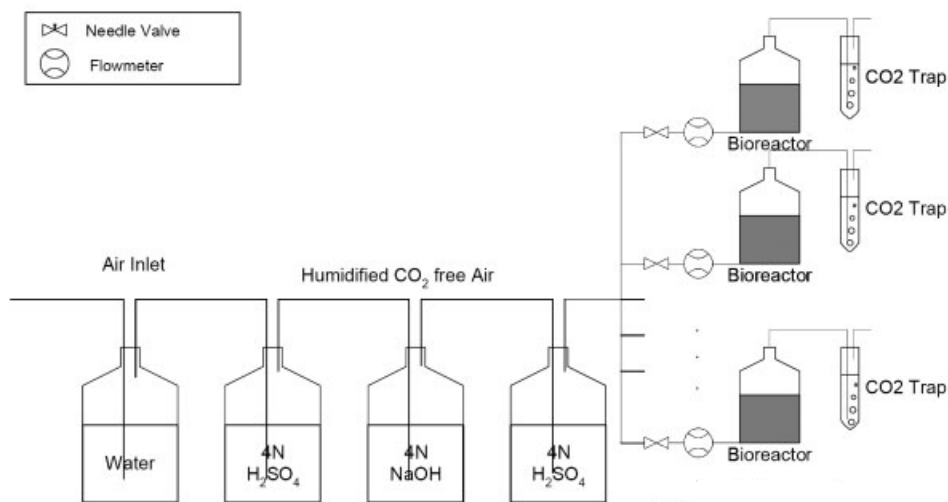
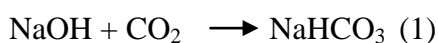


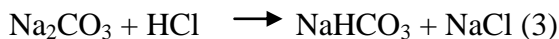
Figure 6.3.2: Schematic of the experimental setup

A solution with 250 ml 0.25N NaOH was used for trapping the CO₂ from the test flasks and the amount of CO₂ content in solution was calculated through acid-base

titration. The NaOH solution was changed every time that CO₂ was calculated. Ten milliliter aliquots were removed from the 250 ml trapping NaOH solution and titrated with 0.186N standardized hydrochloric acid (HCl) solution to obtain the value of CO₂ in the solution. The CO₂ content in the 10 mL solution was correlated with the 250 mL solution and the actual CO₂ amount was determined. The CO₂ trapping reaction was done in a two step reaction as shown below.



Similarly, during titration CO₂ was removed through the following reactions:



Initially, a few drops of phenolphthalein indicator were added to the 10 mL NaOH aliquot and further titrated until it turned from pink to colorless. At this point, the Na₂CO₃ was converted into NaHCO₃ and NaCl. Further, a few drops of Bromocresol green - methyl red indicator were added and titrated till the solution turned from blue to yellow. The NaHCO₃ reacted with HCl to form NaCl, H₂O and CO₂. Hence the amount of HCl consumed could be used to calculate the CO₂ concentration in the solution according to the following formula:

$$\text{gCO}_2 = \frac{V \times C \times 44}{1000}$$

where $g\text{CO}_2$ is the amount of evolved carbon dioxide in grams; V is the volume of HCl consumed; C is the concentration of HCl solution. The percentage biodegradation D_t was further calculated by the following equation:

$$D_t = \frac{\sum(\text{CO}_2)_T - \sum(\text{CO}_2)_B}{\text{ThCO}_2} \times 100$$

where

$\Sigma(\text{CO}_2)_T$ is the amount of carbon dioxide evolved in test flask F_T between the start of the test and time t , expressed in milligrams;

$\Sigma(\text{CO}_2)_B$ is the amount of carbon dioxide evolved in the blank flask F_R between the start of the test and time t , expressed in milligrams;

ThCO_2 is the theoretical amount of carbon dioxide evolved by the test material, expressed in milligrams.

The theoretical amount of CO_2 evolved by the test material ThCO_2 is given by the following equation:

$$\text{ThCO}_2 = m \times X_c \times \frac{44}{12}$$

where m is the mass of test material introduced into the test system;

X_c is the carbon content of the test material, determined from the chemical formula or calculated from an elemental analysis and expressed as a mass fraction; 44 and 12 are the molecular mass of carbon dioxide and the atomic mass of carbon, respectively.

6.3.3 Biodegradation kinetics

The percent biodegradation values at different times that were obtained from the biodegradation tests were further evaluated to better understand the biodegradation kinetics [34]. Figure 6.3.3 shows a typical biodegradation curve of CO₂ evolved evolved as a function of time.

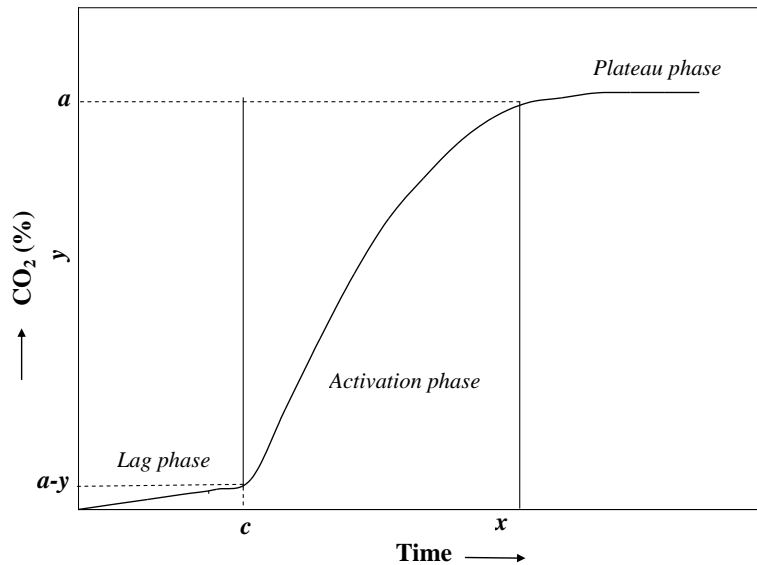


Figure 6.3.3: A typical biodegradation curve showing CO₂ evolved as a function of time

There are typically three different phases involved in the biodegradation reaction, lag phase, activation phase and a plateau phase. In Figure 6.3.3, y denotes CO₂ evolved (percentage), x is time (days), a is the upper asymptote (percentage), and c is the lag time. Considering a biodegradation reaction involving one reactant, such as



The rate law corresponding to a first order reaction can be written as

$$r = -K C_A = K C_p \quad (a)$$

where r is the rate of reaction, K is the rate constant, C_A , C_p are the concentration of reactants and products, respectively; For a first order reaction, the rate law can be written in differential form as

$$\frac{dy}{dt} = k y \quad (b)$$

Integrating both the sides of the equation,

$$\int_{a-y}^a \frac{dy}{y} = \int_c^x k dt \quad (c)$$

$$\ln\left(\frac{a-y}{a}\right) = -k(x-c) \quad (d)$$

$$a - y = a e^{-k(x-c)} \quad (e)$$

$$y = a(1 - e^{-k(x-c)}) \quad (f)$$

for the following boundary conditions: $y = a[1 - e^{-k(x-c)}]$ for $x > c$; $y = 0$ for $x \leq c$

This mathematical model is used for understanding the kinetics of the biodegradation reaction. Lag time and asymptote were introduced into the model as to ascertain the biodegradation only during active phase. The parameters of the model, rate constant, lag time and asymptote were obtained by fitting the experimental percentage versus time data using nonlinear regression analysis. The Correlation Co-efficient R^2 was also determined to estimate the variability derived by the model.

6.3.4 Results and discussion

6.3.4.1 Biodegradation of PVA in non-acclimatized medium

The two different PVA samples, PVA-88 and PVA-99 were investigated for their degradation behaviour under aqueous conditions in aerobic conditions. During aerobic degradation, the carbon in the polymers is converted by the action of microorganisms into carbon dioxide, water, biomass and other residues. The rate and extent of aerobic biodegradability was assessed by determining the amount of carbon dioxide evolved using a cumulative respirometric method. Figure 6.3.4 shows the biodegradation curves of PVA samples done in the presence of non-acclimatized municipal waste water.

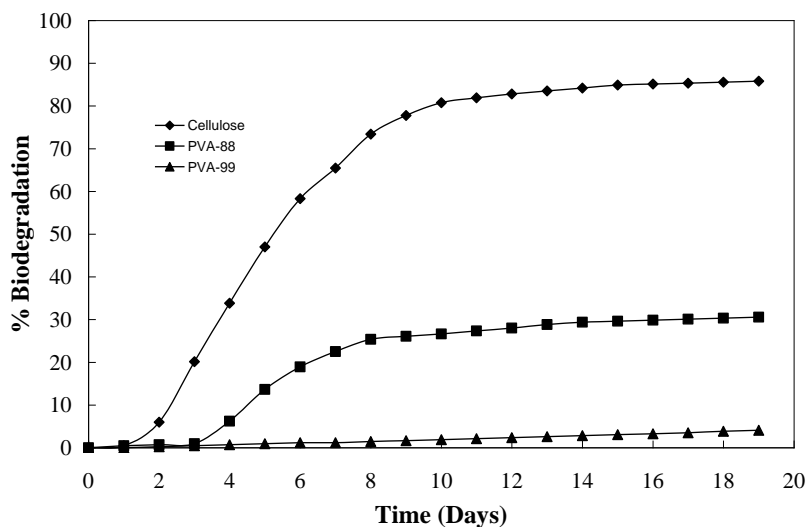


Figure 6.3.4: Biodegradation curves of PVA and cellulose in the presence of municipal sewage sludge.

Cellulose used as a positive control during the test, degraded by $85.8 \pm 0.6\%$ and reached a plateau stage within 19 days. PVA-88, a partially hydrolyzed PVA degraded by $30.6 \pm 0.8\%$, while PVA-99 did not show any signs of significant degradation ($4.1 \pm 0.2\%$). The differences in the degree of biodegradation between the two different grades of PVA

could be explained due to the differences in their degree of hydrolysis. The solubility of PVA in water depends on its degree of polymerization and degree of hydrolysis [32]. As a general rule, a decrease in the degree of polymerization and hydrolysis is accompanied by a rise in the rate of dissolution in water, as is evident from the different dissolving temperatures. PVA-88, a partially hydrolysed polymer (88%) was readily soluble in water at room temperature, while PVA-99, a fully hydrolyzed polymer was soluble in water at a temperature of 90 – 95°C. Moreover partially hydrolyzed PVA tends to be semi-crystalline while fully hydrolyzed PVA tends to be highly crystalline. Amorphous regions of the polymers are easily accessible to the microorganisms compared to the crystalline regions [19,20].

Table 6.3.1: Kinetic parameters of PVA degradation in acclimatized and non-acclimatized inoculum

Sample	Biodegradation, %	Rate constant (day ⁻¹)	Correlation Coefficient, R ²	Lag time (days)
Cellulose ^a	85.8±0.6	0.51±0.00	0.94±0.0	2.0±0.0
PVA-88 ^a	30.6±0.8	0.49±0.02	0.95±0.0	4.0±0.0
PVA-99 ^a	4.1±0.2	-	-	-
Starch ^b	85.6±0.0	0.10±0.00	0.99±0.0	0.0±0.0
PVA-88 ^b	89.0±3.9	0.03±0.00	0.96±0.05	12.0±8.5
PVA-99 ^b	88.9±3.1	0.12±0.00	0.98±0.01	12.0±0.0

^a samples in non-acclimatized inoculum

^b samples in acclimatized inoculum

The parameters of the biodegradation kinetics, rate constants, lag time and correlation co-efficients are shown in Table 6.3.1. Figure 6.3.5 shows the graph of $\ln(1-y/a)$ vs time for cellulose, a straight line fit indicating a first order reaction and the rate constant k obtained from the slope of the curve. It is apparent from the data in Figure 6.3.5 that the biodegradation rate with of cellulose follows a first order reaction with a

rate constant of 0.51 day^{-1} . Cellulose, a natural polymer, is easily assimilated by the microorganisms, while it takes a much longer time for the microbes to get adjusted to the presence of a synthetic polymer. This can be observed from the increased lag time (4 days) in the case of PVA-88, though a rate constant of 0.49 day^{-1} comparable to cellulose was obtained initially.

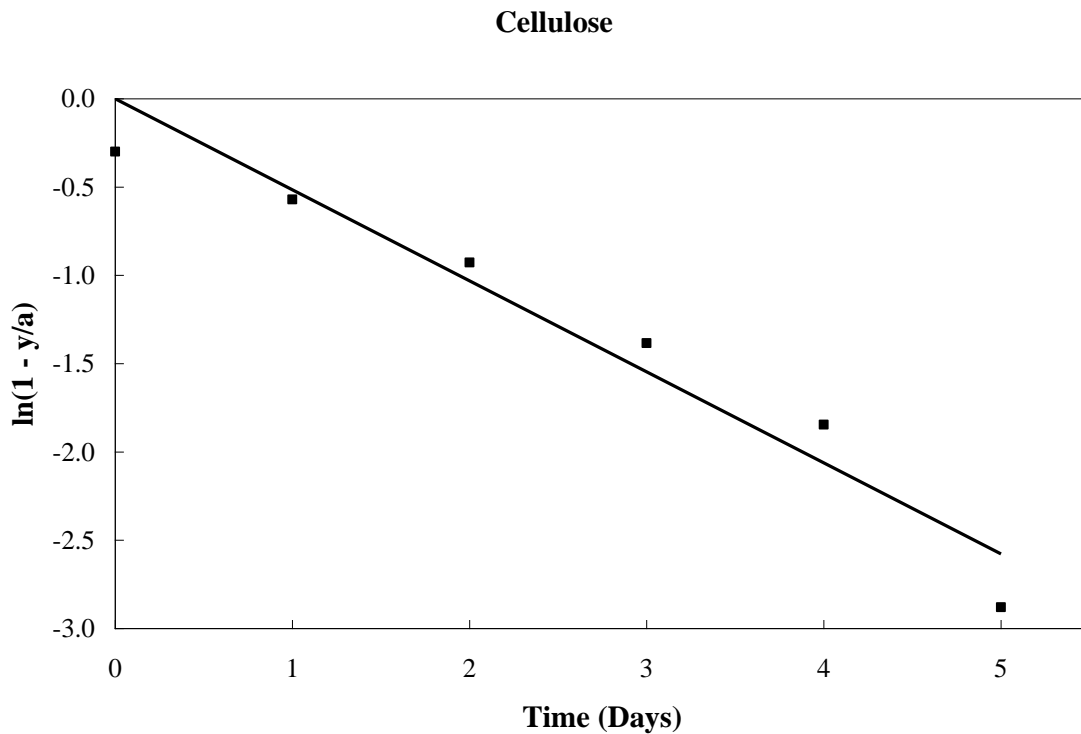


Figure 6.3.5: Graph of $\ln(1-y/a)$ versus time for cellulose in municipal sewage water

The results of the PVA biodegradation tests conducted in the presence of a non-acclimatized inoculum, however, cannot be considered conclusive due to the short incubation time. As reported in the literature, it has been established that a more active and specialized microbial population that assimilates PVA could be established in a longer period of time [35].

6.3.4.2 Biodegradation of PVA in the presence of acclimatized inoculum

The municipal sewage sludge enriched in liquid cultures where PVA was the only organic carbon and energy source was used as an acclimatized inoculum and the results of the test are shown in Figure 6. It is observed that in the presence of acclimatized inoculum, the extents of biodegradation for PVA-88 and PVA-99 were $89.0\pm 3.9\%$ and 88.9 ± 3.1 , respectively. The extent of the biodegradation was comparable to that of starch (85.6%) after an incubation period of 70 days. These values are much larger compared to those recorded in the presence of non-acclimatized municipal sewage sludge. This observed difference could be explained due to the increase in the activation of microbial strains responsible for PVA degradation due to selective pressure exerted by constant exposure in the case of acclimatized inoculum. It has been reported that certain microorganisms identified as *Pseudomonas* species, *Alcaligenes*, and *Bacillus* were particularly active in the PVA-contaminated environments [36].

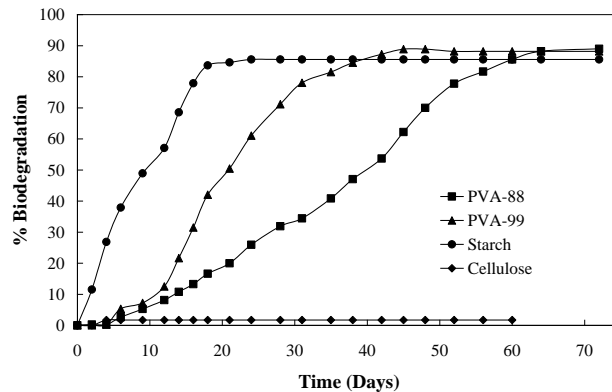


Figure 6.3.6: Biodegradation of PVA, cellulose and starch in the presence of acclimatized inoculum.

The rate constants of starch (0.10 day^{-1}) and PVA-99 (0.12 day^{-1}) are listed in Table 6.3.1 and are very similar, though comparatively a much larger lag time is

observed in the PVA samples (12 days). The degree of hydrolysis of the PVA samples did not seem to have much of an effect on the extent of biodegradation, whereas the degradation rate showed a moderate rate dependence on the degree on hydrolysis. PVA-99 degraded at a faster rate compared to PVA-88 as can be seen from Figure 6.3.6. The graphs of $\ln(1-y/a)$ versus time for both PVA-88 and PVA-99 are shown in Figures 6.3.7 and 6.3.8, respectively. Both the curves show a straight line fit, indicating a first order reaction. The rate constant of PVA-99 (0.12 day^{-1}) showed a four fold increase over the rate constant of PVA-88 (0.03 day^{-1}). It can also be observed that the correlation coefficients R^2 derived in all the cases, from the model is around 0.95 indicating a significant confident of the model, considering the heterogeneity of biodegradation process and diversity of microorganisms associated with it.

Acclimatization of the microbial population to PVA led to a substantial decrease in cellulose assimilation by the same microorganisms as revealed by the very low biodegradation of the cellulose sample (1.7%). However higher degradation values are obtained for starch. In this case, cellulolytic, starch and PVA – degrading activity were conflicting. Therefore particular attention needs to be further devoted to understand the degradation biochemistry and the complexity of mechanisms associated with such biodegradation reactions.

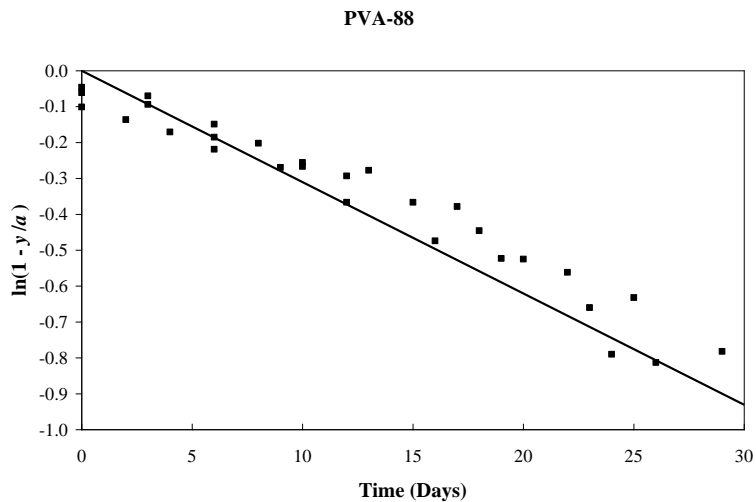


Figure 6.3.7: Biodegradation kinetics of PVA-88 in the presence of acclimatized inoculum

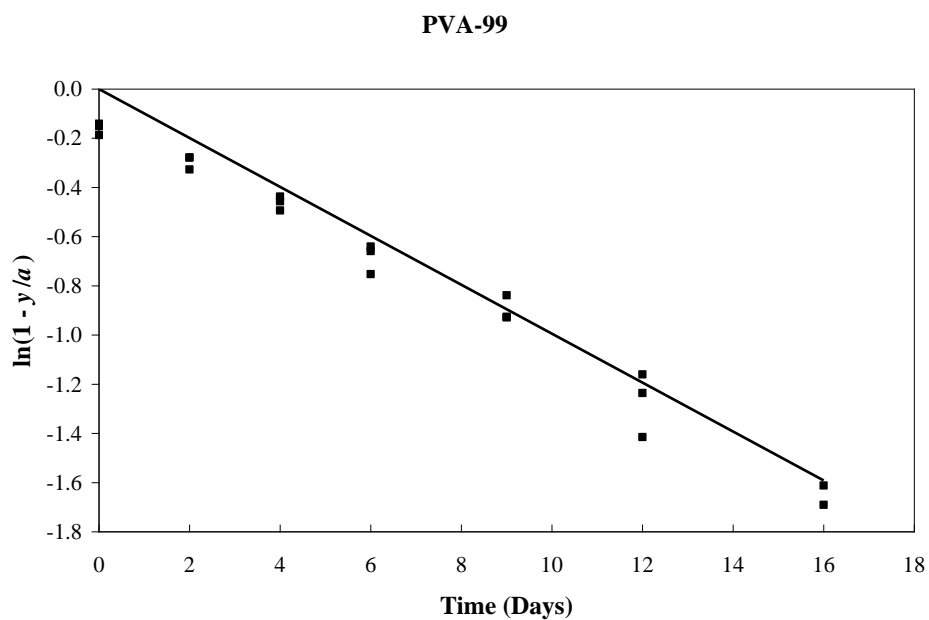


Figure 6.3.8: Biodegradation kinetics of PVA-99 in the presence of acclimatized inoculum

6.3.5 Conclusions

This study was carried to assess the aerobic biodegradability of two different PVA samples under different composting conditions, using acclimatized and non-acclimatized inoculum. The percent biodegradation values were determined using a cumulative respirometric method as specified by standard test method ISO 14852. The experimental data were further fitted into a mathematical model to derive the biodegradation kinetics. Significant levels of PVA biodegradation were reached only in the presence of acclimated PVA degrading microorganisms, most likely because of the selective pressure exerted by the large amounts of PVA in such inoculum. The degree of hydrolysis did not seem to have much of an effect on the extent of biodegradation, whereas the degradation rate showed a moderate dependence on the degree of hydrolysis as evident from the faster degradation rate of PVA-99 compared to PVA-88. The rate constants and the order of the reactions were obtained by fitting the biodegradation data to a mathematical model. The reactions are first order indicating that the rate of the biodegradation reaction depends linearly only on the reactant concentrations

6.4 Biodegradability testing of castor oil PU films and soymeal polyol using Microbial Oxidation Degradation Analyzer (MODA)

6.4.1 Introduction

Polyurethanes (PUs) are an important class of synthetic polymers used in a variety of applications including packaging, paints, coatings, padding and thermal insulation materials. Typically, PUs are prepared by the reaction between polyols and isocyanates, which are generally derived from petro-fossil sources. In the last few years, new PUs are being synthesized using polyols derived from renewable, bio-based sources such as

vegetable oils. It was interesting to determine whether these poly(ester-urethane)s derived from renewable resources were biodegradable. The biodegradability of polyurethanes by microorganisms depends on many properties of the polymer such as molecular orientation, crystallinity, cross-linking and chemical groups present in the main polymer chains. The hydrolysable ester bond in the main chain is considered to be more susceptible to microbial attack by the action of enzymes. The biodegradation of poly(ester-urethane)s is comparatively higher than the poly(ether-urethane)s [37-39]. Further investigations conducted indicated that the PU composed of aliphatic diisocyanates demonstrated a greater rate of biodegradation than PUs composed of aromatic diisocyanates. The rate of biodegradation increased in accordance with the diisocyanates used: MDI < H₁₂MDI < HDI [40].

In this study, the biodegradation of castor oil based PU films and soymeal polyols were conducted according to the standard test method as prescribed by ISO 14855-2. The extent and rates of biodegradation were determined, analyzed and reported.

6.4.2 Experimental methods

6.4.2.1 Materials

Castor oil polyurethane (PU) films having a thickness of 1.68±0.08 mil were provided by a Delhi based PU making company. The PU films were cut into flakes of average dimensions 0.3 x 0.3 cm² and utilized for the test. Cellulose powder (Sigma Aldrich) was used as the positive reference. The organic carbon content of the Indian castor oil PU films was 66.34% which was determined by elemental analysis (Midwest Microlab, LLC, Indianapolis) and cellulose was 44.44% determined from the chemical formula.

The soymeal polyol was synthesized in our lab according to the procedures mentioned in the previous chapters. Soymeal was initially treated with 60% alcohol to remove the soluble carbohydrates, followed by acid hydrolysis using HCl, amination with ethylenediamine and finally reacted with ethylene carbonate to obtain soymeal polyol as shown in chapter 5. The organic carbon content of soymeal was 41.7% as determined by elemental analysis.

6.4.2.2 Gravimetric measurement respirometric system

An ISO 14855-2 method was used as a reference for the biodegradability test. ISO 14855-2 recommends using two blanks, two positive reference materials and two samples to be analyzed for the biodegradation measurement, the compost and sample in a ratio of 6:1 and the commonly used quantity is 60 g of compost to 10 g of sample.

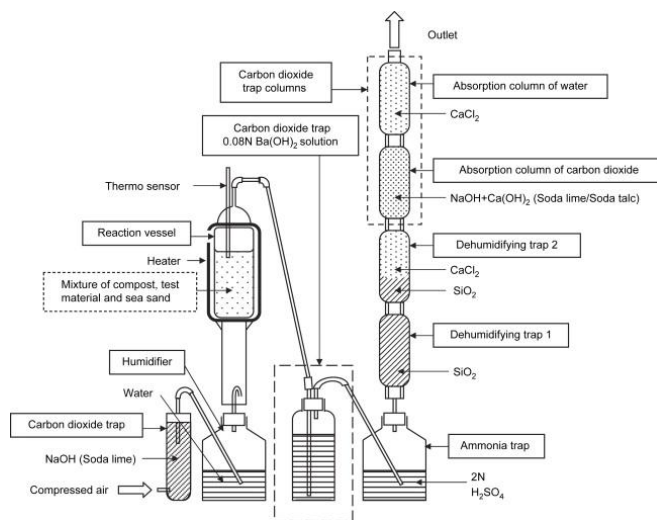


Figure 6.4.1: Schematic representation of the MODA system

A gravimetric measurement respirometric system according to some of the specifications has been built by Hissan Trading Co. Ltd. (Tokyo, Japan), and is commercialized under the name of microbial oxidative degradation analyzer (MODA). A MODA system (Figure 6.4.1) was provided by Saida UMS Inc. (Tokyo, Japan) for the

test presented in this work. The MODA system consists of four bioreactors, one for blank, one for positive control (Cellulose) and two for test samples. In the MODA system, pressurized air is passed through the column containing soda lime (obtained from Airgas) with CO₂ absorption indicator to make it CO₂ free. Later, the air is bubbled through a flask containing deionized water to maintain constant humidity in the compost mixture and in the reaction column. The reaction column consists of a column covered with a heating jacket and a thermosensor to maintain the temperature at 58°C. Air is passed through each bioreactor and later through an ammonia eliminator, moisture remover, and finally to a CO₂ trap column.

6.4.2.3 Preparation of compost

The compost used for the test was made of cow manure, wood shavings and waste feed and was obtained from the Michigan State University composting facility (East Lansing, MI). The compost which was matured for 3 months was screened using a 5 mm mesh and had a relative moisture content and pH of about 65±3% and 8.5±0.5, respectively. Then, 270 grams of the compost by dry weight was added with sufficient moisture to make it to a final moisture content of 80%, left aerated at room temperature for one day and placed in a thermostat at 58 °C overnight. The compost was then mixed well with 270 grams of vermiculite (manufactured by Therm-O-Rock, New Eagle, PA) and a sufficient quantity of water added to bring the moisture content to 65%. This compost-vermiculite mixture was then kept for activation for 7 days at 58°C by mixing twice a day and adding water as necessary to adjust the moisture content.

The activated compost was then introduced into the bioreactors of the MODA such that each column consisted of mature compost (60 g dry weight), vermiculite (60 g

dry weight) and 10 grams by dry weight of the test sample. Compost with no sample was used as the blank to determine the respiration activity of the compost. The bioreactor columns were covered with a thermal jacket at a temperature of 58°C and CO₂ free air was passed through the columns at 25 mL/min flow rate for 30-60 days. In addition to the carbon dioxide, ammonia and water were also generated from the reaction columns, which were eliminated by passing the output of the reactors through 2N sulfuric acid (H₂SO₄) in the ammonia absorption flask, and the neutralization of ammonia by H₂SO₄ was monitored by methyl red indicator. Later the air was passed through moisture removal columns 1 and 2 as shown in Figure 6.4.1. Silica gel was used for the moisture removal (column 1); when the silica gel was saturated it changed color from dark blue to colorless. Moisture removal column 2 consisted of 20% silica gel and 80% calcium chloride (93% granular, anhydrous obtained from Sigma-Aldrich, St.Louis, MO) which completely removed moisture from the air. Column 3 was a carbon dioxide absorption column and contained soda lime (medical grade, Airgas). This chemical reaction generated water, hence the column 4 containing calcium chloride collected the remaining water from the reaction. The produced CO₂ amounts were measured once a day by measuring the weights of an absorption column for carbon dioxide and an absorption column for water. The degree of biodegradation was calculated from the produced CO₂ amount which was subtracted from the respiration CO₂ amount determined from the blank and divided by theoretically produced CO₂ amount of the added sample. The compost mixture was taken out once a week for manual turning to ensure proper mixing of the compost and the sample, and also to improve aeration and maintain accurate moisture in the mixture.

6.4.3 Results and discussion

6.4.3.1 Biodegradation of castor oil based PU films

The cumulative carbon dioxide evolved in the inoculum, castor oil PU films and cellulose columns is shown in Figure 6.4.2. It is obvious that the reference material produced more carbon dioxide than the blank, followed by the CO₂ production of the castor oil PU film. There was a general increase in CO₂ production throughout the test for the blank, indicating the good activity of the compost. Figure 6.4.3 shows the percentage biodegradation of castor oil PU films and cellulose as a function of time. ISO 14855-2 recommends that this test is valid only if cellulose or positive reference control reaches 70% mineralization value before 45 days. These tests fulfilled this condition as was indicated by the results. The cellulose percent biodegradation after 45 days was 69.4%, which was very close to the validity conditions as per ISO 14855-2. However ISO 14855-2 also recommends using two positive controls in the test and the test is only valid if the difference between the biodegradation in the two controls is less than 20%. In our case, we had only one positive control due to the limitation of the MODA equipment.

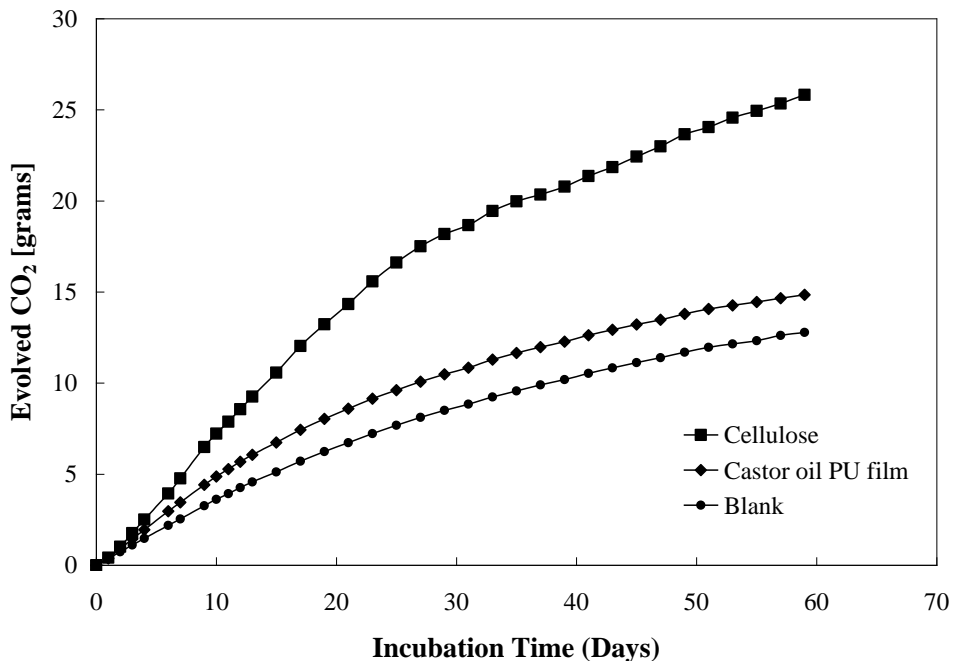


Figure 6.4.2: Evolved carbon dioxide as a function of time for cellulose, blank and castor oil PU film

The biodegradation of castor oil PU films as shown in Figure 6.4.3 reached a plateau phase after 33 days. The percent biodegradation of PU films at this point was 10.2%, while the extent of the biodegradation of cellulose was 62.7%. As shown in Table 6.4.1, the total carbon dioxide evolved from the castor oil PU films was 2.05 g, while the theoretical carbon dioxide expected was 20.16 g and the % mineralization attained was 10.2%. On the other hand, the reference material cellulose reached 79.9% towards the end of the test at 59 days. ASTM D6400, which addresses the compostability of plastic materials, standard specifications and terminologies for biodegradable materials states that for a single polymer (homopolymers or random copolymers) to be certified as biodegradable, 60% of the organic carbon must be converted to carbon dioxide by the end of the test period. Therefore, following the specifications in ASTM D6400 it can be

concluded that the castor oil PU films have not attained satisfactory levels of biodegradation.

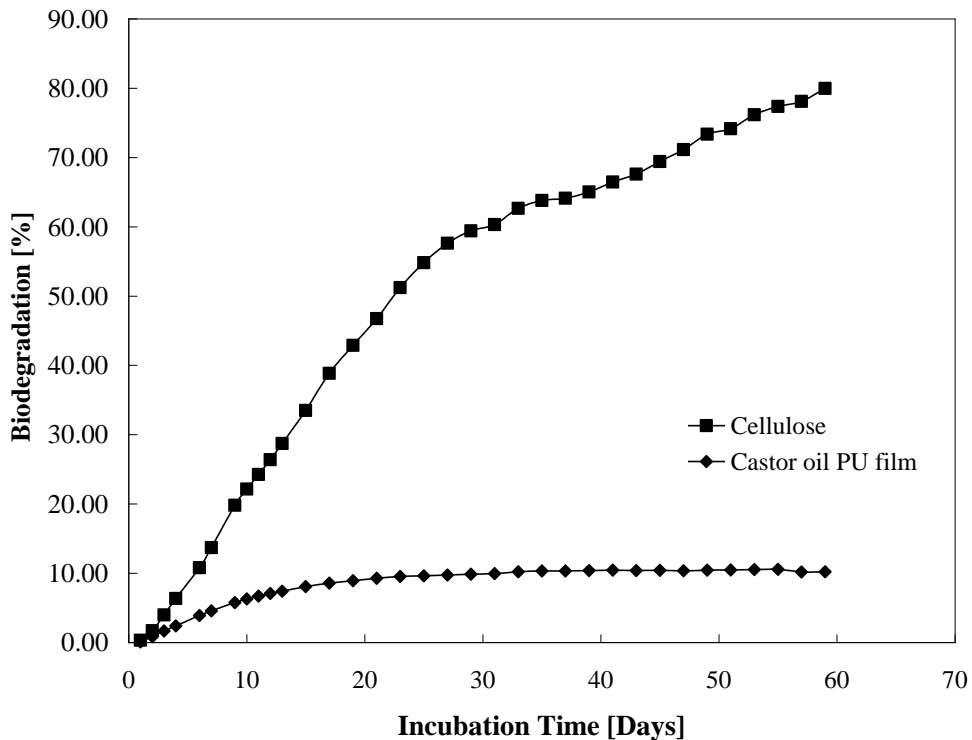


Figure 6.4.3: Percent biodegradation as a function of time for cellulose and castor oil PU film

Table 6.4.1: Percent biodegradation of castor oil PU film as a function of time

Sample	Amount taken, grams	Total carbon content (%)	Expected CO ₂ , grams	Evolved CO ₂ , grams	Biodegradation, (%)
Cellulose	10.01	44.44	16.31	13.03	79.9
Castor oil PU film	8.29	66.34	20.16	2.05	10.2

6.4.3.2 Biodegradation of soymeal polyol

Figure 6.4.4 shows the cumulative carbon dioxide evolved in the blank, soymeal polyols and cellulose columns. The carbon dioxide produced by the cellulose is more

than the CO₂ production of the blank, as was expected. This can be explained due to the action of the microorganisms on the degradable carbon of the reference material. The CO₂ production from the soymeal polyols is higher than the blank; however the rate of CO₂ evolution decreased after the 9th day. There was a steady increase in CO₂ production throughout the test period for the blank, indicating good activity of the microorganisms in the compost. The percent biodegradation of soymeal polyol and cellulose with time is shown in Figure 6.4.5. The percent biodegradation of cellulose attained was 60.2% towards the end of 23 days and can be expected to reach above 70% mineralization after 45 days, thus it can be fairly assumed to fulfill the validity conditions as mentioned in ISO 14855-2 standard.

Soymeal polyols exhibited higher biodegradation rates than cellulose during the initial phases. This could be due to the presence of limited amounts of insoluble carbohydrates present in the soymeal polyol, serving as readily available nutrients to the microorganisms present in the compost. Moreover, soymeal polyol is a liquid and has a much larger surface contact area than the powdery cellulose. The biodegradation curve of the soymeal polyols reached its maximum value of $22.5 \pm 2.1\%$ after 9 days. The plot of soymeal polyol showed a declining trend after 9 days, which does not necessarily mean a decline in percent biodegradation. This negative trend is observed due to subtracting the cumulative CO₂ evolved from the soymeal from the blank. The soymeal polyol has amide-urethane linkages in its structure that are not easily assimilated by the microorganisms, thereby reducing their activity.

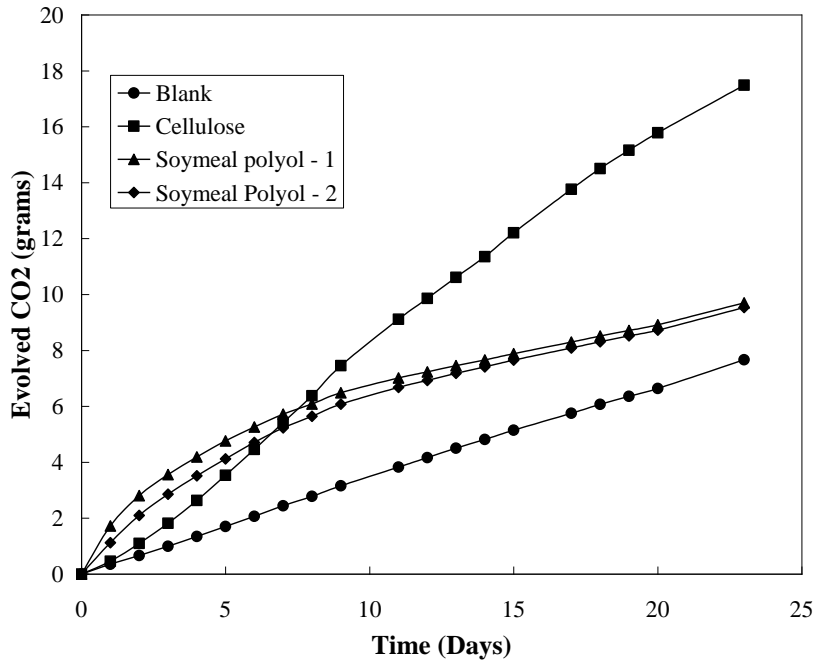


Figure 6.4.4: Cumulative CO₂ evolved over time in soymeal polyols, cellulose and blank

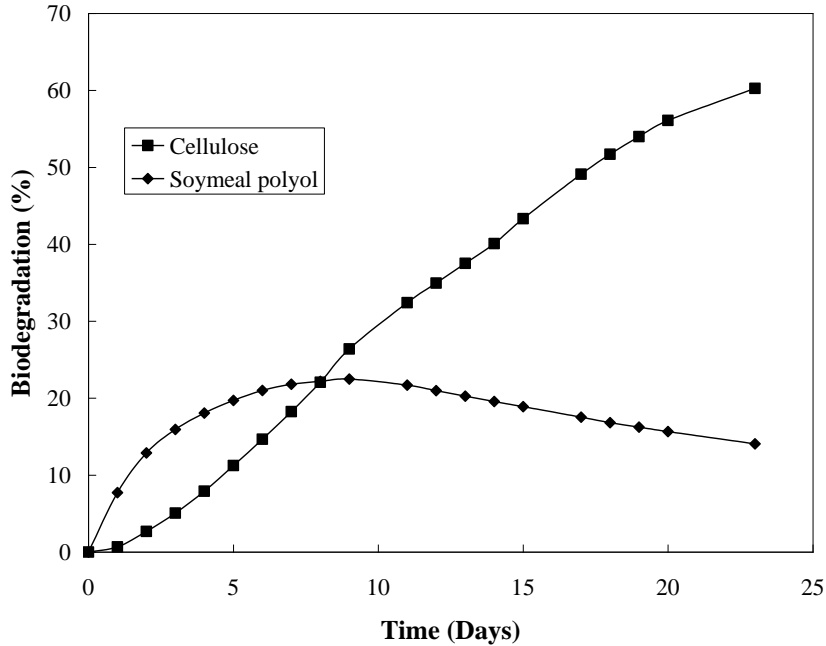


Figure 6.4.5: Percentage biodegradation as a function of time for cellulose and soymeal polyol

6.4.3.3 Biodegradation kinetic studies

The percent biodegradation values versus time data obtained from the tests was further evaluated for understanding the biodegradation kinetics by an exponential product formation model [34] given below.

$$y = a[1 - e^{-k(x-c)}] \text{ for } x > c; y = 0 \text{ for } x \leq c$$

where y is CO₂ evolved (percentage), x is time (days), a is the upper asymptote (percentage), k is the rate constant (per day) and c is the lag time. Lag time and asymptote were introduced into the model so as to ascertain the biodegradation only during active biodegradation. The parameters of the model, rate constant, lag time and asymptote are obtained by fitting the experimental percentage versus time data using nonlinear regression analysis. The correlation co-efficient R^2 is also determined from the model to estimate the variability accounted for the model. The results of the biodegradation kinetic studies of castor oil PU and soymeal polyol are shown in Table 6.4.2.

Table 6.4.2: Biodegradation kinetic parameters of castor oil PU and soymeal polyol

Sample	Biodegradation, %	Rate constant (day ⁻¹)	Correlation Coefficient, R ²	Lag time (days)
Cellulose	79.9±0.0	0.06±0.02	0.98±0.04	0.0±0.0
Castor oil PU	10.2±0.0	0.09±0.02	0.98±0.00	0.0±0.0
Soymeal polyol	22.5±2.1	0.50±0.11	0.97±0.01	0.0±0.0

Figures 6.4.6, 6.4.7 and 6.4.8 show the graphs of $\ln(1-y/a)$ versus time for cellulose, castor oil PU films and soymeal polyol, respectively. The observed linear correlation as indicated by the straight line fit in these log plots confirmed the first order rate of these reactions. The rate constants (day⁻¹) were obtained from the slope of $\ln(1-y/a)$ vs time curves. Similarly the biodegradation reaction was first order with respect to the concentrations of the test samples. The rate constants of cellulose, castor oil and

soymeal polyol are 0.06, 0.09, 0.50 day⁻¹ respectively. The rate constants of soymeal polyol are comparatively higher than cellulose, due to the initial higher biodegradation rates observed in the case of soymeal polyol before it reached the plateau phase within a short time, as was shown in Figure 6.4.5. The correlation coefficients obtained indicated a good fit of the kinetic model to the experimental biodegradation data. Figure 6.4.9 shows the comparison between the experimental data and the calculated data from the kinetic model. The data generated by the kinetic model (shown in dotted lines) closely matches with the experimental data (shown in solid lines).

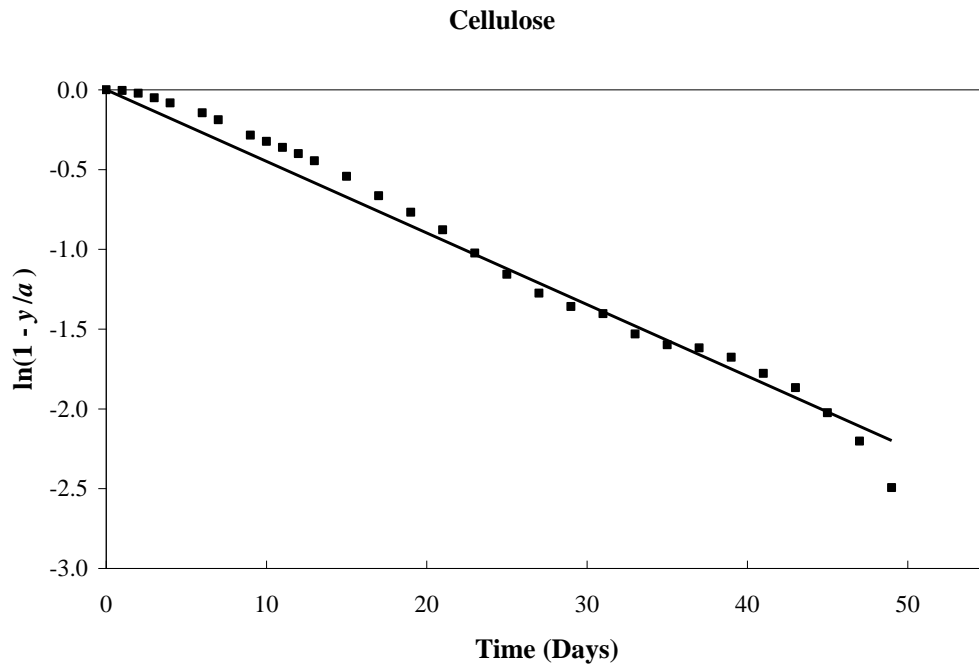


Figure 6.4.6: Graph of $\ln(1-y/a)$ versus time for cellulose

Castor oil PU film

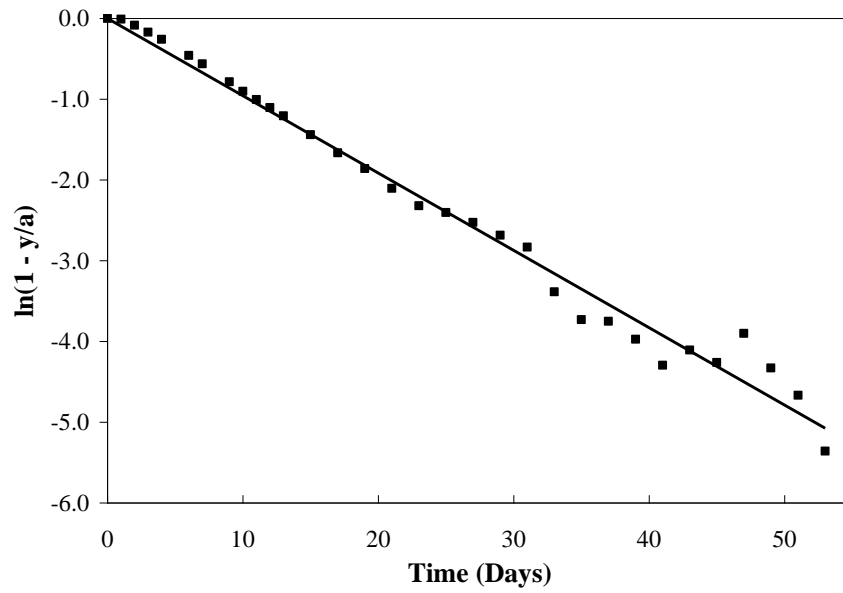


Figure 6.4.7: Graph of $\ln(1-y/a)$ versus time for castor oil PU films.

Soymeal Polyol

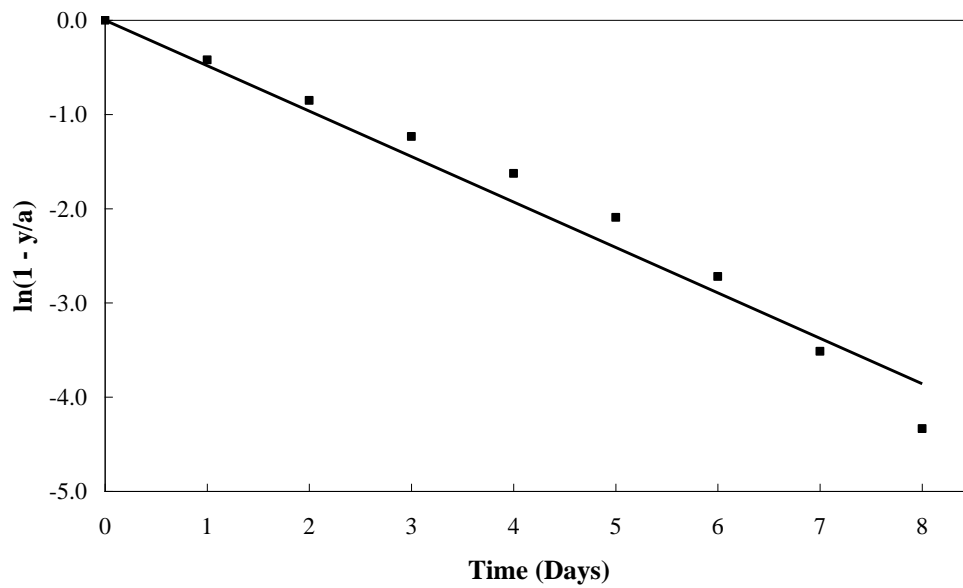


Figure 6.4.8: Graph of $\ln(1-y/a)$ versus time obtained for soymeal polyol

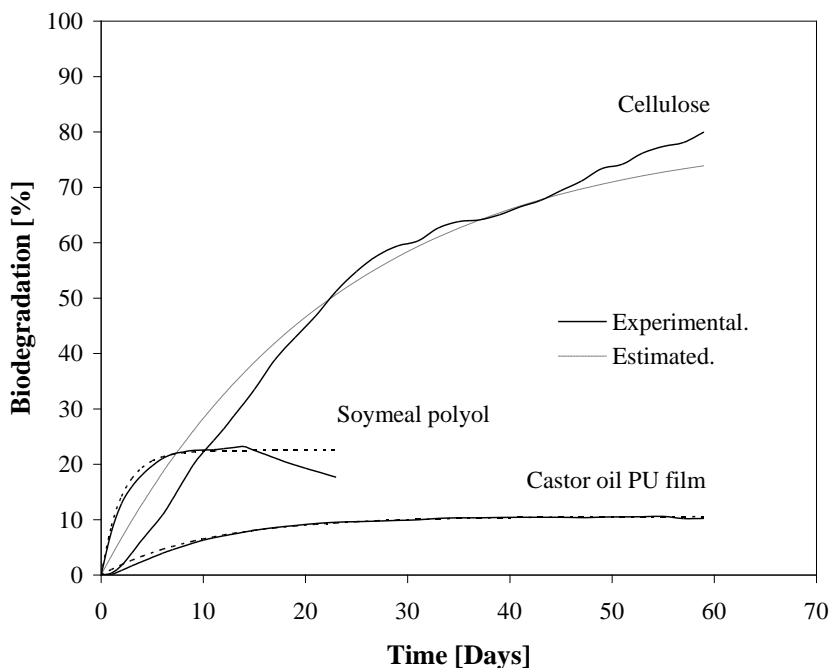


Figure 6.4.9: Comparison between experimental and estimated data generated by the kinetic model

6.4.4 Conclusions

This study was carried out in order to assess the biodegradability of castor oil PU films and soymeal polyols under controlled laboratory conditions according to ISO 14855-2 using MODA. From the results obtained, it can be concluded that both castor oil PU films and soymeal polyols have not reached satisfactory biodegradation levels as indicated by the conditions of the ISO 14855-2 standard. After 59 days, the biodegradation of castor oil PU films was 10.2%. The rate of biodegradation for the reference material reached 69.6% towards the end of the 45 day test period, thereby fulfilling the validity conditions according to ISO 14855-2. Soymeal polyol reached its maximum biodegradability level of $22.5 \pm 2.1\%$. The reaction kinetics indicates that the biodegradation reactions are first order with respect to the concentration of the test materials.

REFERENCES

REFERENCES

1. EPA (2011) Municipal Solid Waste Generation, Recycling, and Disposal in the United States: Facts and Figures for 2011. Environmental Protection Agency, Washington DC
2. ASTM (2004) D6400-04 Standard Specification for Compostable Plastics. West Conshohocken, PA
3. Kale G, Kijchavengkul T, Auras R, Rubino M, Selke SE, Singh SP (2007) An overview of compostability of bioplastic packaging materials. *Macromol Biosci* 7:255-277
4. Kister G, Cassanas G, Bergounhon M, Hoarau D, Vert M (2000) Structural characterization and hydrolytic degradation of solid copolymers of D, L-lactide-co-ε-caprolactone by Raman spectroscopy. *Polymer* 41:925-932
5. Proikakis CS, Mamouzelous NJ, Tarantili PA, Andreopoulos AG (2006) Swelling and hydrolytic degradation of poly(D, L-lactic acid) in aqueous solution. *Polym Degrad Stab*, 91(3):614-619
6. Helbling C, Abanilla M, Lee L, Karbhari VM, (2006) Issues of variability and durability under synergistic exposure conditions related to advanced polymer composites in civil infrastructure, *Compos. Part A-Appl Sci*, 37(8):1102-1110
7. Ipekogulu B, Boke H, Cizer O (2007) Assessment of material use in relation to climate in historical buildings, *Build Environ*. 42:970-978
8. Jakubowicz I, Yarahmadi N, Petersen H, (2006) Evaluation of the rate of abiotic degradation of biodegradable polyethylene in various environments. *Polym Degrad Stab*, 91(6):1556-1562
9. Gu JD, Ford TE, Mitton DB, Mitchell R, (2000) Microbial degradation and deterioration of polymeric materials In: Revie W, editor. *The Uhlig Corrosion Handbook*, 2nd Edition, New York: Wiley b, 439-460
10. Gu JD (2003) Microbiological deterioration and degradation of synthetic polymeric materials: recent research advances. *Int Biodeterior Biodegrad*,52: 69-91
11. Gartiser S, Wallrahenstein M, Stiene G (1998) Assessment of several test methods for the determination of the anaerobic biodegradability of polymers. *J Environ Polym Degrad*. 1998, 6, 159-173.

12. Griffin GJL (1980) Synthetic polymers and the living environment. *Pure Appl Chem* 52:399-407
13. Chandra T, Rustgi R (1998) Biodegradable Polymers. *Prog Polym Sci* 23:1273-1335
14. Kai-Lai GH, Pometto AL III, Hinz PN (1999) Effects of temperature and relative humidity on polylactide acid plastic degradation. *J Environ Polym Degrad* 7(2): 83-92
15. Rafael A, Bruce H, Selke S (2004) An overview of Polylactides as Packaging Materials. *Macromol Biosci* 4:835-864
16. Kai-Lai GH Pometto III AL, Gadea-Rivas A, Briceno JA, Rojas A (1999) Degradation of Polylactic Acid (PLA) Plastic in Costa Rican Soil and Iowa State University Compost Rows. *J Environ Polym Degrad* 7:173-177
17. Artham T, Doble M (2008) Biodegradation of Aliphatic and Aromatic Polycarbonates. *Macromol Biosci* 8(1):14-24
18. Stevens ES (2003) What Makes Green Plastics Green? *Biocycle* 24:24-27
19. Wendy A, Allan A, Brian T (1998) A review of biodegradable polymers: uses, current developments in the synthesis and characterization of biodegradable polyesters, blends of biodegradable polymers and recent advances in biodegradation studies. *Polym Int* 47: 89-144
20. Zhang X, Wyss UP, Pichora D, Goosen MFA (1994) An investigation of poly(lactic acid) degradation. *J Bioactive Compat Polym* 9:80-100
21. Gopferich A (1997) Mechanisms of Polymer Degradation and Elimination", in: *Handbook of Biodegradable Polymers*, Domb AJ, Kost A, Wiseman DM, Eds, Hardwood Academic, Montreux, 451-471
22. Chellini E, Corti A (2003) A simple Method Suitable to Test the Ultimate Biodegradability of Environmentally Degradable Polymers. *Macromol Symp* 197: 381-395
23. Corti A, Muniyasamy S, Vitali M, Imam SH, Chellini E (2010) Oxidation and Biodegradation of Polyethylene Films Containing Pro-oxidant Additives: Synergistic Effects of Sunlight Exposure, Thermal Aging and Fungal Biodegradation. *Polym Degrad Stab* 95:1106-1114

24. ISO (1999) 14855-1: Determination of The Ultimate Aerobic Biodegradability And Disintegration of Plastic Materials Under Controlled Composting Conditions - Method By Analysis of Evolved Carbon Dioxide. ISO, Geneva, Switzerland
25. ASTM (1998) D5338-98^{e1} Standard Test Method for Determining Aerobic Biodegradation of Plastic Materials Under Controlled Composting Conditions. ASTM, West Conshohocken, PA.
26. ISO (2006) 14855-1 Determination of the Ultimate Aerobic Biodegradability of Plastic Materials under Controlled Composting Conditions - Method by Analysis of Evolved Carbon Dioxide. Part 2: Gravimetric Measurement of Carbon Dioxide Evolved in a Laboratory Scale Test. ISO, Geneva, Switzerland.
27. Jegal J, Lee KH (1996) Pervaporation separation of water - ethanol mixtures through PVA-sodium alginate blend membranes. J Appl Polym Sci 61(2):389-392
28. Suzuki F, Nakane K, Piao JS (1996) Formation of a compatible composite of silica poly(vinyl alcohol) through the sol-gel process and a calcinated product of the composite. J Mater Sci 31(5):1335-1340
29. Betty LLO, Amanda IMG, Ligia SG (1999) Biodegradability of poly(vinyl alcohol). Polym Eng Sci 39(8):1346-1352
30. Corti A, Solaro R, Chiellini E (2002) Biodegradation of poly(vinyl alcohol) in selected mixed microbial culture and relevant culture filtrate. Polym Degrad Stab 75:447-458
31. Kim BC, Sohn CK, Lim SK, Lee JW, Park W (2003) Degradation of polyvinyl alcohol by *Sphingomonas* sp. SA3 and its symbiote. J Ind Microbiol Biotechnol 30:70-74
32. Finch CA (1992) Polyvinyl Alcohol - Developments, John Wiley and Sons, Chichester, New York, Brisbane, Toronto, Singapore, pp. 269-312.
33. ISO (2005) 14852 Determination of the Ultimate Aerobic Biodegradability of Plastic Materials In An Aqueous Medium - Method By Analysis of Evolved Carbon Dioxide. ISO, Geneva, Switzerland.
34. Larson RJ, Payne AG (1981) Fate of the benzene ring of linear alkylbenzene sulfonate in natural waters. Appl Environ Microbiol. 41:621-627
35. Chiellini E, Corti A, Solaro R (1999) Biodegradation of poly(vinyl alcohol) based blown films under different environmental conditions. Polym Degrad Stab 64:305-312

36. Chiellini E, Corti A, Solaro R (2003) Biodegradation of poly (vinyl alcohol) based materials. *Prog Polym Sci* 28:963-1014
37. Howard GT (2002) Biodegradation of polyurethane: a review. *Int Biodeterior Biodegrad* 49:245-252
38. Shogren RL, Petrovic Z, Liu Z, Erhan SZ (2004) Biodegradation Behavior of Some Vegetable Oil-Based Polymers. *J Polym Environ* 12(3):173-178
39. Cangemi J, Santos AM, Dos C, Neto S, Chierice GO (2008) Biodegradation of polyurethane derived from castor oil., *Polimeros* 18(3):201-206
40. Kim YD, Kim SC (1998) Effect of chemical structure on the biodegradation of polyurethanes under composting conditions. *Polym Degrad Stabil* 62(2): 343-352

Chapter 7 Summary and recommendations for future work

7.1 Summary

This dissertation work was divided into five parts: (a). synthesis of polyurethanes from soymeal by a non - isocyanate route, (b). rigid polyurethane foams based on soymeal polyols, (c). spectroscopic method for hydroxyl value determination, (d). evaluation of PU coatings based on soymeal polyol and castor oil, (e) biodegradability studies.

7.1.1 Synthesis of polyurethanes from soymeal by a non - isocyanate route

- Successfully synthesized bio-based poly(amide-urethane-ester)s from soymeal without employing the toxic isocyanates
- Higher molecular weights could not be obtained due to the limitations of the polycondensation reactions
- The obtained polyurethanes are amorphous and thermally stable upto 270 °C
- The intermediate hydroxy-terminated urethane monomers can be potentially used as polyols for rigid PU foam formulations

7.1.2 Rigid polyurethane foams based on soymeal polyols

- Foams with 25% and 50% soymeal polyols exhibited properties comparable to the reference model pour-in-place foams
- Soymeal polyols exhibited self catalytic properties, due to the presence of secondary amines

- Partially biobased polyurethane, therefore has a smaller carbon footprint than traditional rigid foams
- High dimensional stability and chemical resistance derived from the amide linkages
- Compatibility with other polyols, blowing agents and other foam additives
- High functionality polyols suitable for high crosslink rigid foams
- Low flammability (charring upon burning) in synergy with flame retardant additives
- Potential applications in Foam-In-Place packaging applications

7.1.3 Spectoscopic method for hydroxyl value determination

- An excellent linear correlation ($R^2 = 0.9783$) was observed between the hydroxyl values and the FTIR peak areas at 1251 cm^{-1}
- Wide range of OHVs (20 - 1800 mg KOH/g) using polyols having different structures were used
- This method is simple, faster, accurate and reproducible than conventional titration methods
- Requires small samples, and does not use toxic or hazardous reagents
- Not susceptible to error due to the presence of water, acid or base contaminants
- This method can be used for routine analysis as well as quality control

7.1.4 Evaluation of PU coatings based on soymeal polyol and castor oil

- Soymeal polyol PU coatings exhibited hydrophilic nature

- Higher OH values (435.7 mg KOH/g) of soymeal polyols resulted in high degree of crosslinking upon reaction with isocyanates; rigid films with higher T_g (87.7 °C)
- Castor oil PU coatings exhibited hydrophobic nature
- Low OH values (163 mg KOH/g) of castor oil resulted in less number of cross links between the polymer chains; flexible films with lower T_g (22.8 °C)*
- Castor oil PU coatings significantly increased the moisture barrier properties of cellophane
- A decline in the oxygen barrier properties of cellophane, due to disruption of intermolecular hydrogen bonding forces upon exposure to aqueous coatings

7.1.5 Biodegradability studies

- Conducted biodegradability studies and determined the reaction kinetics
- Two different grades of poly(vinyl) alcohol, PVA-88 and PVA-99 were tested for their biodegradability in aqueous medium in accordance with ISO 14852 standard
- PVA degraded in the presence of acclimatized inoculum and the percent biodegradation of PVA-88 and PVA-99 are 89.0±3.9% and 88.9±3.1% respectively
- The degree of hydrolysis of the PVA samples did not have an effect on the extent of biodegradation, whereas the rate of degradation showed a moderate dependence on the degree of hydrolysis, as was evident from the rate constants.

- Castor oil PU films and soymeal polyol were tested for their biodegradability using MODA in accordance with ISO 14855-2 standard.
- Both castor oil PU films and soymeal polyol had not reached satisfactory biodegradation levels.
- The biodegradation reactions conducted under standard laboratory conditions were first order reactions and depended linearly only on the reactant concentrations.

7.2 Recommendations for future work

7.2.1 Synthesis of soymeal polyols suitable for flexible polyurethane foams

The hydroxyl values of the polyols play an important role in determining the final properties of the polyurethane foams. The molecular structure of the hydrolyzed soymeal prior to reaction with cyclic carbonates can be modified by reacting with high molecular weight amines such as polyetheramines, to obtain low hydroxyl value polyols suitable for flexible foams. The polyols obtained can be further evaluated in flexible foam formulations and tested for its properties.

7.2.2 Evaluation of soymeal polyols for adhesive formulations

Polyurethanes are widely used in the packaging industry as adhesives. The soymeal polyol can be further evaluated in adhesive formulations and tested for its performance properties.

7.2.3 Shelf life studies for packaging applications

Further, work is needed to be done for understanding and determining if the properties of these soymeal based flexible foams and adhesives can be

utilized for real life packaging applications. By designing an actual package and running shelf life studies on the relevant products can be helpful in understanding and estimating the performance of these materials for real life packaging applications.